CHAPTER 5†: SHIELDING EVALUATION

5.0 INTRODUCTION

The shielding analysis of the HI-STORM FW system is presented in this chapter. As described in Chapter 1, the HI-STORM FW system is designed to accommodate both PWR and BWR MPCs within HI-STORM FW overpacks (see Table 1.0.1).

In addition to storing intact PWR and BWR fuel assemblies, the HI-STORM FW system is designed to store BWR and PWR damaged fuel assemblies and fuel debris. Damaged fuel assemblies and fuel debris are defined in Subsection 2.1. Both damaged fuel assemblies and fuel debris are required to be loaded into Damaged Fuel Containers (DFCs).

PWR fuel assemblies may contain burnable poison rod assemblies (BPRAs), with any number of full-length rods and thimble plug rodlets in the locations without a full-length rod, thimble plug devices (TPDs), control rod assemblies (CRAs) or axial power shaping rod assemblies (APSRs), neutron source assemblies (NSAs), or similarly named devices. These non-fuel hardware devices are an integral yet removable part of PWR fuel assemblies and therefore the HI-STORM FW system has been designed to store PWR fuel assemblies with or without these devices. Since each device occupies the same location within a fuel assembly, a single PWR fuel assembly will not contain multiple devices, with the exception of instrument tube tie rods (ITTRs), which may be stored in the assembly along with other types of non-fuel hardware.

As described in Chapter 1(see Tables 1.2.3 and 1.2.4), the loading of fuel in all HI-STORM FW MPCs will follow specific heat load limitations.

In order to offer the user more flexibility in fuel storage, the HI-STORM FW System offers two heat load patterns, each with a three-region loading configuration, in the MPC-37. The MPC-89 has one heat load pattern with a three-region loading configuration. The regionalized storage patterns are guided by the considerations of minimizing occupational and site boundary dose to comply with ALARA principles.

The sections that follow will demonstrate that the design of the HI-STORM FW dry cask storage system fulfills the following acceptance criteria outlined in the Standard Review Plan, NUREG-1536 [5.2.1]:

---

† This chapter has been prepared in the format and section organization set forth in Regulatory Guide 3.61. However, the material content of this chapter also fulfills the requirements of NUREG-1536. Pagination and numbering of sections, figures, and tables are consistent with the convention set down in Chapter 1, Section 1.0, herein. Finally, all terms-of-art used in this chapter are consistent with the terminology of the glossary and component nomenclature of the Bill-of-Materials (Section 1.5).

Acceptance Criteria

1. The minimum distance from each spent fuel handling and storage facility to the controlled area boundary must be at least 100 meters. The "controlled area" is defined in 10CFR72.3 as the area immediately surrounding an ISFSI or monitored retrievable storage (MRS) facility, for which the licensee exercises authority regarding its use and within which ISFSI operations are performed.

2. The system designer must show that, during both normal operations and anticipated occurrences, the radiation shielding features of the proposed dry cask storage system are sufficient to meet the radiation dose requirements in Sections 72.104(a). Specifically, the vendor must demonstrate this capability for a typical array of casks in the most bounding site configuration. For example, the most bounding configuration might be located at the minimum distance (100 meters) to the controlled area boundary, without any shielding from other structures or topography.

3. Dose rates from the cask must be consistent with a well established "as low as reasonably achievable" (ALARA) program for activities in and around the storage site.

4. After a design-basis accident, an individual at the boundary or outside the controlled area shall not receive a dose greater than the limits specified in 10CFR72.106.

5. The proposed shielding features must ensure that the dry cask storage system meets the regulatory requirements for occupational and radiation dose limits for individual members of the public, as prescribed in 10CFR Part 20, Subparts C and D.

Consistent with the Standard Review Plan, NUREG-1536, this chapter contains the following information:

- A description of the shielding features of the HI-STORM FW system, including the HI-TRAC transfer cask.
- A description of the source terms.
- A general description of the shielding analysis methodology.
- A description of the analysis assumptions and results for the HI-STORM FW system, including the HI-TRAC transfer cask.
- Analyses are presented for each MPC showing that the radiation dose rates follow As-Low-As-Reasonably-Achievable (ALARA) practices.
- Analyses to show that the 10CFR72.106 controlled area boundary radiation dose limits can be met during accident conditions of storage for non-effluent radiation from illustrative ISFSI configurations at a minimum distance of 100 meters. Since only representative dose rate values for normal conditions are presented for this chapter, compliance with the radiation and

exposure objectives of 10CFR72.104 is not being evaluated herein but will be performed as part of the site specific evaluations.

Chapter 2 contains a detailed description of structures, systems, and components important to safety.

Chapter 7 contains a discussion on the release of radioactive materials from the HI-STORM FW system. Therefore, this chapter only calculates the dose from direct neutron and gamma radiation emanating from the HI-STORM FW system.

Chapter 11, Radiation Protection, contains the following information:

- A discussion of the estimated occupational exposures for the HI-STORM FW system, including the HI-TRAC transfer cask.
- A summary of the estimated radiation exposure to the public.

The safety analyses summarized in this chapter demonstrate that under accident conditions, acceptable margins to allowable limits exist under all design basis loading conditions. For normal and off-normal conditions, the analyses in this chapter simply provide a generic evaluation that demonstrates that the dose requirements as specified in 10CFR72.104 can be met under site specific conditions. Minor changes to the design parameters that inevitably occur during the product's life cycle which are treated within the purview of 10CFR72.48 and are ascertained to have an insignificant effect on the computed dose rates in this chapter may not prompt a formal reanalysis and revision of the results and associated data in the tables of this chapter unless the cumulative effect of all such unquantified changes cannot be deemed any more to be insignificant. For accident conditions, the dose limit as specified in 10CFR72.106 is 5 rem. The only accident which impacts dose rates is the loss of water in the water jacket for the HI-TRAC VW. For the purposes of determining if the changes to the HI-TRAC VW are insignificant, an insignificant loss of margin with reference to the 5 rem acceptance criteria is defined as the estimated reduction that is no more than one order of magnitude less than the available margin reported in the FSAR. For normal and off-normal conditions, site specific dose evaluations are required to demonstrate compliance with 10CFR72.104. Incorporating any minor changes into those site specific evaluations is only warranted if it would be expected, on a site specific basis, that those changes could result in a situation where the limits are no longer met and where therefore other compensatory measures are required, such as a change in the loading plan or the concrete density. Incorporating changes into the analyses in this chapter for normal and off-normal conditions will only be performed under extenuating circumstances, e.g. major changes to the shielding design, in order to provide an updated template for the site specific dose analyses.

To ensure rigorous configuration control, the information in the Licensing drawings in Section 1.5 should be treated as the authoritative source for numerical analysis at all times. Reliance on the input data and associated results in this chapter for additional mathematical computations

may not be appropriate as they serve the sole purpose of establishing safety compliance in accordance with the acceptance criteria set down in Chapter 2 and in this chapter.

5.1 DISCUSSION AND RESULTS

The principal sources of radiation in the HI-STORM FW system are:

- Gamma radiation originating from the following sources:

  1. Decay of radioactive fission products
  2. Secondary photons from neutron capture in fissile and non-fissile nuclides
  3. Hardware activation products generated during core operations

- Neutron radiation originating from the following sources

  1. Spontaneous fission
  2. α,n reactions in fuel materials
  3. Secondary neutrons produced by fission from subcritical multiplication
  4. γ,n reactions (this source is negligible)

During loading, unloading, and transfer operations, shielding from gamma radiation is provided by the stainless steel structure and the basket of the MPC and the steel, lead, and water in the HI-TRAC transfer cask. For storage, the gamma shielding is provided by the MPC, and the steel and concrete ("Metcon" structure) of the overpack. Shielding from neutron radiation is provided by the concrete of the overpack during storage and by the water of the HI-TRAC transfer cask during loading, unloading, and transfer operations. It is worth noting that the models, used to evaluate the dose calculations in this chapter, are constructed with minimum concrete densities and minimum lead thicknesses.

The shielding analyses were performed with MCNP5 [5.1.1] developed by Los Alamos National Laboratory (LANL). The source terms for the design basis fuels were calculated with the SAS2H and ORIGEN-S sequences from the SCALE 5 system [5.1.2, 5.1.3]. A detailed description of the MCNP models and the source term calculations are presented in Sections 5.3 and 5.2, respectively.

The design basis zircaloy clad fuel assemblies used for calculating the dose rates presented in this chapter are Westinghouse (W) 17x17 and the General Electric (GE) 10x10, for PWR and BWR fuel types, respectively. Required site specific shielding evaluations will verify whether those assemblies and assembly parameters are appropriate for the site-specific analyses. Subsection 2.1 specifies the acceptable fuel characteristics, including the acceptable maximum burnup levels and minimum cooling times for storage of fuel in the HI-STORM FW MPCs.

The following presents a discussion that explains the rationale behind the burnup and cooling time combinations that are evaluated in this chapter for normal and accident conditions.

10CFR72 contains two sections that set down main dose rate requirements: §104 for normal and off-normal conditions, and §106 for accident conditions. The relationship of these requirements

to the analyses in this Chapter 5, and the burnup and cooling times selected for the various analyses, are as follows:

- 10CFR72.104 specifies the dose limits from an ISFSI (and other operations) at a site boundary under normal and off-normal conditions. Compliance with §104 can therefore only be demonstrated on a site-specific basis, since it depends not only on the design of the cask system and the loaded fuel, but also on the ISFSI layout, the distance to the site boundary, and possibly other factors such as use of higher density concrete or the terrain around the ISFSI. The purpose of this chapter is therefore to present a general overview over the expected dose rates, next to the casks and at various distances, to aid the user in applying ALARA considerations and planning of the ISFSI. To that extent, it is sufficient to present reasonably conservative dose rate values, based on a reasonable conservative choice of burnups and cooling times of the assemblies.
- For the accident dose limit in 10CFR72.106 it is desirable to show compliance in this Chapter 5 on a generic basis, so that calculations on a site-by-site basis are not required. To that extend, a burnup and cooling time calculation that maximizes the dose rate under accident conditions needs to be selected.

The HI-STORM FW System offers three-region loading configurations as shown in Table 1.2.3 and Table 1.2.4 in Chapter 1.

- For the MPC-37, there are two heat load patterns, each with a three-region loading configuration – Loading Pattern A and Loading Pattern B. An important difference between Pattern A and Pattern B loading is the loading is the maximum allowed heat load of the cells on the periphery of the MPC-37. Pattern A contains the cells with the lowest decay heat on the periphery, while Pattern B contains the cells with the highest decay heat on the periphery. In Pattern A, fuel assemblies with higher heat loads are loaded in the inner region allowing the user to take advantage of self-shielding from the fuel assemblies with lower heat loads in the outer regions. However, for Pattern B, the fuel assemblies with the higher heat loads could be loaded in the outer region (Region 3). Based on this difference it is expected that Pattern B will have higher dose rates than Pattern A. Therefore, for dose calculations Pattern B is selected, as it is the more limiting of the two loading patterns. Furthermore, uniform loading of MPC-37 cells is assumed for dose calculations. The burnup and cooling time combination is selected as representative of the cells on the periphery. This is a conservative approach, as it assumes that all thirty seven cells have a decay heat per cell equal to or slightly exceeding the decay heat of the periphery cells.

- For the MPC-89, there is only one heat load pattern with a three-region loading configuration. Based on the configuration for the MPC-89, fuel assemblies with higher heat loads would be loaded in the inner region allowing the user to take advantage of self-shielding from fuel assemblies with lower heat loads in the outer regions (see Table 1.2.4). However, for simplification, the shielding analyses are performed for a single region, i.e. assuming all assemblies in the basket have the same burnup and cooling time.

In the case of the MPC-89 the burnup and cooling time combination is selected as a representative average for the entire basket.

While Loading Pattern B for the MPC-37 allows assemblies with higher heat loads and therefore higher source terms in the outer region (Region 3) of the MPC, the guiding principle in selecting fuel loading should still be to preferentially place assemblies with higher source terms in the inner regions of the basket as far as reasonably possible.

It is recognized that for a given heat load, an infinite number of burnup and cooling time combination could be selected, which would result in slightly different dose rate distributions around the cask. For a high burnup with a corresponding longer cooling time, dose locations with a high neutron contribution would show higher dose values, due to the non-linear relationship between burnup and neutron source term. At other locations dose rates are more dominated by contribution from the gamma sources. In these cases, short cooling time and lower burnup combinations with heat load comparable to the higher burnup and corresponding longer cooling time combinations would result in higher dose rates. However, in those cases, there would always be a compensatory effect, since for each dose location, higher neutron dose rates would be partly offset by lower gamma dose rates and vice versa.

Based on these considerations, average burnup and cooling time values are selected for all calculations for normal conditions, i.e values that are away from the extreme values. The selected values are shown in Table 5.0.1, and are based on a total heat loads presented in Table 1.2.3. For the accident conditions however, it is recognized that the bounding accident condition is the loss of water in the HI-TRAC VW, a condition that is neutron dominated due to the removal of the principal neutron absorber in the HI-TRAC VW (water). For this case, the upper bound burnup is selected, in order to maximize the neutron source strength of all assemblies in the basket, and a corresponding higher cooling time is selected in order to meet the overall heat load limit in the cask. The resulting burnup and cooling times values for accidents are therefore different from those for normal conditions and are listed in Table 5.0.2. In all cases, low initial enrichments are selected, which further increases the neutron source terms from the assemblies

With the burnup and cooling times selected based on above considerations, dose rates calculated for normal conditions will be reasonably conservative, while for accident conditions those will represent reasonable upper bound limits.

Table 5.0.1

DESIGN BASIS FUEL BURNUP, COOLING TIME AND ENRICHMENT FOR NORMAL CONDITIONS

Design Basis Burnup and Cooling Times Zircaloy Clad Fuel	
MPC-37	**MPC-89**
45,000 MWD/MTU 4.5 Year Cooling 3.6 wt% U-235 Enrichment	45,000 MWD/MTU 5 Year Cooling 3.2 wt% U-235 Enrichment

Table 5.0.2

DESIGN BASIS FUEL BURNUP, COOLING TIME AND ENRICHMENT FOR ACCIDENT CONDITIONS

Design Basis Burnup and Cooling Times Zircaloy Clad Fuel	
MPC-37	**MPC-89**
65,000 MWD/MTU 8 Year Cooling 4.8 wt% U-235 Enrichment	65,000 MWD/MTU 10 Year Cooling 4.8 wt% U-235 Enrichment

5.1.1 Normal and Off-Normal Operations

Chapter 12 discusses the potential off-normal conditions and their effect on the HI-STORM FW system. None of the off-normal conditions have any impact on the shielding analysis. Therefore, off-normal and normal conditions are identical for the purpose of the shielding evaluation.

The 10CFR72.104 criteria for radioactive materials in effluents and direct radiation during normal operations are:

1. During normal operations and anticipated occurrences, the annual dose equivalent to any real individual who is located beyond the controlled area, must not exceed 25 mrem to the whole body, 75 mrem to the thyroid and 25 mrem to any other critical organ.

2. Operational restrictions must be established to meet as low as reasonably achievable (ALARA) objectives for radioactive materials in effluents and direct radiation.

10CFR20 Subparts C and D specify additional requirements for occupational dose limits and radiation dose limits for individual members of the public. Chapter 11 specifically addresses these regulations.

In accordance with ALARA practices, design objective dose rates are established for the HI-STORM FW system and presented in Table 2.3.2.

Figure 5.1.1 identifies the locations of the dose points referenced in the dose rate summary tables for the HI-STORM FW overpack. Dose Point #2 is located on the side of the cask at the axial mid-height. Dose Points #1 and #3 are the locations of the inlet and outlet air ducts, respectively. The dose values reported for these locations (adjacent and 1 meter) were averaged over the duct opening. Dose Point #4 is the dose location on the overpack lid. The dose values reported at the locations shown on Figure 5.1.1 are averaged over a region that is approximately 1 foot in width.

Figure 5.1.2 identifies the location of the dose points for the HI-TRAC VW transfer cask. Dose Point Locations #1 and #3 are situated below and above the water jacket, respectively. Dose Point #4 is the dose location on the HI-TRAC VW lid and dose rates below the HI-TRAC VW are estimated with Dose Point #5. Dose Point Location #2 is situated on the side of the cask at the axial mid-height.

The total dose rates presented are presented for two cases: with and without BPRAs. The dose from the BPRAs was conservatively assumed to be the maximum calculated in Subsection 5.2.4.

Tables 5.1.1 and 5.1.2 provides dose rates adjacent to and one meter from the HI-TRAC VW during normal conditions for the MPC-37 and MPC-89. The dose rates listed in Table 5.1.1 correspond to the normal condition in which the MPC is dry and the HI-TRAC water jacket is filled with water.

Tables 5.1.5 and 5.1.6 provide the design basis dose rates adjacent to the HI-STORM FW overpack during normal conditions for the MPC-37 and MPC-89. Tables 5.1.7 and 5.1.8 provide the design basis dose rates at one meter from the HI-STORM FW overpack containing the MPC-37 and MPC-89, respectively.

The dose to any real individual at or beyond the controlled area boundary is required to be below 25 mrem per year. The minimum distance to the controlled area boundary is 100 meters from the ISFSI. Table 5.1.3 presents the annual dose to an individual from a single HI-STORM FW cask and various storage cask arrays, assuming an 8760 hour annual occupancy at the dose point location. The minimum distance required for the corresponding dose is also listed. It is noted that these data are provided for illustrative purposes only. A detailed site-specific evaluation of dose at the controlled area boundary must be performed for each ISFSI in accordance with 10CFR72.212. The site-specific evaluation will consider dose from other portions of the facility and will consider the actual conditions of the fuel being stored (burnup and cooling time).

Figure 5.1.3 is an annual dose versus distance graph for the HI-STORM FW cask array configurations provided in Table 5.1.3. This curve, which is based on an 8760 hour occupancy, is provided for illustrative purposes only and will be re-evaluated on a site-specific basis.

Subsection 5.2.3 discusses the BPRAs, TPDs, CRAs and APSRs that are permitted for storage in the HI-STORM FW system. Subsection 5.4.4 discusses the increase in dose rate as a result of adding non-fuel hardware in the MPCs.

The analyses summarized in this section demonstrate that the HI-STORM FW system is in compliance with the radiation and exposure objectives of 10CFR72.106. Since only representative dose rate values for normal conditions are presented in this chapter, compliance with 10CFR72.104 is not being evaluated. This will be performed as part of the site specific evaluations.

5.1.2 Accident Conditions

The 10CFR72.106 radiation dose limits at the controlled area boundary for design basis accidents are:

> Any individual located on or beyond the nearest boundary of the controlled area may not receive from any design basis accident the more limiting of a total effective dose equivalent of 5 Rem, or the sum of the deep-dose equivalent and the committed dose equivalent to any individual organ or tissue (other than the lens of the eye) of 50 Rem. The lens dose equivalent shall not exceed 15 Rem and the shallow dose equivalent to skin or to any extremity shall not exceed 50 Rem. The minimum distance from the spent fuel or high-level radioactive waste handling and storage facilities to the nearest boundary of the controlled area shall be at least 100 meters.

Structural evaluations, presented in Chapter 3, shows that a freestanding HI-STORM FW storage overpack containing a loaded MPC remains standing during events that could potentially lead to a tip-over event. Therefore, the tip-over accident is not considered as part of the shielding evaluation.

Design basis accidents which may affect the HI-STORM FW overpack can result in limited and localized damage to the outer shell and radial concrete shield. As the damage is localized and the vast majority of the shielding material remains intact, the effect on the dose at the site boundary is negligible. Therefore, the site boundary doses for the loaded HI-STORM FW overpack for accident conditions are equivalent to the normal condition doses, which meet the 10CFR72.106 radiation dose limits. However the adjacent and one meter dose rates may be increased, which should be considered in any post-accident activities near the affected cask.

The design basis accidents analyzed in Chapter 11 have one bounding consequence that affects the shielding materials of the HI-TRAC transfer cask. It is the potential for damage to the water jacket shell and the loss of the neutron shield (water). In the accident consequence analysis, it is conservatively assumed that the neutron shield (water) is completely lost and replaced by a void.

Throughout all design basis accident conditions the axial location of the fuel will remain fixed within the MPC because of the MPC's design features (see Chapter 1). Further, the structural evaluation of the HI-TRAC VW in Chapter 3 shows that the inner shell, lead, and outer shell remain intact throughout all design basis accident conditions. Localized damage of the HI-TRAC outer shell is possible; however, localized deformations will have only a negligible impact on the dose rate at the boundary of the controlled area.

The complete loss of the HI-TRAC neutron shield significantly affects the dose at mid-height (Dose Point #2) adjacent to the HI-TRAC. Loss of the neutron shield has a small effect on the dose at the other dose points. To illustrate the impact of the design basis accident, the dose rates at Dose Point #2 (see Figure 5.1.2) are provided in Table 5.1.4 (MPC-37) for the HI-TRAC VW at a distance of 1 meter and at a distance of 100 meters. The normal condition dose rates are provided for reference. The dose for a period of 30 days is shown in Table 5.1.9, where 30 days is used to illustrate the radiological impact for a design basis accident. Based on this dose rate and the short duration of use for the loaded HI-TRAC transfer cask, it is evident that the dose as a result of the design basis accident cannot exceed 5 rem at the controlled area boundary for the short duration of the accident.

Analyses summarized in this section demonstrate that the HI-STORM FW system, including the HI-TRAC VW transfer cask, is in compliance with the 10CFR72.106 limits.

Table 5.1.1

DOSE RATES FROM THE HI-TRAC VW FOR NORMAL CONDITIONS
MPC-37 DESIGN BASIS FUEL
45,000 MWD/MTU AND 4.5-YEAR COOLING

Dose Point Location	Fuel Gammas (mrem/hr)	(n,γ) Gammas (mrem/hr)	^{60}Co Gammas (mrem/hr)	Neutrons (mrem/hr)	Totals (mrem/hr)	Totals with BPRAs (mrem/hr)
ADJACENT TO THE HI-TRAC VW						
1	975	25	808	67	1874	1874
2	2939	75	<1	154	3169	3169
3	20	5	339	6	371	561
4	98	1	530	225	854	1147
5	940	3	2074	1022	4038	4038
ONE METER FROM THE HI-TRAC VW						
1	695	12	99	30	835	835
2	1382	22	10	58	1472	1474
3	268	6	142	9	425	501
4	80	<1	295	73	449	613
5	470	1	1129	297	1897	1897

Notes:

- Refer to Figure 5.1.2 for dose locations.
- Values are rounded to nearest integer.
- Dose rates are based on no water within the MPC, an empty annulus, and a water jacket full of water. For the majority of the duration that the HI-TRAC bottom lid is installed, the MPC cavity will be flooded with water. The water within the MPC greatly reduces the dose rate.
- Streaming may occur through the annulus. However, during handling/operations the annulus is filled with water and lead snakes are typically present to reduce the streaming effects. Further, operators are not present on top of the transfer cask.
- The "Fuel Gammas" category includes gammas from the spent fuel, ^{60}Co from the spacer grids, and ^{60}Co from the BPRAs in the active fuel region.

Table 5.1.2

DOSE RATES FROM THE HI-TRAC VW FOR NORMAL CONDITIONS
MPC-89 DESIGN BASIS FUEL
45,000 MWD/MTU AND 5-YEAR COOLING

Dose Point Location	Fuel Gammas (mrem/hr)	(n,γ) Gammas (mrem/hr)	^{60}Co Gammas (mrem/hr)	Neutrons (mrem/hr)	Totals (mrem/hr)
ADJACENT TO THE HI-TRAC VW					
1	244	18	2247	40	2549
2	2466	107	<1	219	2793
3	3	3	581	4	591
4	25	<1	505	138	669
5	132	2	2135	720	2989
ONE METER FROM THE HI-TRAC VW					
1	411	13	291	29	744
2	1142	30	21	74	1267
3	119	5	280	8	412
4	16	<1	300	43	360
5	79	<1	1202	202	1484

Notes:

- Refer to Figure 5.1.2 for dose locations.
- Values are rounded to nearest integer.
- Dose rates are based on no water within the MPC, an empty annulus, and a water jacket full of water. For the majority of the duration that the HI-TRAC bottom lid is installed, the MPC cavity will be flooded with water. The water within the MPC greatly reduces the dose rate.
- Streaming may occur through the annulus. However, during handling/operations the annulus is filled with water and lead snakes are typically present to reduce the streaming effects. Further, operators are not present on top of the transfer cask.
- The "Fuel Gammas" category includes gammas from the spent fuel and ^{60}Co from the spacer grids.

Table 5.1.3

DOSE RATES FOR ARRAYS OF HI-STORM FWs with MPC-37

Array Configuration	1 cask	2x2	2x3	2x4	2x5
HI-STORM FW Overpack					
45,000 MWD/MTU AND 4.5-YEAR COOLING					
Annual Dose (mrem/year)	18	15	23	11	14
Distance to Controlled Area Boundary (meters)	300	400	400	500	500

Notes:

- Values are rounded to nearest integer.
- 8760 hour annual occupancy is assumed.
- Dose location is at the center of the long side of the array.

Table 5.1.4

DOSE RATES FROM HI-TRAC VW WITH MPC-37
FOR ACCIDENT CONDITIONS
AT BOUNDING BURNUP AND COOLING TIMES

Dose Point Location	Fuel Gammas (mrem/hr)	(n,γ) Gammas (mrem/hr)	^{60}Co Gammas (mrem/hr)	Neutrons (mrem/hr)	Totals (mrem/hr)	Totals with BPRAs (mrem/hr)
ONE METER FROM HI-TRAC VW						
65,000 MWD/MTU AND 8-YEAR COOLING						
2 (Accident Condition)	1735	3	13	2651	4403	4407
2 (Normal Condition)	893	50	7	122	1071	1074
100 METERS FROM HI-TRAC VW						
65,000 MWD/MTU AND 8-YEAR COOLING						
2 (Accident Condition)	0.7	<0.1	0.1	1.4	2.3	2.4

Notes:

- Refer to Figure 5.1.2 for dose locations.
- Values are rounded to nearest integer where appropriate.
- The "Fuel Gammas" category includes gammas from the spent fuel, ^{60}Co from the spacer grids, and ^{60}Co from the BPRAs in the active fuel region.

Table 5.1.5

DOSE RATES ADJACENT TO HI-STORM FW OVERPACK
FOR NORMAL CONDITIONS
MPC-37
BURNUP AND COOLING TIME
45,000 MWD/MTU AND 4.5-YEAR COOLING

Dose Point Location	Fuel Gammas (mrem/hr)	(n,γ) Gammas (mrem/hr)	^{60}Co Gammas (mrem/hr)	Neutrons (mrem/hr)	Totals (mrem/hr)	Totals with BPRAs (mrem/hr)
1	273	2	14	4	292	292
2	135	1	<1	1	141	141
3 (surface)	11	1	25	2	39	53
3 (overpack edge)	13	<1	63	1	78	113
4 (center)	<1	1	<1	<1	<4	<4
4 (mid)	1	1	4	1	7	10
4 (outer)	10	<1	30	<1	42	59

Notes:

- Refer to Figure 5.1.1 for dose locations.
- Values are rounded to nearest integer where appropriate.
- Dose location 3 (surface) is at the surface of the outlet vent. Dose location 3 (overpack edge) is in front of the outlet vent, but located radially above the overpack outer diameter.
- Dose location 4 (center) is at the center of the top surface of the top lid. Dose location 4 (mid) is situated directly above the vertical section of the outlet vent. Dose location 4 (outer) is extended along the top plane of the top lid, located radially above the overpack outer diameter.
- The "Fuel Gammas" category includes gammas from the spent fuel, ^{60}Co from the spacer grids, and ^{60}Co from the BPRAs in the active fuel region.

Table 5.1.6

DOSE RATES ADJACENT TO HI-STORM FW OVERPACK
FOR NORMAL CONDITIONS
MPC-89
BURNUP AND COOLING TIME
45,000 MWD/MTU AND 5-YEAR COOLING

Dose Point Location	Fuel Gammas (mrem/hr)	(n,γ) Gammas (mrem/hr)	^{60}Co Gammas (mrem/hr)	Neutrons (mrem/hr)	Totals (mrem/hr)
1	172	2	31	3	208
2	92	2	<1	1	96
3 (surface)	3	<1	29	2	35
3 (overpack edge)	5	<1	69	<1	76
4 (center)	0.1	0.4	0.4	0.1	1
4 (mid)	0.2	0.5	4.3	0.5	6
4 (outer)	2	<1	33	<1	37

Notes:

- Refer to Figure 5.1.1 for dose locations.
- Values are rounded to nearest integer where appropriate.
- Dose location 3 (surface) is at the surface of the outlet vent. Dose location 3 (overpack edge) is in front of the outlet vent, but located radially above the overpack outer diameter.
- Dose location 4 (center) is at the center of the top surface of the top lid. Dose location 4 (mid) is situated directly above the vertical section of the outlet vent. Dose location 4 (outer) is extended along the top plane of the top lid, located radially above the overpack outer diameter.
- The "Fuel Gammas" category includes gammas from the spent fuel and ^{60}Co from the spacer grids.

Table 5.1.7

DOSE RATES AT ONE METER FROM HI-STORM FW OVERPACK
FOR NORMAL CONDITIONS
MPC-37
BURNUP AND COOLING TIME
45,000 MWD/MTU AND 4.5-YEAR COOLING

Dose Point Location	Fuel Gammas (mrem/hr)	(n,γ) Gammas (mrem/hr)	^{60}Co Gammas (mrem/hr)	Neutrons (mrem/hr)	Totals (mrem/hr)	Totals with BPRAs (mrem/hr)
1	57	1	4	1	62	62
2	75	1	1	1	77	78
3	6	<1	5	<1	13	15
4 (center)	0.6	0.3	1.0	0.2	2.1	2.7

Notes:

- Refer to Figure 5.1.1 for dose locations.
- Values are rounded to nearest integer where appropriate.
- The "Fuel Gammas" category includes gammas from the spent fuel, ^{60}Co from the spacer grids, and ^{60}Co from the BPRAs in the active fuel region.

Table 5.1.8

DOSE RATES AT ONE METER FROM HI-STORM FW OVERPACK
FOR NORMAL CONDITIONS
MPC-89
BURNUP AND COOLING TIME
45,000 MWD/MTU AND 5-YEAR COOLING

Dose Point Location	Fuel Gammas (mrem/hr)	(n,γ) Gammas (mrem/hr)	^{60}Co Gammas (mrem/hr)	Neutrons (mrem/hr)	Totals (mrem/hr)
1	38	<1	7	<1	47
2	47	<1	<1	<1	50
3	3	<1	5	<1	10
4 (center)	0.2	0.2	1	0.1	2

Notes:

- Refer to Figure 5.1.1 for dose locations.
- Values are rounded to nearest integer where appropriate.
- The "Fuel Gammas" category includes gammas from the spent fuel and ^{60}Co from the spacer girds.

Table 5.1.9

DOSE FROM HI-TRAC VW WITH MPC-37
FOR ACCIDENT CONDITIONS
AT 100 METERS
65,000 MWD/MTU AND 8-YEAR COOLING

Dose Point Location	**Dose Rate (rem/hr)**	**Accident Duration (days)**	**Total Dose (rem)**	**Regulatory Limit (rem)**	**Time to Reach Regulatory Limit (days)**
2 (Accident Condition)	2.3E-3	30	1.66	5	90

Notes:

- Refer to Figure 5.1.2 for dose locations.
- Values are rounded to nearest integer where appropriate.
- Dose rates used to evaluated " Total Dose (rem)" are from Table 5.1.4
- Regulatory Limit is from 10CFR72.106.

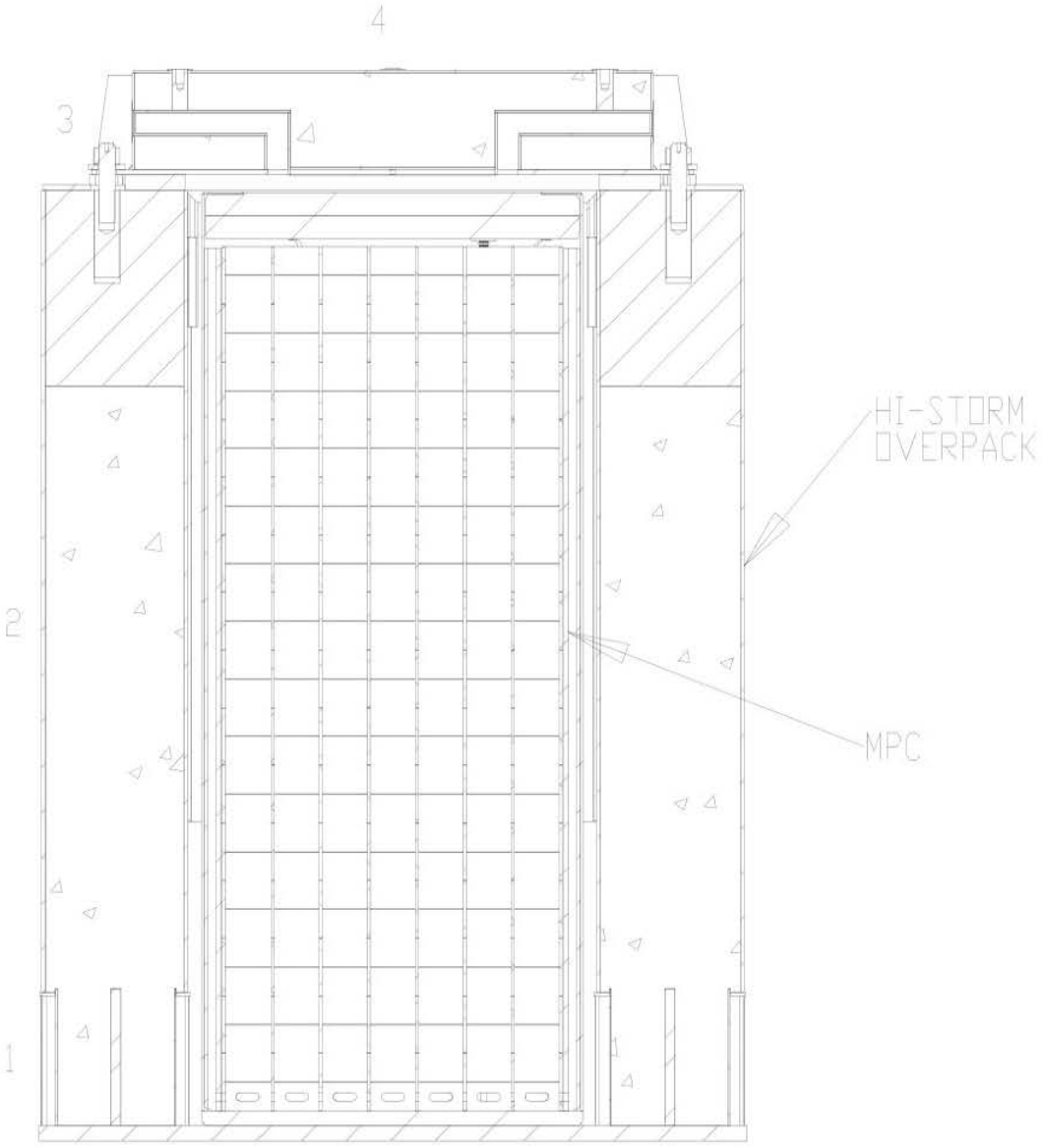

Figure 5.1.1

CROSS SECTION ELEVATION VIEW OF HI-STORM FW OVERPACK WITH DOSE POINT LOCATIONS

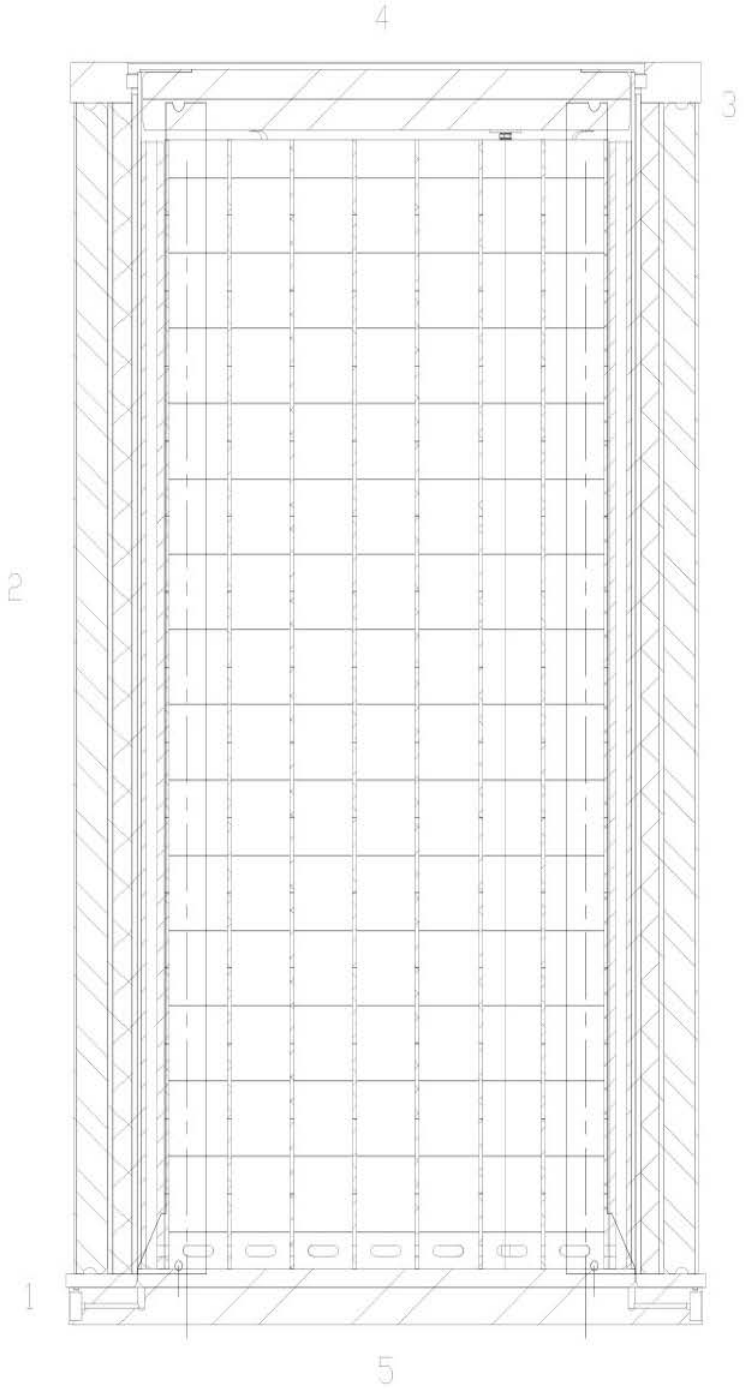

Figure 5.1.2
CROSS SECTION ELEVATION VIEW OF HI-TRAC VW TRANSFER CASK WITH DOSE POINT LOCATIONS

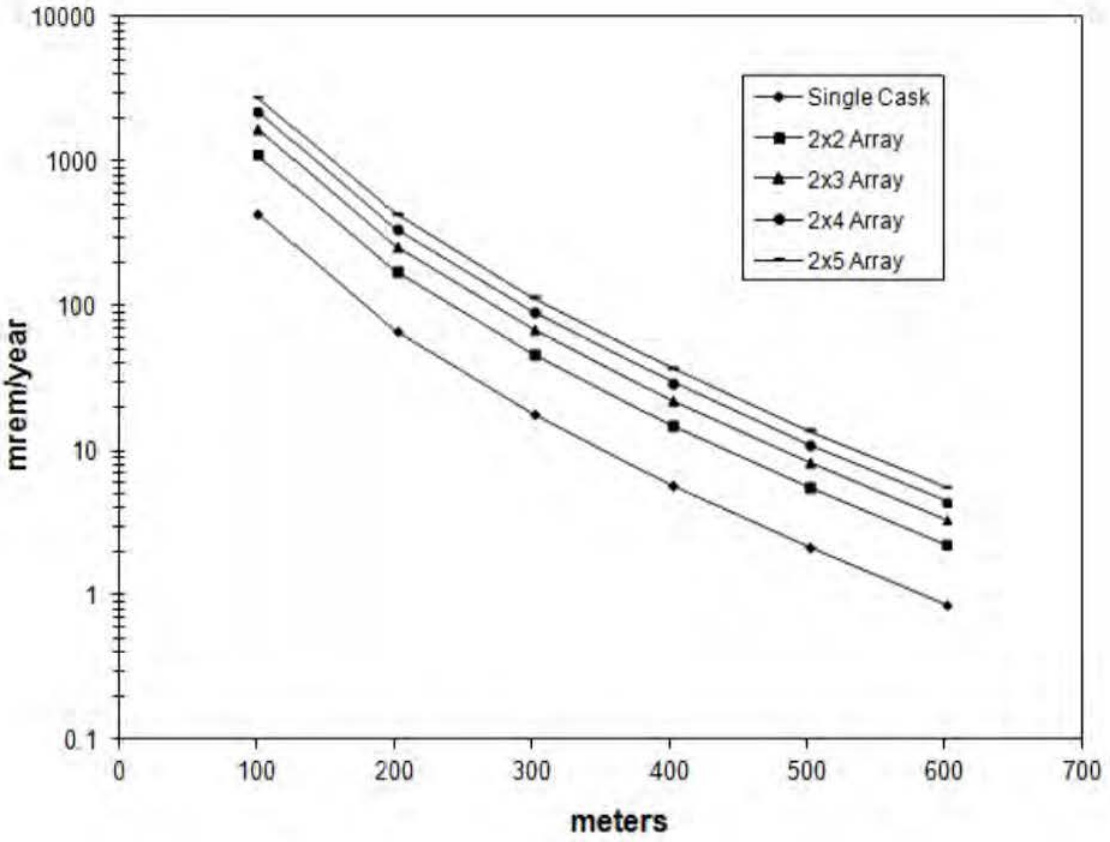

Figure 5.1.3

ANNUAL DOSE VERSUS DISTANCE FOR VARIOUS CONFIGURATIONS OF THE MPC-37 FOR 45,000 MWD/MTU AND 4.5 YEAR COOLING (8760 HOUR OCCUPANCY ASSUMED)

5.2 SOURCE SPECIFICATION

The neutron and gamma source terms, decay heat values, and quantities of radionuclides available for release were calculated with the SAS2H and ORIGEN-S modules of the SCALE 5 system [5.1.2, 5.1.3]. SAS2H has been extensively compared to experimental isotopic validations and decay heat measurements. References [5.2.8] through [5.2.12] and [5.2.15] present isotopic comparisons for PWR and BWR fuels for burnups ranging to 47 GWD/MTU and reference [5.2.13] presents results for BWR measurements to a burnup of 57 GWD/MTU. A comparison of calculated and measured decays heats is presented in reference [5.2.14]. All of these studies indicate good agreement between SAS2H and measured data. Additional comparisons of calculated values and measured data are being performed by various institutions for high burnup PWR and BWR fuel. These new results, when published, are expected to further confirm the validity of SAS2H for the analysis of PWR and BWR fuel.

Sample input files for SAS2H and ORIGEN-S are provided in Appendix 5.A. The gamma source term is actually comprised of three distinct sources. The first is a gamma source term from the active fuel region due to decay of fission products. The second source term is from ^{60}Co activity of the stainless steel structural material in the fuel element above and below the active fuel region. The third source is from (n,γ) reactions described below.

A description of the design basis fuel for the source term calculations is provided in Table 5.2.1. Subsection 5.2.5 discusses, in detail, the determination of the design basis fuel assemblies.

In performing the SAS2H and ORIGEN-S calculations, a single full power cycle was used to achieve the desired burnup. This assumption, in conjunction with the above-average specific powers listed in Table 5.2.1 resulted in conservative source term calculations.

5.2.1 Gamma Source

Tables 5.2.2 through 5.2.5 provide the gamma source in MeV/s and photons/s as calculated with SAS2H and ORIGEN-S for the design basis zircaloy clad fuel at the burnups and cooling times used for normal and accident conditions.

Previous analyses were performed for the HI-STORM 100 system to determine the dose contribution from gammas as a function of energy [5.2.17]. The results of these analyses have revealed that, due to the magnitude of the gamma source at lower energies, photons with energies as low as 0.45 MeV must be included in the shielding analysis, but photons with energies below 0.45 MeV are too weak to penetrate the HI-STORM overpack or HI-TRAC. The effect of gammas with energies above 3.0 MeV, on the other hand, was found to be insignificant. This is due to the fact that the source of gammas in this range (i.e., above 3.0 MeV) is extremely low. Therefore, all photons with energies in the range of 0.45 to 3.0 MeV are included in the shielding calculations.

The primary source of activity in the non-fuel regions of an assembly arises from the activation of ^{59}Co to ^{60}Co. The primary source of ^{59}Co in a fuel assembly is impurities in the steel structural material above and below the fuel. The zircaloy in these regions is neglected since it does not have a significant ^{59}Co impurity level. Reference [5.2.2] indicates that the impurity level in steel is 800 ppm or 0.8 gm/kg. Therefore, inconel and stainless steel in the non-fuel regions are both assumed to have the same 0.8 gm/kg impurity level.

Some of the PWR fuel assembly designs (B&W and WE 15x15) utilized inconel in-core grid spacers while other PWR fuel designs use zircaloy in-core grid spacers. In the mid 1980s, the fuel assembly designs using inconel in-core grid spacers were altered to use zircaloy in-core grid spacers. Since both designs may be loaded into the HI-STORM FW system, the gamma source for the PWR zircaloy clad fuel assembly includes the activation of the in-core grid spacers. Although BWR assembly grid spacers are zircaloy, some assembly designs have inconel springs in conjunction with the grid spacers. The gamma source for the BWR zircaloy clad fuel assembly includes the activation of these springs associated with the grid spacers.

The non-fuel data listed in Table 5.2.1 were taken from References [5.2.2], [5.2.4], and [5.2.5]. As stated above, a Cobalt-59 impurity level of 0.8 gm/kg was used for both inconel and stainless steel. Therefore, there is little distinction between stainless steel and inconel in the source term generation and since the shielding characteristics are similar, stainless steel was used in the MCNP calculations instead of inconel. The BWR masses for an 8x8 fuel assembly were used. These masses are also appropriate for the 10x10 assembly since the masses of the non-fuel hardware from a 10x10 and an 8x8 are approximately the same. The masses listed are those of the steel components. The zircaloy in these regions was not included because zircaloy does not produce significant activation.

The masses in Table 5.2.1 were used to calculate a ^{59}Co impurity level in the fuel assembly material. The grams of impurity were then used in ORIGEN-S to calculate a ^{60}Co activity level for the desired burnup and decay time. The methodology used to determine the activation level was developed from Reference [5.2.3] and is described here.

1. The activity of the ^{60}Co is calculated using ORIGEN-S. The flux used in the calculation was the in-core fuel region flux at full power.

2. The activity calculated in Step 1 for the region of interest was modified by the appropriate scaling factors listed in Table 5.2.6. These scaling factors were taken from Reference [5.2.3].

Tables 5.2.7 through 5.2.10 provide the ^{60}Co activity utilized in the shielding calculations for normal and accident conditions for the non-fuel regions of the assemblies in the MPC-37 and the MPC-89.

In addition to the two sources already mentioned, a third source arises from (n,γ) reactions in the material of the MPC and the overpack. This source of photons is properly accounted for in

MCNP when a neutron calculation is performed in a coupled neutron-gamma mode.

5.2.2 Neutron Source

It is well known that the neutron source strength increases as enrichment decreases, for a constant burnup and decay time. This is due to the increase in Pu content in the fuel, which increases the inventory of other transuranium nuclides such as Cm. The gamma source also varies with enrichment, although only slightly. Because of this effect and in order to obtain conservative source terms, low initial fuel enrichments of 3.2 and 3.6 wt% were chosen for the BWR and PWR design basis fuel assemblies under normal conditions, respectively. For the accident conditions, a fuel enrichment of 4.8 wt% was chosen to accommodate the higher burnups of the selected source terms (see Table 5.0.2) in accordance with Table 5.2.24 of reference [5.2.17].

The neutron source calculated for the design basis fuel assemblies for the MPCs and the design basis fuel are listed in Tables 5.2.11 through 5.2.14 in neutrons/s for the selected burnup and cooling times used in the shielding evaluations for normal and accident conditions. The neutron spectrum is generated in ORIGEN-S.

5.2.3 Non-Fuel Hardware

Burnable poison rod assemblies (BPRAs), thimble plug devices (TPDs), control rod assemblies (CRAs), and axial power shaping rods (APSRs) are permitted for storage in the HI-STORM FW system as an integral part of a PWR fuel assembly. BPRAs and TPDs may be stored in any fuel location while CRAs and APSRs are restricted as specified in Subsection 2.1.

5.2.3.1 BPRAs and TPDs

Burnable poison rod assemblies (BPRA) (including wet annular burnable absorbers) and thimble plug devices (TPD) (including orifice rod assemblies, guide tube plugs, and water displacement guide tube plugs) are an integral, yet removable, part of a large portion of PWR fuel. The TPDs are not used in all assemblies in a reactor core but are reused from cycle to cycle. Therefore, these devices can achieve very high burnups. In contrast, BPRAs are burned with a fuel assembly in core and are not reused. In fact, many BPRAs are removed after one or two cycles before the fuel assembly is discharged. Therefore, the achieved burnup for BPRAs is not significantly different from that of a fuel assembly. Vibration suppressor inserts are considered to be in the same category as BPRAs for the purposes of the analysis in this chapter since these devices have the same configuration (long non-absorbing thimbles which extend into the active fuel region) as a BPRA without the burnable poison.

TPDs are made of stainless steel and contain a small amount of inconel. These devices extend down into the plenum region of the fuel assembly but typically do not extend into the active fuel region. Since these devices are made of stainless steel, there is a significant amount of cobalt-60 produced during irradiation. This is the only significant radiation source from the activation of steel and inconel.

BPRAs are made of stainless steel in the region above the active fuel zone and may contain a small amount of inconel in this region. Within the active fuel zone the BPRAs may contain 2-24 rodlets which are burnable absorbers clad in either zircaloy or stainless steel. The stainless steel clad BPRAs create a significant radiation source (Co-60) while the zircaloy clad BPRAs create a negligible radiation source. Therefore, the stainless steel clad BPRAs are bounding.

SAS2H and ORIGEN-S were used to calculate a radiation source term for the TPDs and BPRAs. In the ORIGEN-S calculations the cobalt-59 impurity level was conservatively assumed to be 0.8 gm/kg for stainless steel and 4.7 gm/kg for inconel. These calculations were performed by irradiating the appropriate mass of steel and inconel using the flux calculated for the design basis W 17x17 fuel assembly. The mass of material in the regions above the active fuel zone was scaled by the appropriate scaling factors listed in Table 5.2.6 in order to account for the reduced flux levels above the fuel assembly. The total curies of cobalt were calculated for the TPDs and BPRAs as a function of burnup and cooling time.

Since the HI-STORM FW cask system is designed to store many varieties of PWR fuel, a representative TPD and BPRA had to be determined for the purposes of the analysis. This was accomplished in the HI-STORM 100 FSAR [5.2.17] by analyzing all of the BPRAs and TPDs (Westinghouse and B&W 14x14 through 17x17) found in references [5.2.5] and [5.2.7] to determine the TPD and BPRA which produced the highest Cobalt-60 source term and decay heat for a specific burnup and cooling time. The TPD was determined to be the Westinghouse 17x17 guide tube plug and the BPRA was actually determined by combining the higher masses of the Westinghouse 17x17 and 15x15 BPRAs into a single hypothetical BPRA. The masses of these devices are listed in Table 5.2.15.

Table 5.2.16 shows the curies of Co-60 that were calculated for BPRAs and TPDs in each region of the fuel assembly (e.g. incore, plenum, top). A burnup and cooling time, separate from the fuel assemblies, is used for BPRAs and TPDs. Table 2.1.25 of the HI-STORM 100 [5.2.17] lists the allowable burnups and cooling times for non-fuel hardware that corresponds to the BPRA. These burnup and cooling times assure that the Co-60 activity remains below the levels specified above. For specific site boundary evaluations, these levels/values can be used if they are bounding. Alternatively, more realistic values can be used.

The HI-STORM 100 [5.2.17] presents dose rates for both BPRAs and TPDs. The results indicate that BPRAs are bounding, therefore all dose rates in this chapter will contain a BPRA in every PWR fuel location. However, Section 5.4 also contains a quantitative dose rates comparison from BPRAs and TPDs to validate this approach. Subsection 5.4.4 discusses the increase in the cask dose rates due to the insertion of BPRAs into fuel assemblies.

5.2.3.2 CRAs and APSRs

Control rod assemblies (CRAs) (including control element assemblies and rod cluster control assemblies) and axial power shaping rod assemblies (APSRs) are an integral portion of a PWR

fuel assembly. These devices are utilized for many years (upwards of 20 years) prior to discharge into the spent fuel pool. The manner in which the CRAs are utilized vary from plant to plant. Some utilities maintain the CRAs fully withdrawn during normal operation while others may operate with a bank of rods partially inserted (approximately 10%) during normal operation. Even when fully withdrawn, the ends of the CRAs are present in the upper portion of the fuel assembly since they are never fully removed from the fuel assembly during operation. The result of the different operating styles is a variation in the source term for the CRAs. In all cases, however, only the lower portion of the CRAs will be significantly activated. Therefore, when the CRAs are stored with the PWR fuel assembly, the activated portion of the CRAs will be in the lower portion of the cask. CRAs are fabricated of various materials. The cladding is typically stainless steel, although inconel has been used. The absorber can be a single material or a combination of materials. AgInCd is possibly the most common absorber although B_4C in aluminum is used, and hafnium has also been used. AgInCd produces a noticeable source term in the 0.3-1.0 MeV range due to the activation of Ag. The source term from the other absorbers is negligible, therefore the AgInCd CRAs are the bounding CRAs.

APSRs are used to flatten the power distribution during normal operation and as a result these devices achieve a considerably higher activation than CRAs. There are two types of B&W stainless steel clad APSRs: gray and black. According to reference [5.2.5], the black APSRs have 36 inches of AgInCd as the absorber while the gray ones use 63 inches of inconel as the absorber. Because of the cobalt-60 source from the activation of inconel, the gray APSRs produce a higher source term than the black APSRs and therefore are the bounding APSR.

Since the level of activation of CRAs and APSRs can vary, the quantity that can be stored in an MPC is being limited. These devices are required to be stored in the locations as outlined in Subsection 2.1.

Subsection 5.4.4 discusses the effect on dose rate of the insertion of APSRs or CRAs into fuel assemblies.

5.2.4 Choice of Design Basis Assembly

The Westinghouse 17x17 and GE 10x10 assemblies were selected as design basis assemblies since they are widely used throughout the industry. Site specific shielding evaluations should verify that those assemblies and assembly parameters are appropriate for the site-specific analyses.

5.2.5 Decay Heat Loads and Allowable Burnup and Cooling Times

Subsection 2.1 describes the MPC maximum decay heat limits per assembly. The allowable burnup and cooling time limits are derived based on the allowable decay heat limits.

5.2.6 Fuel Assembly Neutron Sources

Neutron source assemblies (NSAs) are used in reactors for startup. There are different types of neutron sources (e.g. californium, americium-beryllium, plutonium-beryllium, polonium-beryllium, antimony-beryllium). These neutron sources are typically inserted into the water rod of a fuel assembly and are usually removable.

During in-core operations, the stainless steel and inconel portions of the NSAs become activated, producing a significant amount of Co-60. A detailed discussion about NSAs is provided in reference [5.2.17], where it is concluded that activation from NSAs are bounded by activation from BPRAs.

For ease of implementation in the CoC, the restriction concerning the number of NSAs is being applied to all types of NSAs. In addition, conservatively NSAs are required to be stored in the inner region of the MPC basket as specified in Subsection 2.1. Further limitations allow for only one NSA to be stored in the MPC-37 (see Table 2.1.1).

Table 5.2.1

DESCRIPTION OF DESIGN BASIS CLAD FUEL

	PWR	**BWR**
Assembly type/class	WE 17×17	GE 10×10
Active fuel length (in.)	144	144
No. of fuel rods	264	92
Rod pitch (in.)	0.496	0.51
Cladding material	Zircaloy-4	Zircaloy-2
Rod diameter (in.)	0.374	0.404
Cladding thickness (in.)	0.0225	0.026
Pellet diameter (in.)	0.3232	0.345
Pellet material	UO_2	UO_2
Pellet density (gm/cc)	10.412 (95% of theoretical)	10.522 (96% of theoretical)
Enrichment (w/o ^{235}U)	3.6	3.2
Specific power (MW/MTU)	43.48	30
Weight of UO_2 (kg)[††]	532.150	213.531
Weight of U (kg)[††]	469.144	188.249
No. of Water Rods/ Guide Tubes	25	2
Water Rod/ Guide Tube O.D. (in.)	0.474	0.98
Water Rod/ Guide Tube Thickness (in.)	0.016	0.03

[††] Derived from parameters in this table.

Table 5.2.1 (continued)

DESCRIPTION OF DESIGN BASIS FUEL

	PWR	**BWR**
Lower End Fitting (kg)	5.9 (steel)	4.8 (steel)
Gas Plenum Springs (kg)	1.150 (steel)	1.1 (steel)
Gas Plenum Spacer (kg)	0.793 (inconel) 0.841 (steel)	N/A
Expansion Springs (kg)	N/A	0.4 (steel)
Upper End Fitting (kg)	6.89 (steel) 0.96 (inconel)	2.0 (steel)
Handle (kg)	N/A	0.5 (steel)
Incore Grid Spacers (kg)	4.9 (inconel)	0.33 (inconel springs)

Table 5.2.2

CALCULATED MPC-37 PWR FUEL GAMMA SOURCE PER ASSEMBLY FOR DESIGN BASIS BURNUP AND COOLING TIME FOR NORMAL CONDITIONS

Lower Energy	**Upper Energy**	**45,000 MWD/MTU 4.5-Year Cooling**	
(MeV)	(MeV)	(MeV/s)	(Photons/s)
0.45	0.7	2.11E+15	3.68E+15
0.7	1.0	7.67E+14	9.02E+14
1.0	1.5	1.74E+14	1.39E+14
1.5	2.0	1.45E+13	8.30E+12
2.0	2.5	1.01E+13	4.47E+12
2.5	3.0	4.05E+11	1.47E+11
Total		3.08E+15	4.73E+15

Table 5.2.3

CALCULATED MPC-37 PWR FUEL GAMMA SOURCE PER ASSEMBLY FOR BURNUP AND COOLING TIME FOR ACCIDENT CONDITIONS

Lower Energy	**Upper Energy**	**65,000 MWD/MTU 8-Year Cooling**	
(MeV)	(MeV)	(MeV/s)	(Photons/s)
0.45	0.7	2.05E+15	3.56E+15
0.7	1.0	4.16E+14	4.89E+14
1.0	1.5	1.30E+14	1.04E+14
1.5	2.0	8.66E+12	4.95E+12
2.0	2.5	6.46E+11	2.87E+11
2.5	3.0	4.49E+10	1.63E+10
Total		2.60E+15	4.16E+15

Table 5.2.4

CALCULATED MPC-89 BWR FUEL GAMMA SOURCE PER ASSEMBLY FOR DESIGN BASIS BURNUP AND COOLING TIME FOR NORMAL CONDITIONS

Lower Energy	**Upper Energy**	**45,000 MWD/MTU 5-Year Cooling**	
(MeV)	(MeV)	(MeV/s)	(Photons/s)
0.45	0.7	7.52E+14	1.31E+15
0.7	1.0	2.40E+14	2.82E+14
1.0	1.5	5.53E+13	4.42E+13
1.5	2.0	4.15E+12	2.37E+12
2.0	2.5	2.02E+12	8.97E+11
2.5	3.0	9.74E+10	3.54E+10
Total		1.05E+15	2.04E+15

Table 5.2.5

CALCULATED MPC-89 BWR FUEL GAMMA SOURCE PER ASSEMBLY FOR BURNUP AND COOLING TIME FOR ACCIDENT CONDITIONS

Lower Energy	**Upper Energy**	**65,000 MWD/MTU 10-Year Cooling**	
(MeV)	(MeV)	(MeV/s)	(Photons/s)
0.45	0.7	6.98E+14	1.21E+15
0.7	1.0	8.37E+13	9.85E+13
1.0	1.5	3.50E+13	2.80E+13
1.5	2.0	2.52E+12	1.44E+12
2.0	2.5	4.49E+10	2.00E+10
2.5	3.0	3.90E+09	1.42E+09
Total		8.19E+14	1.34E+15

Table 5.2.6

SCALING FACTORS USED IN CALCULATING THE ^{60}Co SOURCE

Region	PWR	BWR
Handle	N/A	0.05
Upper End Fitting	0.1	0.1
Gas Plenum Spacer	0.1	N/A
Expansion Springs	N/A	0.1
Gas Plenum Springs	0.2	0.2
Incore Grid Spacer	1.0	1.0
Lower End Fitting	0.2	0.15

Table 5.2.7

CALCULATED MPC-37 ^{60}Co SOURCE PER ASSEMBLY FOR DESIGN BASIS FUEL AT DESIGN BASIS BURNUP AND COOLING TIME FOR NORMAL CONDITIONS

Location	**45,000 MWD/MTU and 4.5-Year Cooling (curies)**
Lower End Fitting	86.02
Gas Plenum Springs	16.77
Gas Plenum Spacer	11.91
Expansion Springs	NA
Incore Grid Spacers	357.19
Upper End Fitting	57.22
Handle	NA

Table 5.2.8

CALCULATED MPC-37 ^{60}Co SOURCE PER ASSEMBLY FOR DESIGN BASIS FUEL AT BURNUP AND COOLING TIME FOR ACCIDENT CONDITIONS

Location	**65,000 MWD/MTU and 8-Year Cooling (curies)**
Lower End Fitting	64.89
Gas Plenum Springs	12.65
Gas Plenum Spacer	8.99
Expansion Springs	NA
Incore Grid Spacers	269.46
Upper End Fitting	43.17
Handle	NA

Table 5.2.9

CALCULATED MPC-89 ^{60}Co SOURCE PER ASSEMBLY FOR DESIGN BASIS FUEL AT DESIGN BASIS BURNUP AND COOLING TIME FOR NORMAL CONDITIONS

Location	**45,000 MWD/MTU and 5-Year Cooling (curies)**
Lower End Fitting	158.66
Gas Plenum Springs	48.48
Gas Plenum Spacer	N/A
Expansion Springs	8.81
Grid Spacer Springs	72.72
Upper End Fitting	44.07
Handle	5.51

Table 5.2.10

CALCULATED MPC-89 ^{60}Co SOURCE PER ASSEMBLY FOR DESIGN BASIS FUEL AT BURNUP AND COOLING TIME FOR ACCIDENT CONDITIONS

Location	**65,000 MWD/MTU and 10-Year Cooling (curies)**
Lower End Fitting	90.17
Gas Plenum Springs	27.55
Gas Plenum Spacer	N/A
Expansion Springs	5.01
Grid Spacer Springs	41.33
Upper End Fitting	25.05
Handle	3.13

Table 5.2.11

CALCULATED MPC-37 PWR NEUTRON SOURCE PER ASSEMBLY
FOR 45,000 MWD/MTU BURNUP AND 4.5 YEAR COOLING

Lower Energy (MeV)	**Upper Energy (MeV)**	**45,000 MWD/MTU 4.5-Year Cooling (Neutrons/s)**
1.0e-01	4.0e-01	3.05E+07
4.0e-01	9.0e-01	6.64E+07
9.0e-01	1.4	6.63E+07
1.4	1.85	5.30E+07
1.85	3.0	9.88E+07
3.0	6.43	8.97E+07
6.43	20.0	8.56E+06
Totals		4.13E+08

Table 5.2.12

CALCULATED MPC-37 PWR NEUTRON SOURCE PER ASSEMBLY
FOR 65,000 MWD/MTU BURNUP AND 8 YEAR COOLING

Lower Energy (MeV)	**Upper Energy (MeV)**	**65,000 MWD/MTU 8-Year Cooling (Neutrons/s)**
1.0e-01	4.0e-01	6.80E+07
4.0e-01	9.0e-01	1.48E+08
9.0e-01	1.4	1.47E+08
1.4	1.85	1.17E+08
1.85	3.0	2.18E+08
3.0	6.43	1.98E+08
6.43	20.0	1.89E+07
Totals		9.16E+08

Table 5.2.13

CALCULATED MPC-89 BWR NEUTRON SOURCE
PER ASSEMBLY
FOR DESIGN BASIS FUEL
FOR 45,000 MWD/MTU BURNUP AND 5 YEAR COOLING

Lower Energy (MeV)	**Upper Energy (MeV)**	**45,000 MWD/MTU 5-Year Cooling (Neutrons/s)**
1.0e-01	4.0e-01	1.37E+07
4.0e-01	9.0e-01	2.99E+07
9.0e-01	1.4	2.99E+07
1.4	1.85	2.38E+07
1.85	3.0	4.44E+07
3.0	6.43	4.03E+07
6.43	20.0	3.86E+06
Totals		1.86E+08

Table 5.2.14

CALCULATED MPC-89 BWR NEUTRON SOURCE
PER ASSEMBLY
FOR DESIGN BASIS FUEL
FOR 65,000 MWD/MTU BURNUP AND 10 YEAR COOLING

Lower Energy (MeV)	**Upper Energy (MeV)**	**65,000 MWD/MTU 10-Year Cooling (Neutrons/s)**
1.0e-01	4.0e-01	2.40E+07
4.0e-01	9.0e-01	5.22E+07
9.0e-01	1.4	5.20E+07
1.4	1.85	4.15E+07
1.85	3.0	7.71E+07
3.0	6.43	7.00E+07
6.43	20.0	6.68E+06
Totals		3.24E+08

Table 5.2.15
DESCRIPTION OF DESIGN BASIS BURNABLE POISON ROD ASSEMBLY AND THIMBLE PLUG DEVICE

Region	**BPRA**	**TPD**
Upper End Fitting (kg of steel)	2.62	2.3
Upper End Fitting (kg of inconel)	0.42	0.42
Gas Plenum Spacer (kg of steel)	0.77488	1.71008
Gas Plenum Springs (kg of steel)	0.67512	1.48992
In-core (kg of steel)	13.2	N/A

Table 5.2.16
DESIGN BASIS COBALT-60 ACTIVITIES FOR BURNABLE POISON ROD
ASSEMBLIES AND THIMBLE PLUG DEVICES

Region	**BPRA**	**TPD**
Upper End Fitting (curies Co-60)	32.7	25.21
Gas Plenum Spacer (curies Co-60)	5.0	9.04
Gas Plenum Springs (curies Co-60)	8.9	15.75
In-core (curies Co-60)	848.4	N/A

5.3 MODEL SPECIFICATIONS

The shielding analysis of the HI-STORM FW system was performed with MCNP5 [5.1.1]. MCNP is a Monte Carlo transport code that offers a full three-dimensional combinatorial geometry modeling capability including such complex surfaces as cones and tori. This means that no gross approximations were required to represent the HI-STORM FW system, including the HI-TRAC transfer casks, in the shielding analysis. A sample input file for MCNP is provided in Appendix 5.A.

As discussed in Subsection 5.1.1, off-normal conditions do not have any implications for the shielding analysis. Therefore, the MCNP models and results developed for the normal conditions also represent the off-normal conditions. Subsection 5.1.2 discussed the accident conditions and stated that the only accident that would impact the shielding analysis would be a loss of the neutron shield (water) in the HI-TRAC. Therefore, the MCNP model of the normal HI-TRAC condition has the neutron shield in place while the accident condition replaces the neutron shield with void. Subsection 5.1.2 also mentioned that there is no credible accident scenario that would impact the HI-STORM shielding analysis. Therefore, models and results for the normal and accident conditions are identical for the HI-STORM overpack.

5.3.1 Description of the Radial and Axial Shielding Configuration

Chapter 1 provides the drawings that describe the HI-STORM FW system, including the HI-TRAC transfer cask. These drawings, using nominal dimensions, were used to create the MCNP models used in the radiation transport calculations. Modeling deviations from these drawings are discussed below. Figures 5.3.1 and 5.3.2, as well as Figures 5.3.12 and 5.3.13, show cross sectional views of the HI-STORM FW overpack, MPCs, and basket cells as they are modeled in MCNP. Figures 5.3.1 and 5.3.2 were created in VISED and are drawn to scale. The inlet and outlet vents were modeled explicitly, therefore, streaming through these components is accounted for in the calculations of the dose adjacent to the overpack and at 1 meter. Figures 5.3.3 and 5.3.4 show a cross sectional view of the HI-TRAC VW with the MPC-37 and MPC-89, respectively, as it was modeled in MCNP. These figures were created in VISED and are drawn to scale.

Figure 5.3.5 shows a cross sectional view of the HI-STORM FW overpack with the as-modeled thickness of the various materials.

Figure 5.3.6 shows the axial representation of the HI-STORM FW overpack with the various as-modeled dimensions indicated.

Figure 5.3.7 shows axial cross-sectional views of the HI-TRAC VW transfer casks with the as-modeled dimensions and materials specified. Figures 5.3.8 and 5.3.9 shows fully labeled radial cross-sectional view of the HI-TRAC VW transfer casks and each of the MPCs.

Calculations were performed for the HI-STORM 100 [5.2.17] to determine the acceptability of homogenizing the fuel assembly versus explicit modeling. Based on these calculations it was concluded that it is acceptable to homogenize the fuel assembly without loss of accuracy. The width of the PWR and BWR homogenized fuel assembly is equal to 17 times the pitch and 10 times the pitch, respectively. Homogenization results in a noticeable decrease in run time.

Several conservative approximations were made in modeling the MPC. The conservative approximations are listed below.

1. The fuel shims are not modeled because they are not needed on all fuel assembly types. However, most PWR fuel assemblies will have fuel shims. The fuel shim length for the design basis fuel assembly type determines the positioning of the fuel assembly for the shielding analysis. This is conservative since it removes steel that would provide a small amount of additional shielding.

2. The MPC basket supports are not modeled. This is conservative since it removes material that would provide a small increase in shielding.

The zircaloy flow channels are included in the modeling of the BWR assemblies. The expected impact of this assumption on the dose rates is insignificant. Additionally, site specific analysis should consider site specific fuel characteristics as applicable.

All dose calculations presented in this Chapter were performed with the standard lid design, shown in Figure 5.3.6. An additional lid design, the Version XL lid, with the increased height of the Version XL cask body has been developed for the HI-STORM FW system to further optimize the shielding performance of the system. With respect to shielding and dose rates, this design has the following characteristics that make it superior to the initial lid design:

- A larger diameter of the lid. This significantly reduces the dose rates directly outside of the outlet vents. This is important from an occupational dose perspective for the operational steps to install lid bolts connecting the lid to the cask body. Those bolts are located directly outside the outlet vents in the standard lid design shown in Figure 5.3.6. For the Version XL lid design, the bolts are on top of the lid.
- The Version XL lid contains an inner shield ring above the annulus, which reduces the radiation streaming up from the annulus quite substantially. Therefore, despite the fact that the lid is overall slightly thinner, the average dose rate across the top is lower than that for the standard lid.

Since the overall dose rates above the Version XL lid are bounded by those for the standard lid shown in Figure 5.3.6, no separate dose rates are reported for the Version XL lid and body design in this chapter. However for the site specific calculations that show compliance with the requirements in 10CFR72.104, this Version XL lid and body design should be considered in the analyses if it is used.

As discussed in Chapter 1, because of a thicker section of steel and concrete in the domed lid directly above the canister, the shielding performance of the domed lid against sky shine is substantially better than the Version XL lid. For the site specific calculations that show compliance with the requirements in 10CFR72.104, the domed lid and Version XL body design should be considered in the analysis if it is used.

5.3.1.1 Fuel Configuration

As described earlier, the active fuel region is modeled as a homogenous zone. The end fittings and the plenum regions are also modeled as homogenous regions of steel. The masses of steel used in these regions are shown in Table 5.2.1. The axial description of the design basis fuel assemblies is provided in Table 5.3.1. Figures 5.3.10 and 5.3.11 graphically depict the location of the PWR and BWR fuel assemblies within the HI-STORM FW system. The axial locations of the basket, inlet vents, and outlet vents are shown in these figures.

Intact fuel assemblies can be stored in damaged fuel containers (DFCs) in all 37 locations within MPC-37, if allowed by the certificate of compliance. The DFCs add additional shielding material and is therefore conservatively neglected in the shielding models.

5.3.1.2 Streaming Considerations

The MCNP model of the HI-STORM overpack completely describes the inlet and outlet vents, thereby properly accounting for their streaming effect. Further, the top lid is properly modeled with its reduced diameter, which accounts for higher localized dose rates on the top surface of the HI-STORM.

The MCNP model of the HI-TRAC transfer cask accounts for the fins through the HI-TRAC water jacket, as discussed in Subsection 5.4.1, as well as the open annulus.

5.3.2 Regional Densities

Composition and densities of the various materials used in the HI-STORM FW system and HI-TRAC shielding analyses are given in Table 5.3.2. All of the materials and their actual geometries are represented in the MCNP model.

The concrete density shown in Table 5.3.2 is the minimum concrete density analyzed in this chapter. The HI-STORM FW overpacks are designed in such a way that the concrete density in the body of the overpack can be increased to approximately 3.2 g/cm^3 (200 lb/cu-ft). Increasing the density beyond the value in Table 5.3.2 would result in a significant reduction in the dose rates. This may be beneficial based on on-site and off-site ALARA considerations.

The water density inside the MPC corresponds to the maximum allowable water temperature within the MPC. The water density in the water jacket corresponds to the maximum allowable temperature at the maximum allowable pressure. As mentioned, the HI-TRAC transfer cask may be equipped with a water jacket to provide radial neutron shielding. Demineralized water (borated water) will be utilized in the water jacket. To ensure operability for low temperature conditions, ethylene glycol (25% in solution) may be added to reduce the freezing point for low temperature operations. Calculations were performed for the HI-STORM 100 system [5.2.17] to determine the effect of the ethylene glycol on the shielding effectiveness of the radial neutron shield. Based on these calculations, it was concluded that the addition of ethylene glycol (25% in solution) does not reduce the shielding effectiveness of the radial neutron shield.

Subsections 4.4 and 4.5 demonstrate that all materials used in the HI-STORM and HI-TRAC remain below their design temperatures as specified in Table 2.2.3 during all normal conditions. Therefore, the shielding analysis does not address changes in the material density or composition as a result of temperature changes.

Chapter 11 discusses the effect of the various accident conditions on the temperatures of the shielding materials and the resultant impact on their shielding effectiveness. As stated in Subsection 5.1.2, there is only one accident that has any significant impact on the shielding configuration. This accident is the loss of the neutron shield (water) in the HI-TRAC as a result of fire or other damage. The change in the neutron shield was conservatively analyzed by assuming that the entire volume of the liquid neutron shield was replaced by void.

Table 5.3.1

DESCRIPTION OF THE AXIAL MCNP MODEL OF THE FUEL ASSEMBLIES[†]

Region	Start (in.)	Finish (in.)	Length (in.)	Actual Material	Modeled Material
PWR					
Lower End Fitting	0.0	2.738	2.738	SS304	SS304
Space	2.738	3.738	1.0	zircaloy	void
Fuel	3.738	147.738	144.0	fuel & zircaloy	fuel & zircaloy
Gas Plenum Springs	147.738	151.916	4.178	SS304 & inconel	SS304
Gas Plenum Spacer	151.916	156.095	4.179	SS304 & inconel	SS304
Upper End Fitting	156.095	159.765	3.670	SS304 & inconel	SS304
BWR					
Lower End Fitting	0.0	7.385	7.385	SS304	SS304
Fuel	7.385	151.385	144.0	fuel & zircaloy	fuel & zircaloy
Space	151.385	157.385	6.0	zircaloy	void
Gas Plenum Springs	157.385	166.865	9.48	SS304 & zircaloy	SS304
Expansion Springs	166.865	168.215	1.35	SS304	SS304
Upper End Fitting	168.215	171.555	3.34	SS304	SS304
Handle	171.555	176	4.445	SS304	SS304

[†] All dimensions start at the bottom of the fuel assembly. The length of the fuel shims must be added to the distances to determine the distance from the top of the MPC baseplate.

Table 5.3.2

COMPOSITION OF THE MATERIALS IN THE HI-STORM FW SYSTEM

Component	Density (g/cm³)	Elements	Mass Fraction (%)
Metamic-HT†	2.61 (9% B_4C)	(b)(4)	
SS304	7.94	Cr	19
		Mn	2
		Fe	69.5
		Ni	9.5
Carbon Steel	7.82	C	1.0
		Fe	99.0
Zircaloy	6.55	Zr	98.24
		Sn	1.45
		Fe	0.21
		Cr	0.10

† All B-10 loadings in the Metamic compositions are conservatively lower than the values defined in the Bill of Materials.

Table 5.3.2 (continued)

COMPOSITION OF THE MATERIALS IN THE HI-STORM FW SYSTEM

Component	Density (g/cm^3)	Elements	Mass Fraction (%)
BWR Fuel Region Mixture	4.781 (5.0 wt% U-235)	^{235}U	3.207
		^{238}U	60.935
		O	8.623
		Zr	26.752
		N	0.014
		Cr	0.027
		Fe	0.034
		Sn	0.409
PWR Fuel Region Mixture	3.769 (5.0 wt% U-235)	^{235}U	3.709
		^{238}U	70.474
		O	9.972
		Zr	15.565
		Cr	0.016
		Fe	0.033
		Sn	0.230

Table 5.3.2 (continued)

COMPOSITION OF THE MATERIALS IN THE HI-STORM FW SYSTEM

Component	Density (g/cm^3)	Elements	Mass Fraction (%)
Lower End Fitting (PWR)	1.849	SS304	100
Gas Plenum Springs (PWR)	0.23626	SS304	100
Gas Plenum Spacer (PWR)	0.33559	SS304	100
Upper End Fitting (PWR)	1.8359	SS304	100
Lower End Fitting (BWR)	1.5249	SS304	100
Gas Plenum Springs (BWR)	0.27223	SS304	100
Expansion Springs (BWR)	0.69514	SS304	100
Upper End Fitting (BWR)	1.4049	SS304	100
Handle (BWR)	0.26391	SS304	100
Lead	11.3	Pb	99.9
		Cu	0.08
		Ag	0.02
Water	0.919 (water jacket)	H	11.2
	0.958 (inside MPC)	O	88.8

Table 5.3.2 (continued)

COMPOSITION OF THE MATERIALS IN THE HI-STORM FW SYSTEM

Component	Density (g/cm^3)	Elements	Mass Fraction (%)
Water w/ 2000 ppm	0.958	B-10	0.036
		B-11	0.164
		H	11.17
		O	88.63
Concrete	2.4	H	1.0
		O	53.2
		Si	33.7
		Al	3.4
		Na	2.9
		Ca	4.4
		Fe	1.4

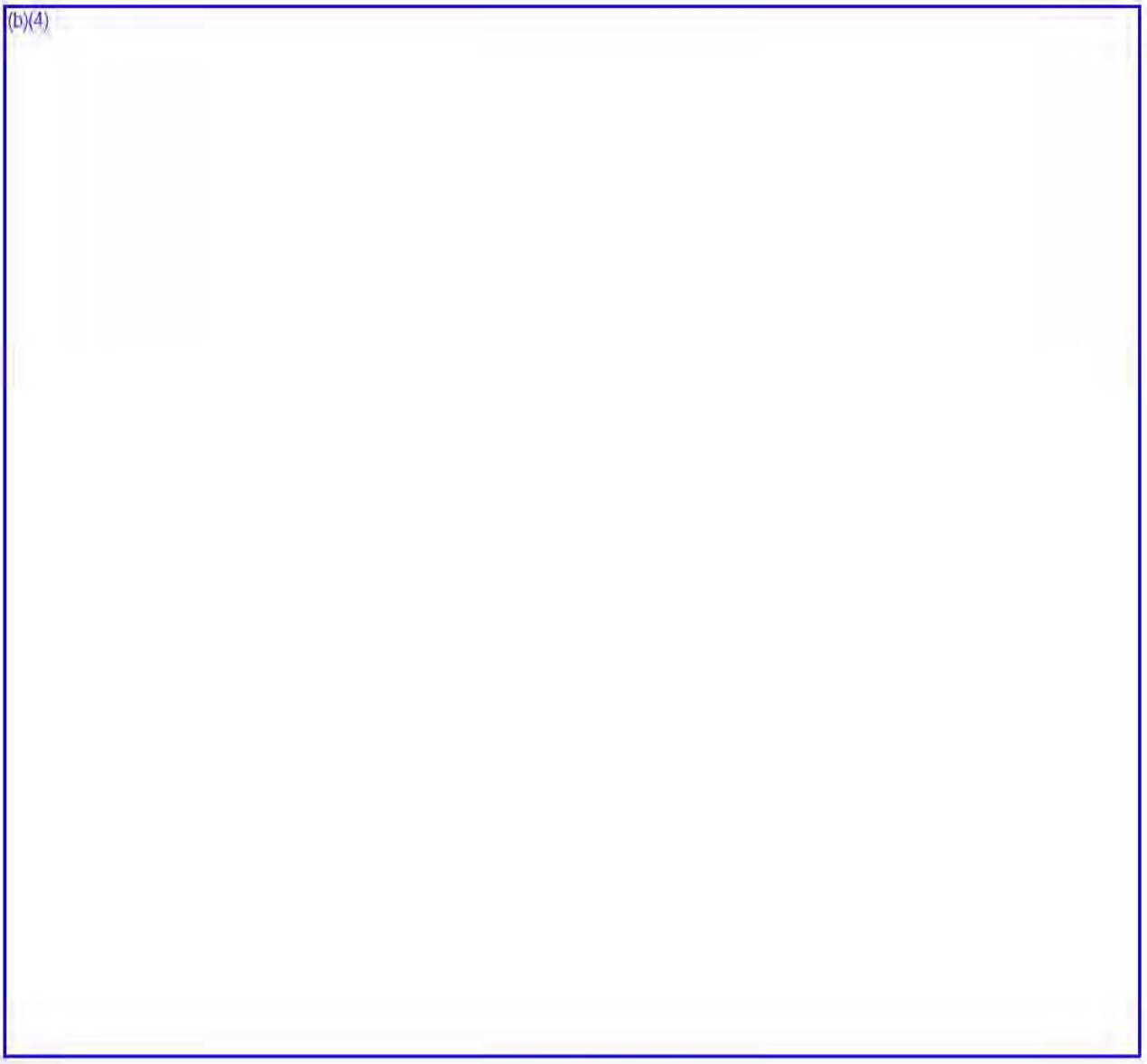

Figure 5.3.1
HI-STORM FW OVERPACK WITH MPC-37 CROSS SECTIONAL VIEW AS MODELED IN MCNP†

† This figure is drawn to scale using VISED.

Figure 5.3.2

HI-STORM FW OVERPACK WITH MPC-89 CROSS SECTIONAL VIEW AS MODELED IN MCNP†

† This figure is drawn to scale using VISED.

(b)(4)

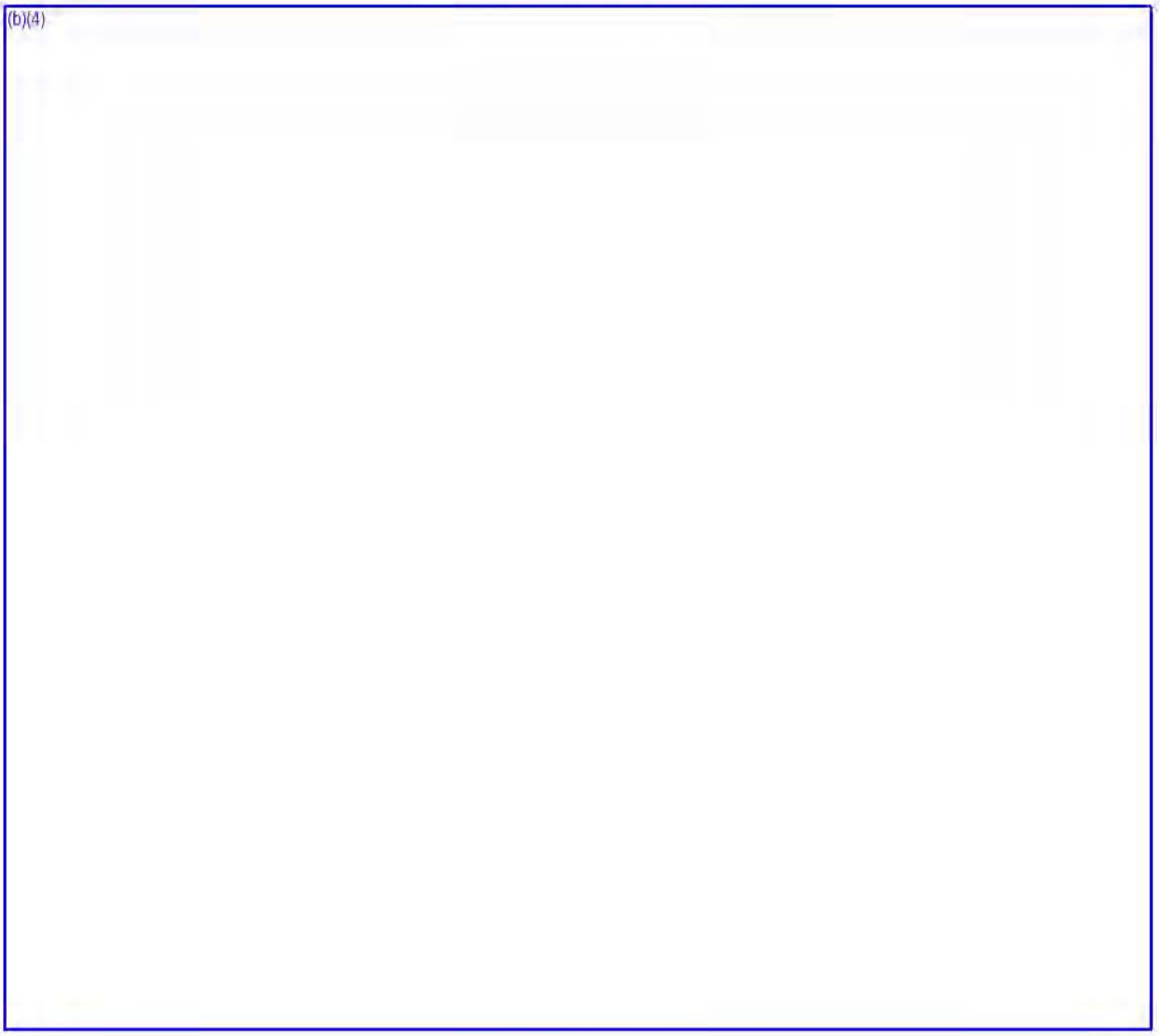

Figure 5.3.3

HI-TRAC VW OVERPACK WITH MPC-37 CROSS SECTIONAL VIEW AS MODELED IN MCNP†

† This figure is drawn to scale using VISED.

(b)(4)

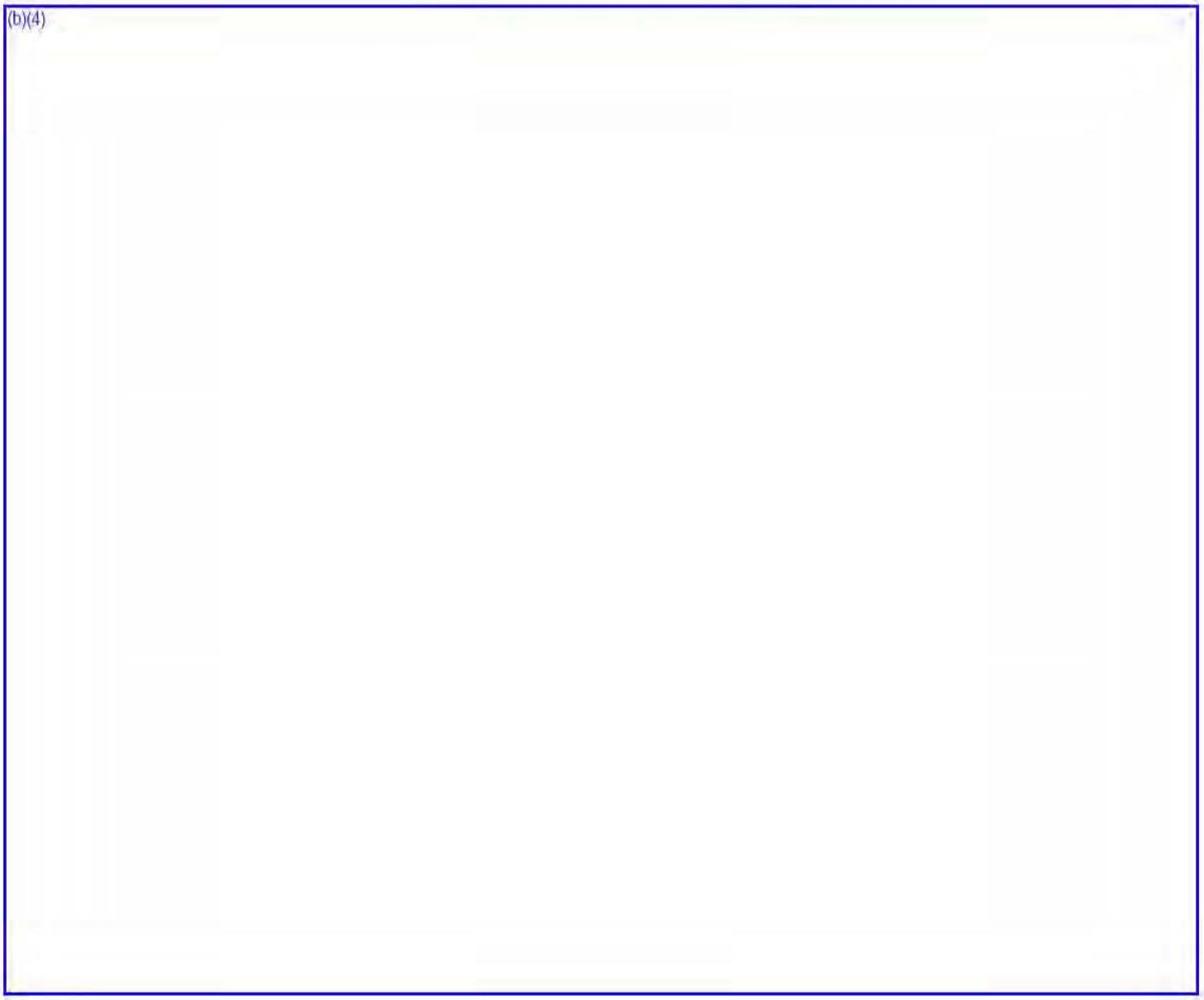

Figure 5.3.4

HI-TRAC VW OVERPACK WITH MPC-89 CROSS SECTIONAL VIEW AS MODELED IN MCNP†

† This figure is drawn to scale using VISED.

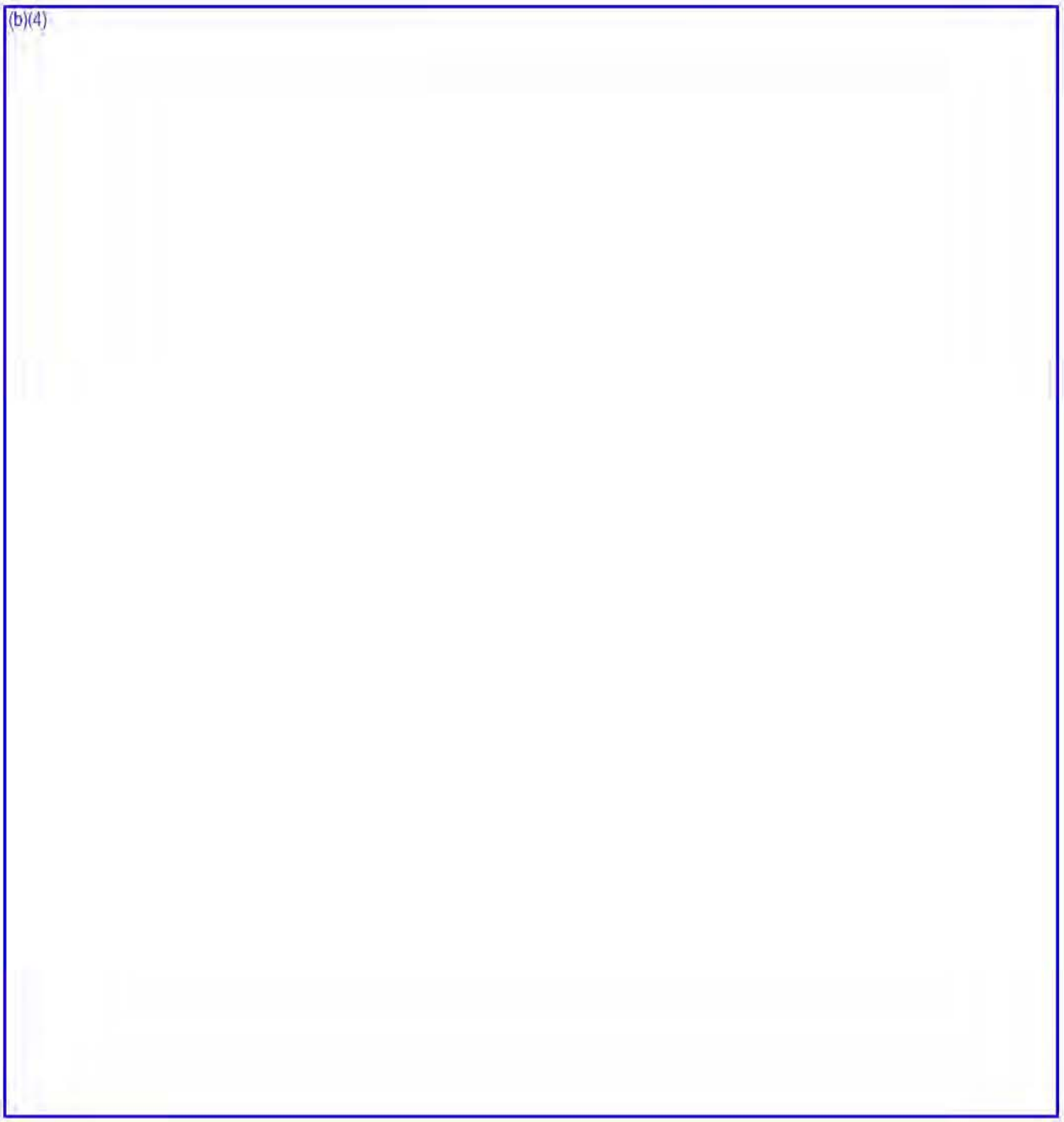

Figure 5.3.5
CROSS SECTION OF HI-STORM FW OVERPACK

(b)(4)

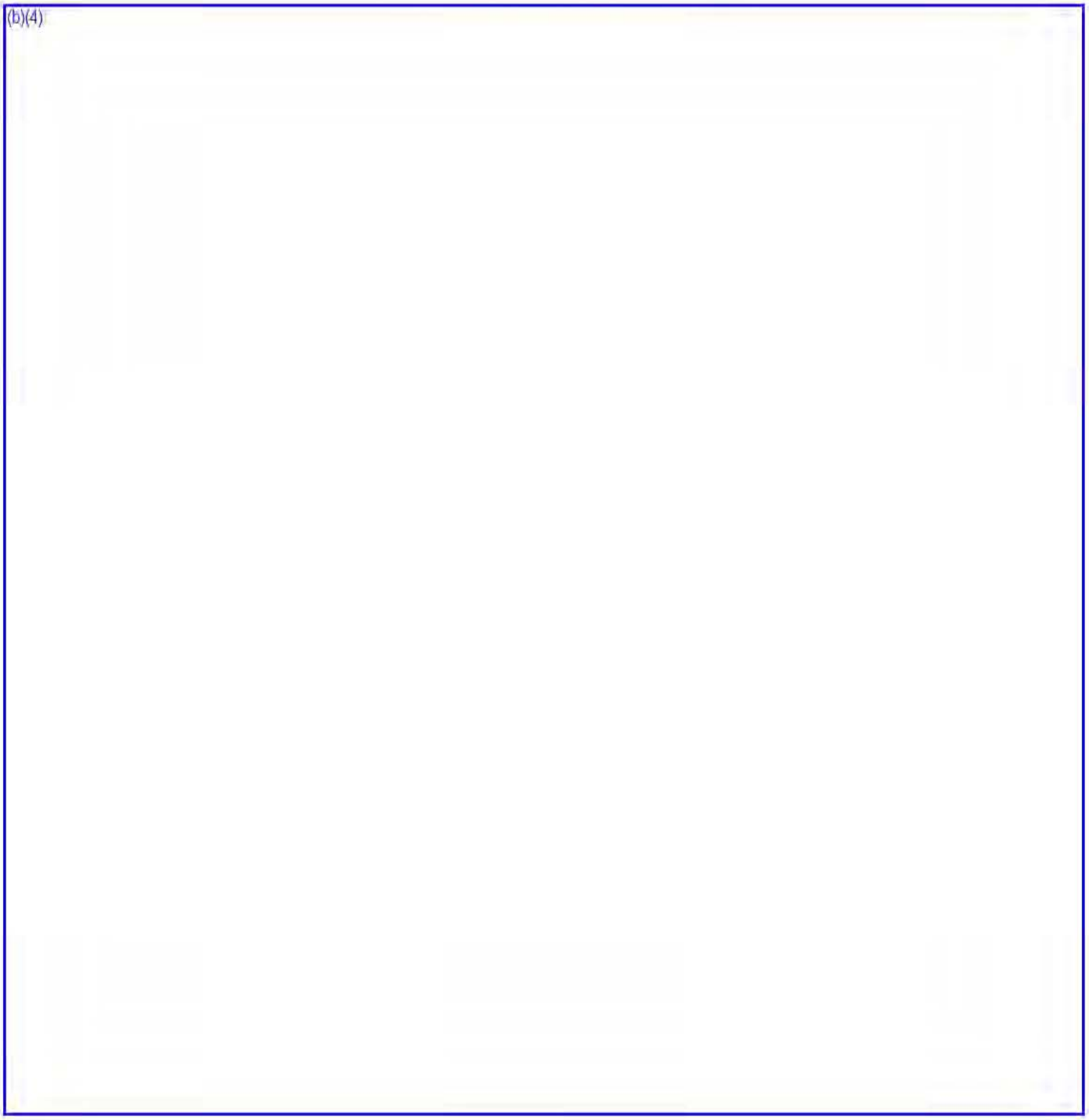

Figure 5.3.6
HI-STORM FW OVERPACK CROSS SECTIONAL ELEVATION VIEW

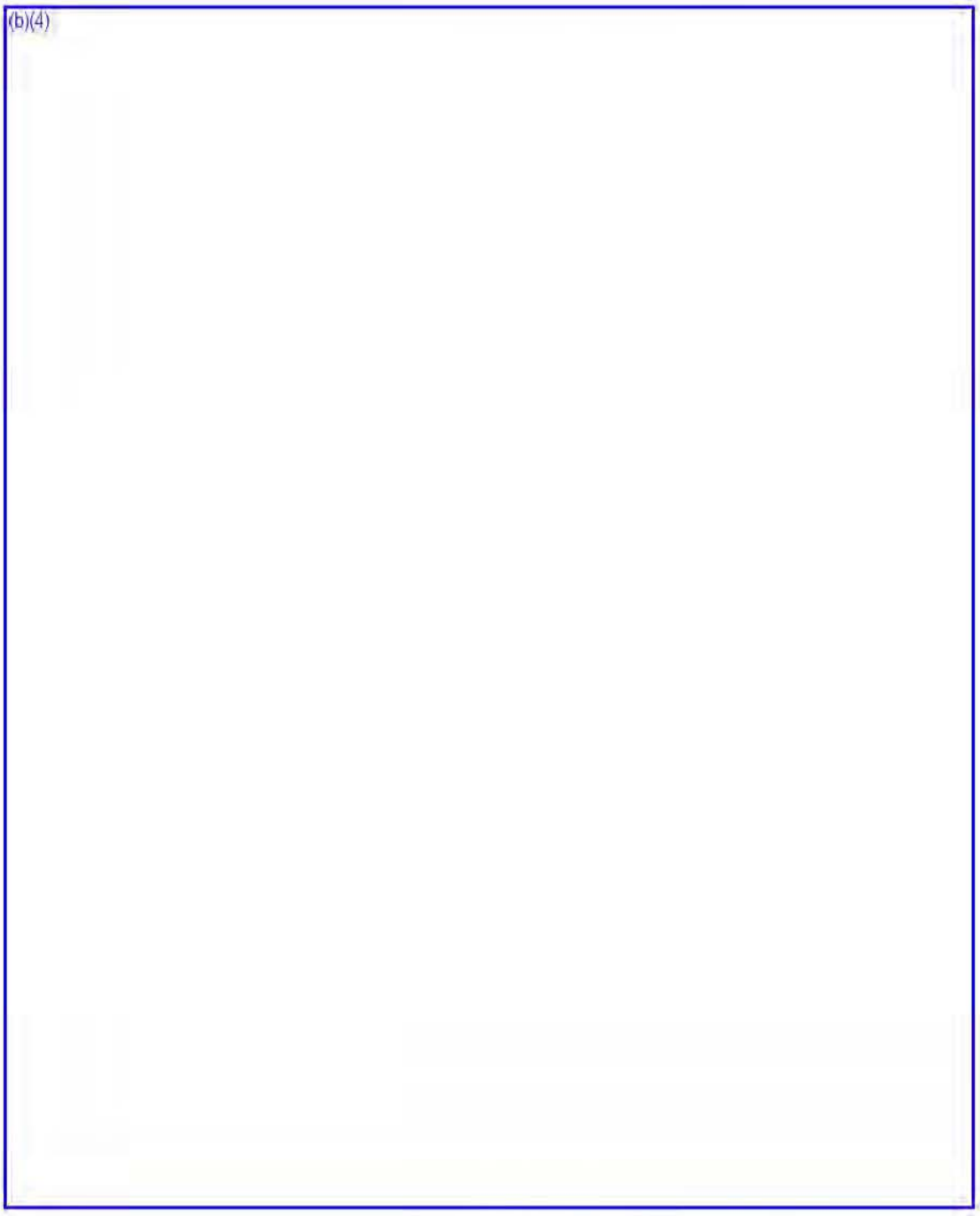

Figure 5.3.7
HI-TRAC VW TRANSFER CASK WITH POOL LID CROSS SECTIONAL ELEVATION VIEW (AS MODELED)

(b)(4)

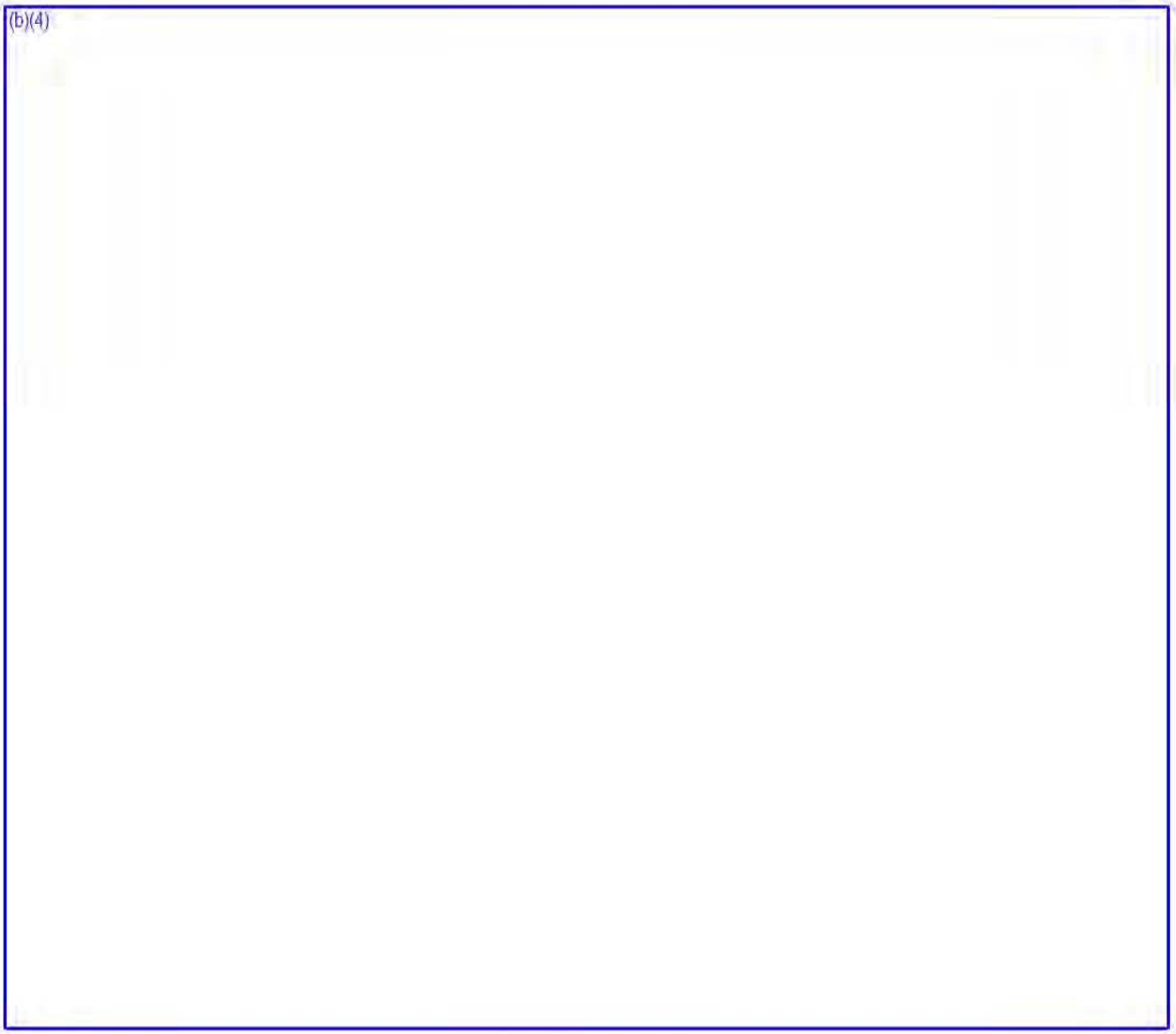

Figure 5.3.8

HI-TRAC VW TRANSFER CASK CROSS SECTIONAL VIEW WITH MPC-37 (AS MODELED)

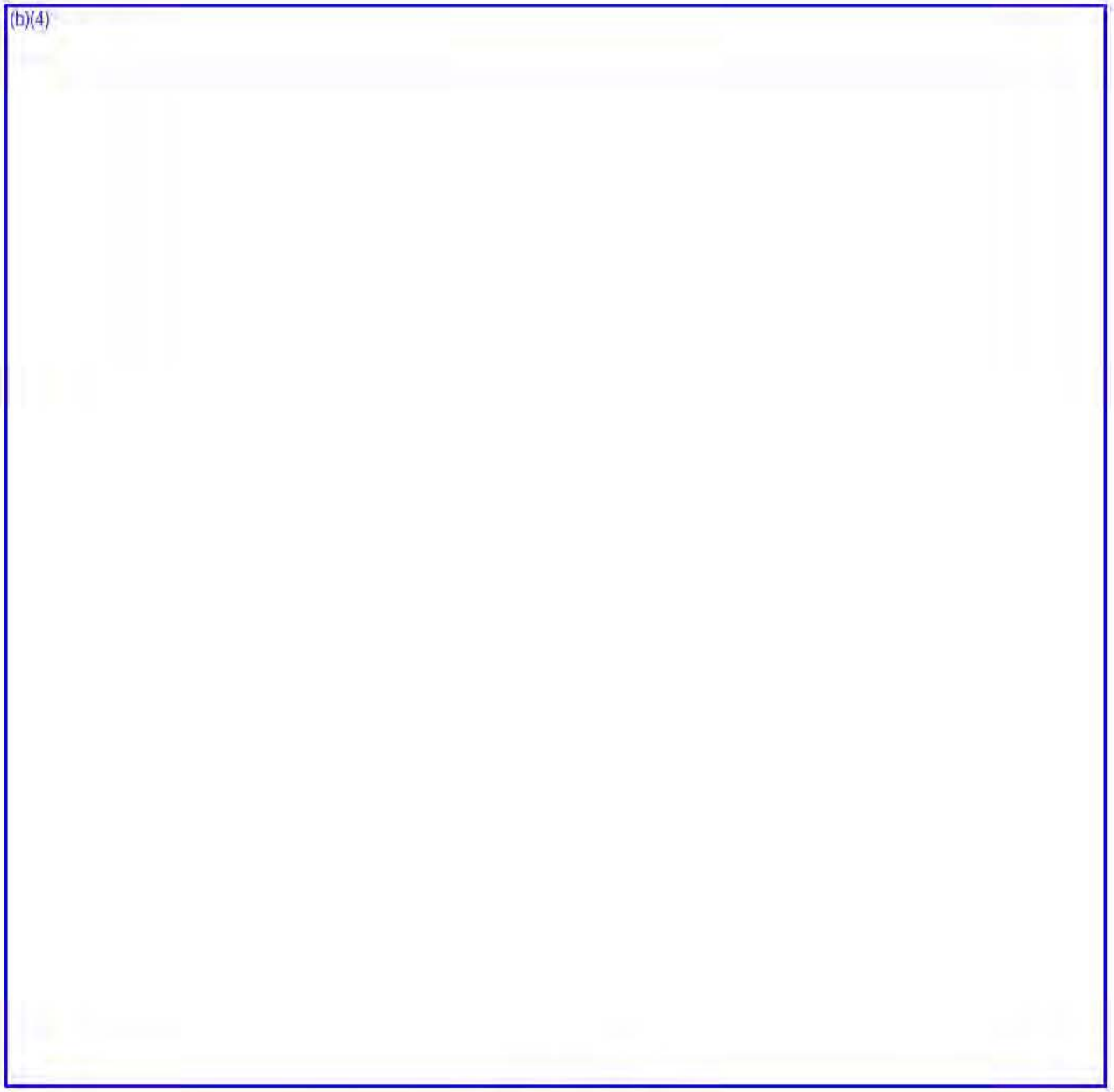

Figure 5.3.9

HI-TRAC VW TRANSFER CASK CROSS SECTIONAL VIEW WITH MPC-89 (AS MODELED)

(b)(4)

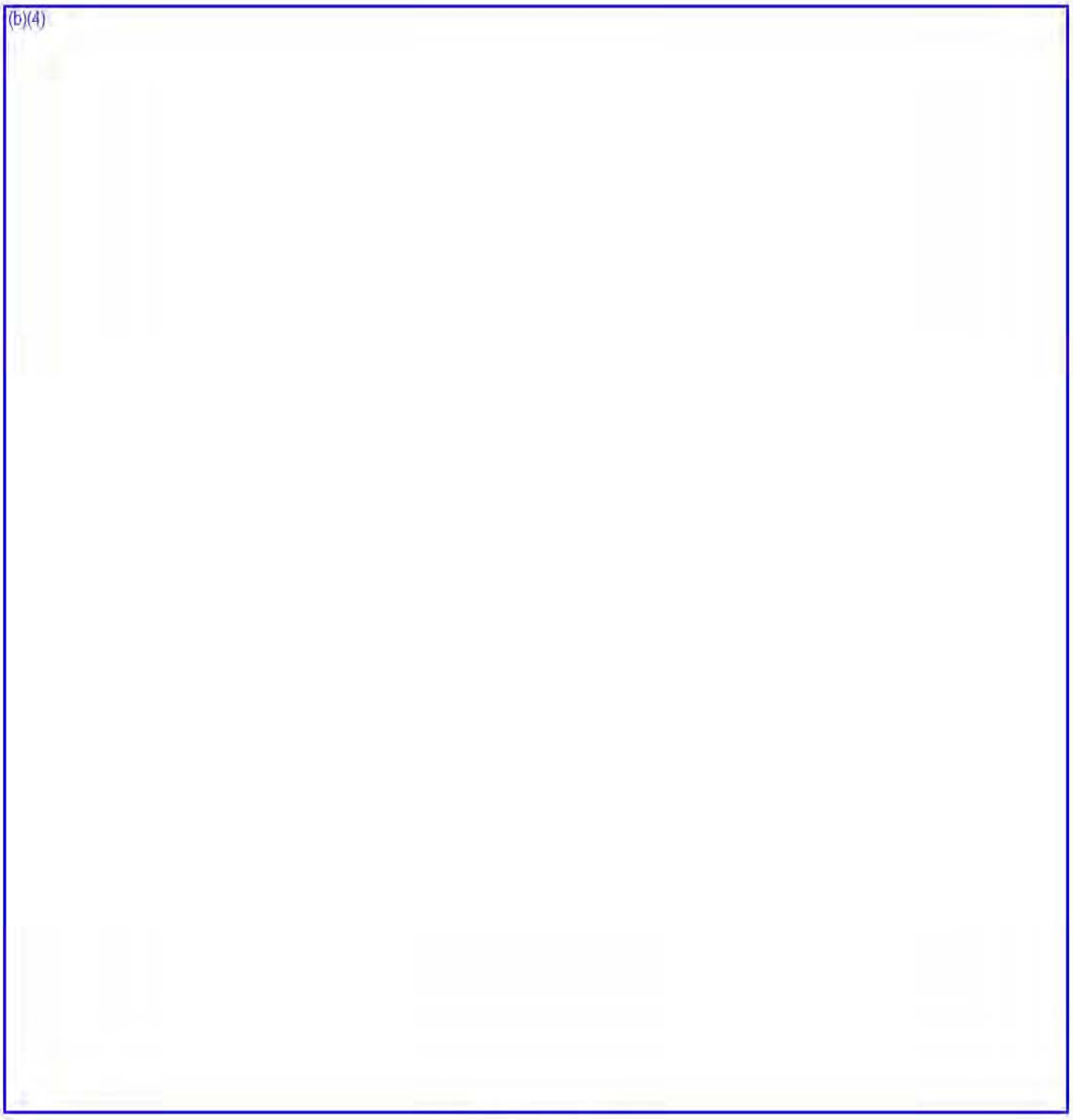

Figure 5.3.10

AXIAL LOCATION OF PWR DESIGN BASIS FUEL IN THE HI-STORM FW OVERPACK

(b)(4)

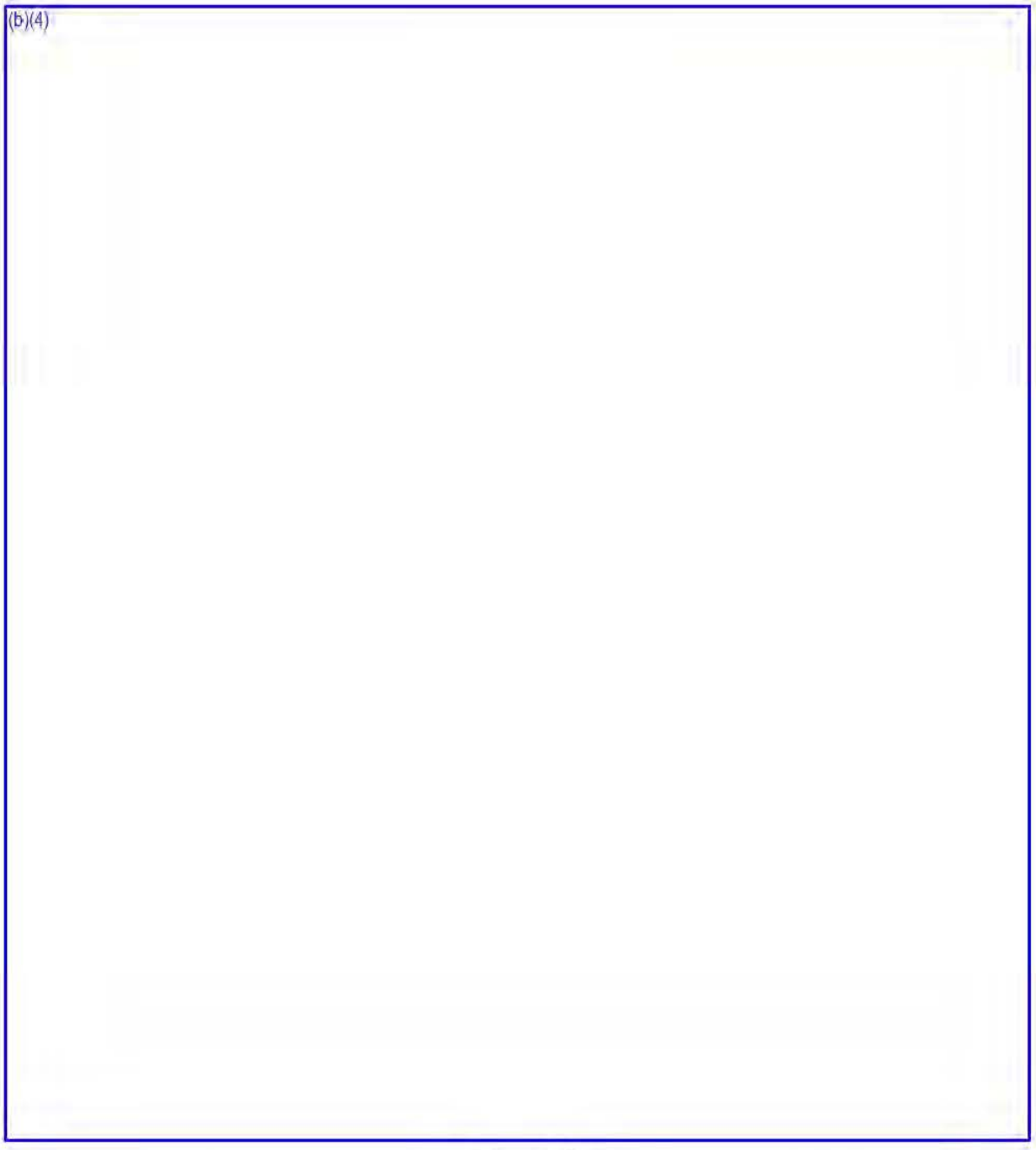

Figure 5.3.11

AXIAL LOCATION OF BWR DESIGN BASIS FUEL IN THE HI-STORM FW OVERPACK

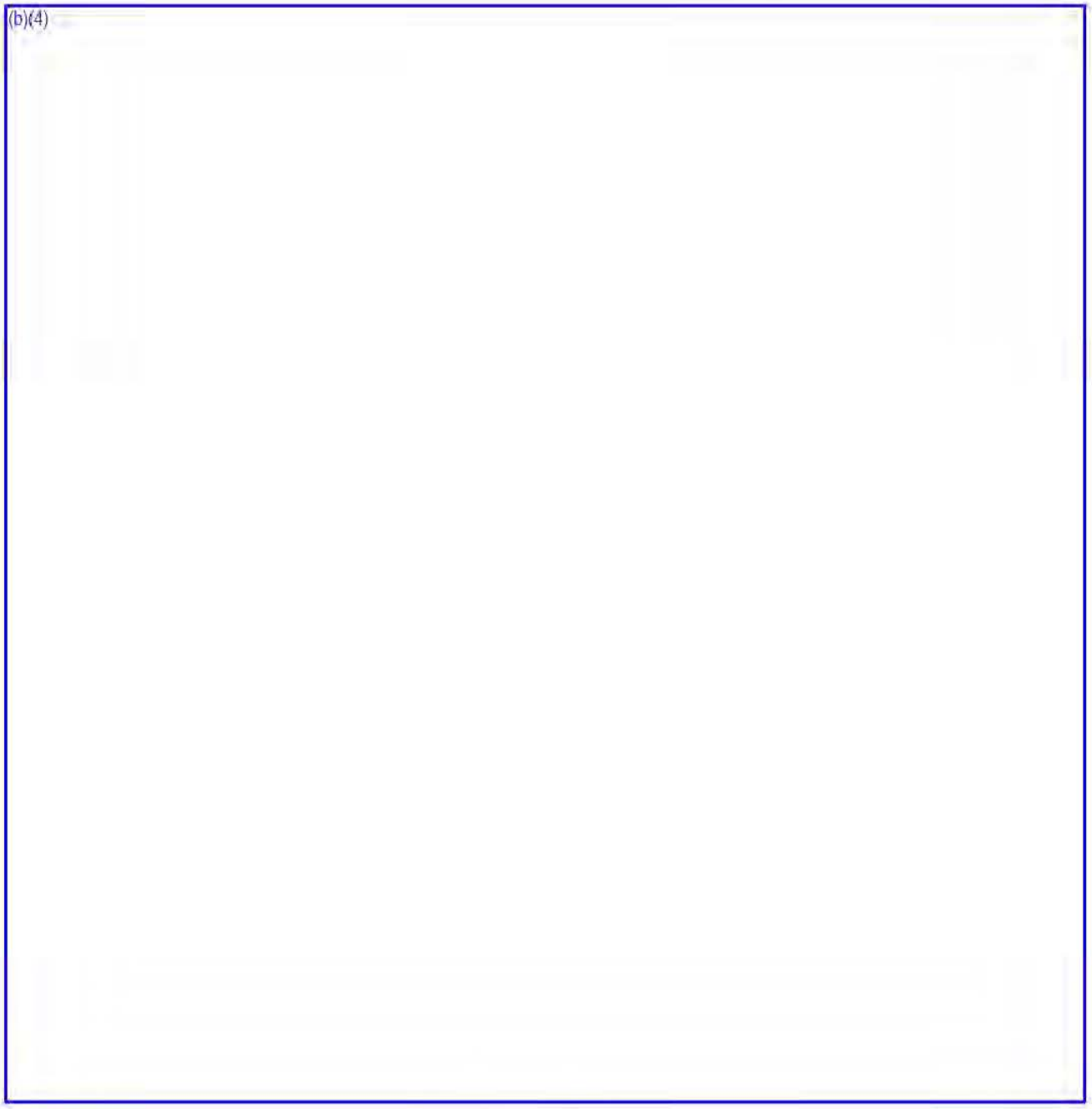

Figure 5.3.12

CROSS SECTIONAL VIEW OF AN MPC-37 BASKET CELL AS MODELED IN MCNP

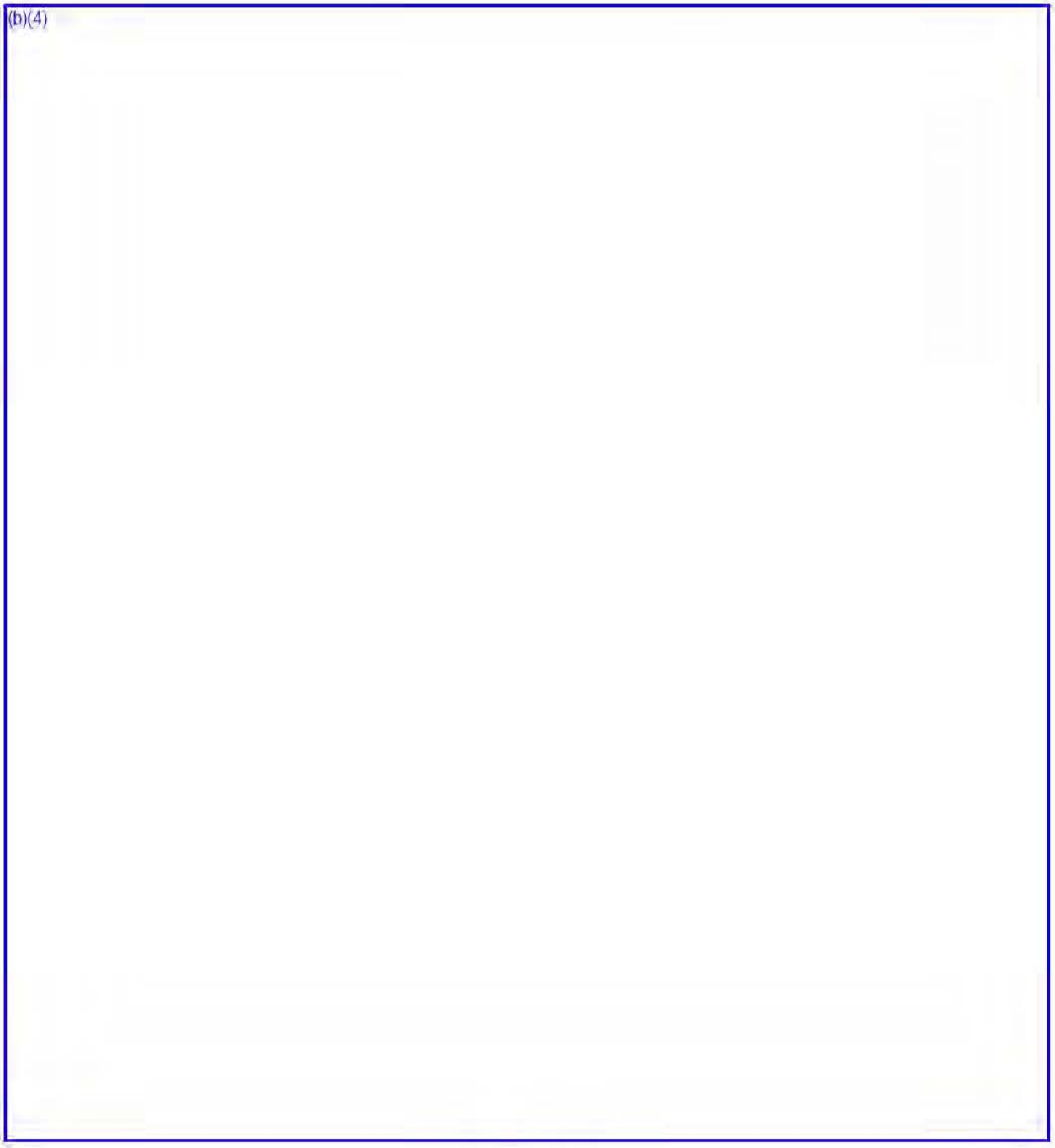

Figure 5.3.13

CROSS SECTIONAL VIEW OF AN MPC-89 BASKET CELL AS MODELED IN MCNP

5.4 SHIELDING EVALUATION

The MCNP-5 code was used for all of the shielding analyses [5.1.1]. MCNP is a continuous energy, three-dimensional, coupled neutron-photon-electron Monte Carlo transport code. Continuous energy cross section data are represented with sufficient energy points to permit linear-linear interpolation between points. The individual cross section libraries used for each nuclide are those recommended by the MCNP manual Cross section libraries are based on ENDF/B-V and ENDF/B-VI, except for Sn isotopes where the ENDL92 library is used, and uranium isotopes where LANL/T16 libraries are used. These are the default libraries for the MCNP code version used here [5.1.1]. MCNP has been extensively benchmarked against experimental data by the large user community. References [5.4.2], [5.4.3], and [5.4.4] are three examples of the benchmarking that has been performed.

The energy distribution of the source term, as described earlier, is used explicitly in the MCNP model. A different MCNP calculation is performed for each of the three source terms (neutron, decay gamma, and ^{60}Co). The axial distribution of the fuel source term is described in Table 2.1.5 and Figures 2.1.3 and 2.1.4. The PWR and BWR axial burnup distributions were obtained from References [5.4.5] and [5.4.6], respectively and have previously been utilized in the HI-STORM FSAR [5.2.17]. These axial distributions were obtained from operating plants and are representative of PWR and BWR fuel with burnups greater than 30,000 MWD/MTU. The ^{60}Co source in the hardware was assumed to be uniformly distributed over the appropriate regions.

It has been shown that the neutron source strength varies as the burnup level raised by the power of 4.2. Since this relationship is non-linear and since the burnup in the axial center of a fuel assembly is greater than the average burnup, the neutron source strength in the axial center of the assembly is greater than the relative burnup times the average neutron source strength. In order to account for this effect, the neutron source strength in each of the 10 axial nodes listed in Table 2.1.5 was determined by multiplying the average source strength by the relative burnup level raised to the power of 4.2. The peak relative burnups listed in Table 2.1.5 for the PWR and BWR fuels are 1.105 and 1.195 respectively. Using the power of 4.2 relationship results in a 37.6% ($1.105^{4.2}/1.105$) and 76.8% ($1.195^{4.2}/1.195$) increase in the neutron source strength in the peak nodes for the PWR and BWR fuel, respectively. The total neutron source strength increases by 15.6% for the PWR fuel assemblies and 36.9% for the BWR fuel assemblies.

MCNP was used to calculate doses at the various desired locations. MCNP calculates neutron or photon flux and these values can be converted into dose by the use of dose response functions. This is done internally in MCNP and the dose response functions are listed in the input file in Appendix 5.A. The response functions used in these calculations are listed in Table 5.4.1 and were taken from ANSI/ANS 6.1.1, 1977 [5.4.1].

The dose rates at the various locations were calculated with MCNP using a two-step process. The first step was to calculate the dose rate for each dose location per starting particle for each neutron and gamma group in each basket region for each axial and azimuthal dose location. The second step is to multiply the dose rate per starting particle for each energy group and basket location (i.e., tally output/quantity) by the source strength (i.e. particles/sec) in that group and sum the resulting dose rates for all groups and basket locations in each dose location. The normalization of these results and calculation of the total dose rate from neutrons, fuel gammas or Co-60 gammas is performed with the following equation.

$$T_{final} = \sum_{j=1}^{M}\left[\sum_{i=1}^{N}\frac{T_{i,j}}{Fm_i} * F_{i,j}\right] \qquad \text{(Equation 5.4.1)}$$

where,

T_{final} = Final dose rate (rem/h) from neutrons, fuel gammas, or Co-60

N = Number of groups (neutrons, fuel gammas) or Number of axial sections (Co-60 gammas)

M = Number of regions in the basket

$T_{i,j}$ = Tally quantity from particles originating in MCNP in group/section i and region j (rem/h)(particles/sec)

$F_{i,j}$ = Fuel Assembly source strength in group i and region j (particles/sec)

Fm_i = Source fraction used in MCNP for group i

Note that dividing by Fm_i (normalization) is necessary to account for the number of MCNP particles that actually start in group i. Also note that T_i is already multiplied by a dose conversion factor in MCNP.

The standard deviations of the various results were statistically combined to determine the standard deviation of the total dose in each dose location. The estimated variance of the total dose rate, S^2_{total}, is the sum of the estimated variances of the individual dose rates S^2_i. The estimated total dose rate, estimated variance, and relative error [5.1.1] are derived according to Equations 5.4.2 through 5.4.5.

$$R_i = \frac{\sqrt{S_i^2}}{T_i} \qquad \text{(Equation 5.4.2)}$$

$$S_{Total}^2 = \sum_{i=1}^{n} S_i^2 \qquad \text{(Equation 5.4.3)}$$

$$T_{Total} = \sum_{i=1}^{n} T_i \qquad \text{(Equation 5.4.4)}$$

$$R_{Total} = \frac{\sqrt{S_{Total}^2}}{T_{Total}} = \frac{\sqrt{\sum_{i=1}^{n} S_i^2}}{T_{Total}} = \frac{\sqrt{\sum_{i=1}^{n} (R_i \times T_i)^2}}{T_{Total}} \qquad \text{(Equation 5.4.5)}$$

where,

i	=	tally component index
n	=	total number of components
T_{Total}	=	total estimated tally
T_i	=	tally i component
S^2_{Total}	=	total estimated variance
S^2_i	=	variance of the i component
R_i	=	relative error of the i component
R_{Total}	=	total estimated relative error

Note that the two-step approach outlined above allows the accurate consideration of the neutron and gamma source spectrum, and the location of the individual assemblies, since the tallies are calculated in MCNP as a function of the starting energy group and the assembly location, and then in the second step multiplied with the source strength in each group in each location. It is therefore equivalent to a one-step calculation where source terms are directly specified in the MCNP input files, except for the following approximations:

The first approximation is that fuel is modeled as fresh UO_2 fuel (rather than spent fuel) in MCNP, with an upper bound enrichment. The second approximation is related to the axial burnup profile. The profile is modeled by assigning a source probability to each of the 10 axial sections of the active region, based on a representative axial burnup profile [5.2.17]. For fuel gammas, the probability is proportional to the burnup, since the gamma source strength changes essentially linearly with burnup. For neutrons, the probability is proportional to the burnup raised to the power of 4.2, since the neutron source strength is proportional to the burnup raised to about that power [5.4.7]. This is a standard approach that has been previously used in the licensing calculations for the HI-STAR 100 cask [5.4.8] and HI-STORM 100 system [5.2.17].

Tables 5.1.6 and 5.1.7 provide the design basis dose rates adjacent to the HI-STORM overpack during normal conditions for the MPC types in Table 1.0.1. Table 5.1.8 provides the design basis dose rates at one meter from the overpack containing the MPC-37. A detailed discussion of the normal, off-normal, and accident condition dose rates is provided in Subsections 5.1.1 and 5.1.2.

Table 5.4.2 shows the corresponding dose rates adjacent to and one meter away from the HI-TRAC for the fully flooded MPC-37 condition with an empty water-jacket (condition in which the HI-TRAC is removed from the spent fuel pool). Table 5.4.3 shows the dose rates adjacent to and one meter away from the HI-TRAC for the fully flooded MPC-37 condition with the water jacket filled with water (condition in which welding operations are performed). For the conditions involving a fully flooded MPC-37, the internal water level was 5 inches below the MPC lid. These dose rates represent the various conditions of the HI-TRAC during operations. Comparing these results to Table 5.1.1 (dry MPC-37 and HI-TRAC water jacket filled with water) indicates that the dose rates in the upper and lower portions of the HI-TRAC are significantly reduced with water in the MPC.

Table 5.4.4 shows the corresponding dose rates adjacent to and one meter away from the HI-TRAC for the fully flooded MPC-89 condition with an empty water-jacket. Table 5.4.5 shows the dose rates adjacent to and one meter away from the HI-TRAC for the fully flooded MPC-89 condition with the water jacket filled with water. These results demonstrate that the dose rates on contact at the top and bottom of the HI-TRAC VW are somewhat higher in the MPC-89 case than in the MPC-37 case. However, the MPC-37 produces higher dose rates than the MPC-89 at the center of the HI-TRAC, on-contact, and at locations 1 meter away from the HI-TRAC. Therefore, the MPC-37 is used for the exposure calculations in Chapter 11 of the SAR.

The calculations presented herein are using a uniform loading pattern. All MPCs, however, also offer regionalized loading patterns, as mentioned in Section 5.0 and described in Subsection 1.2. These loading patterns authorize fuel of higher decay heat (i.e., higher burnups and shorter cooling times) to be stored in certain regions of the basket. Evaluations have been performed for the HI-STORM 100 [5.2.17] where analysis of the MPC-32 and MPC-68 using the same burnup and cooling times in Region 1 and Region 2. Region 1 contains 38% of total number of assemblies for the MPC-32 and 47% for the MPC-68. The evaluations show that approximately 21% and 27% of the neutron dose at the edge of the water jacket comes from region 1 fuel assemblies in the MPC-32 and MPC-68, respectively. Further, approximately 1% and 2% of the photon dose at the edge of the water jacket comes from region 1 fuel assemblies in the MPC-32 and MPC-68, respectively. These results clearly indicate that the outer fuel assemblies shield almost the entire gamma source from the inner assemblies in the radial direction and a significant percentage of the neutron source. The conclusion from this analysis is that the total dose rate on the external radial surfaces of the cask can be greatly reduced by placing longer cooled and lower burnup fuels on the outside of the basket. Using a uniform loading pattern, rather than

employing the regionalized loading scheme, in these HI-STORM FW calculations is therefore acceptable as it produces conservative dose rate values on the radial surfaces.

Since MCNP is a statistical code, there is an uncertainty associated with the calculated values. In MCNP the uncertainty is expressed as the relative error which is defined as the standard deviation of the mean divided by the mean. Therefore, the standard deviation is represented as a percentage of the mean. The relative error for the total dose rates presented in this chapter were typically less than 5% and the relative error for the individual dose components was typically less than 10%.

5.4.1 Streaming Through Radial Steel Fins

The HI-STORM FW overpack and the HI-TRAC VW cask utilize radial steel fins for structural support and cooling. The attenuation of neutrons through steel is substantially less than the attenuation of neutrons through concrete and water. Therefore, it is possible to have neutron streaming through the fins that could result in a localized dose peak. The reverse is true for photons, which would result in a localized reduction in the photon dose.

Analysis of the steel fins in the HI-TRAC has previously been performed in the HI-STORM 100 FSAR [5.2.17] and indicates that neutron streaming is noticeable at the surface of the cask. The neutron dose rate on the surface of the steel fin is somewhat higher than the circumferential average dose rate at that location. The gamma dose rate, however, is slightly lower than the circumferential average dose rate at that location. At one meter from the cask surface there is little difference between the dose rates calculated over the fins compared to the other areas of the water jackets.

These conclusions indicate that localized neutron streaming is noticeable on the surface of the transfer casks. However, at one meter from the surface the streaming has dissipated. Since most HI-TRAC operations will involve personnel moving around the transfer cask at some distance from the cask, only surface average dose rates are reported in this chapter.

5.4.2 Damaged Fuel Post-Accident Shielding Evaluation

The Holtec Generic PWR and BWR DFCs are designed to accommodate any PWR or BWR fuel assembly that can physically fit inside the DFC. Damaged fuel assemblies under normal conditions, for the most part, resemble intact fuel assemblies from a shielding perspective. Under accident conditions, it cannot be guaranteed that the damaged fuel assembly will remain intact. As a result, the damaged fuel assembly may begin to resemble fuel debris in its possible configuration after an accident.

Since damaged fuel is identical to intact fuel from a shielding perspective no specific analysis is required for damaged fuel under normal conditions. However, a generic shielding evaluation was previously performed for the HI-STORM 100 [5.2.17] to demonstrate that fuel debris under normal or accident conditions, or damaged fuel in a post-accident configuration, will not result in a significant increase in the dose rates around the 100-ton HI-TRAC. Since the 100-ton HI-TRAC and the HI-TRAC VW are similar in design, the conclusions from the 100-ton HI-RAC evaluations are also applicable to the HI-TRAC VW.

The scenario analyzed to determine the potential change in dose rate as a result of fuel debris or a damaged fuel assembly collapse in the HI-STORM 100 [5.2.17] feature fuel debris or a damaged fuel assembly that has collapsed (which can have a higher average fuel density than an intact fuel assembly). If the damaged fuel assembly would fully or partially collapse, the fuel density in one portion of the assembly would increase and the density in the other portion of the assembly would decrease. The analysis consisted of modeling the fuel assemblies in the damaged fuel locations in the MPC-24 and MPC-68 with a fuel density that was twice the normal fuel density and correspondingly increasing the source rate for these locations by a factor of two. A flat axial power distribution was used which is approximately representative of the source distribution if the top half of an assembly collapsed into the bottom half of the assembly. Increasing the fuel density over the entire fuel length, rather than in the top half or bottom half of the fuel assembly, is conservative and provides the dose rate change in both the top and bottom portion of the cask.

The results for the MPC-24 and MPC-68 calculations [5.2.17] show that the potential effect on the dose rate is not very significant for the storage of damaged fuel and/or fuel debris. This conclusion is further reinforced by the fact that the majority of the significantly damaged fuel assemblies in the spent fuel inventories are older assemblies from the earlier days of nuclear plant operations. Therefore, these assemblies will have a considerably lower burnup and longer cooling times than the assemblies analyzed in this chapter. In addition, since the dose rate change is not significant for the 100-ton HI-TRAC, the dose rate change will not be significant for the HI-TRAC VW or the HI-STORM FW overpacks.

5.4.3 Site Boundary Evaluation

NUREG-1536 [5.2.1] states that detailed calculations need not be presented since SAR Chapter 12 assigns ultimate compliance responsibilities to the site licensee. Therefore, this subsection describes, by example, the general methodology for performing site boundary dose calculations. The site-specific fuel characteristics, burnup, cooling time, and the site characteristics would be factored into the evaluation performed by the licensee.

The methodology of calculating the dose from a single HI-STORM overpack loaded with an MPC and various arrays of loaded HI-STORMs at distances equal to and greater than 100 meters is described in the HI-STORM 100 FSAR [5.2.17]. A back row factor of 0.20 was calculated in

[5.2.17], and utilized herein to calculate dose value C below, based on the results that the dose from the side of the back row of casks is approximately 16 % of the total dose.

The annual dose, assuming 100% occupancy (8760 hours), at 300 meters from a single HI-STORM FW cask is presented in Table 5.4.6 for the design basis burnup and cooling time analyzed.

The annual dose, assuming 8760 hour occupancy, at distance from an array of casks was calculated in three steps.

1. The annual dose from the radiation leaving the side of the HI-STORM FW overpack was calculated at the distance desired. Dose value = A.

2. The annual dose from the radiation leaving the top of the HI-STORM FW overpack was calculated at the distance desired. Dose value = B.

3. The annual dose from the radiation leaving the side of a HI-STORM FW overpack, when it is behind another cask, was calculated at the distance desired. The casks have an assumed 15-foot pitch. Dose value = C.

The doses calculated in the steps above are listed in Table 5.4.7. Using these values, the annual dose (at the center of the long side) from an arbitrary 2 by Z array of HI-STORM FW overpacks can easily be calculated. The following formula describes the method.

Z = number of casks along long side

Dose = ZA + 2ZB + ZC

The results for various typical arrays of HI-STORM overpacks can be found in Section 5.1. While the off-site dose analyses were performed for typical arrays of casks containing design basis fuel, compliance with the requirements of 10CFR72.104(a) can only be demonstrated on a site-specific basis, as stated earlier. Therefore, a site-specific evaluation of dose at the controlled area boundary must be performed for each ISFSI in accordance with 10CFR72.212. The site-specific evaluation will consider the site-specific characteristics (such as exposure duration and the number of casks deployed), dose from other portions of the facility and the specifics of the fuel being stored (burnup and cooling time).

5.4.4 Non-Fuel Hardware

As discussed in Subsection 5.2.3, non-fuel hardware in the form of BPRAs, TPDs, CRAs, and APSRs are permitted for storage, integral with a PWR fuel assembly, in the HI-STORM FW system. Since each device occupies the same location within an assembly, only one device will be present in a given assembly. ITTRs, which are installed after core discharge and do not contain radioactive material, may also be stored in the assembly. BPRAs, TPDs and ITTRs are authorized for unrestricted storage in an MPC. The permissible locations of the CRAs and APSRs are shown in Figure 2.1.5.

Table 5.4.8 provides the dose rates at various locations on the surface and one meter from the HI-TRAC VW due to the BPRAs and TPDs for the MPC-37. The results in Table 5.4.8 show that the BPRAs essentially bound TPDs. All dose rates with NFH in this chapter therefore assume BPRA in every assembly. Note that, even for calculations without NFH, the dose from the active region conservatively contains the contribution of the BPRA. This mainly affects dose location 1 and 2, and results for these locations are therefore identical in most tables, and don't show the dose rate difference indicated in Table 5.4.8.

The analyses in this chapter that consider presence of BPRAs assume that a full-length rod with burnable poison is present in all principal locations. In reality, many BPRAs contain full-length poison rods in some locations, and thimble rodlets in others. The burnup and cooling time combinations listed in Table 2.1.25 of HI-STORM 100 FSAR [5.2.17] for BPRAs and TPDs were selected to ensure the Co-60 activity of those devices is below the value of 895 Ci (BPRA) and 50 Ci (TPD). These activities are used in the dose evaluations presented in this chapter. Apart from the total activity, the axial distribution of the material in those devices is important for the dose rates. This axial distribution is shown in Table 5.2.15 (masses) and 5.2.16 (activities). It can be observed from Table 5.2.16, while TPDs have a lower overall activity, their activity in the gas plenum region of the assembly is higher compared to that of the BPRAs. These activities were used to calculate the dose rates in Table 5.4.8. The results in this table show that the maximum dose effect for BPRAs is at the side of the cask, while the maximum dose effect of TPDs is near and on the top of the cask. Nevertheless, Table 5.4.8 demonstrates that even near and on the top of the cask, the TPD doses are bounded by the BPRA doses. It is to be noted that BPRAs with several thimble plugs may result higher dose rate near and on the top of the cask than that reported in Table 5.4.8. However, the potential local increase in dose near and on the top of the cask due the presence of several thimble plug rodlets instead of full length BPRA rods would be more than compensated by the reduction of the dose from the side of the cask at larger distances. Therefore, using BPRAs with all burnable poison rods in the analyses that demonstrate compliance with the site boundary dose limits would be bounding, and hence the burnup and cooling time combinations for BPRAs in Table 2.1.25 of the HI-STORM 100 FSAR [5.2.17] are conservative.

Two different configurations were analyzed for CRAs and three different configurations were analyzed for APSRs in the HI-STORM FSAR [5.2.17]. The dose rate due to CRAs and APSRs was explicitly calculated for dose locations around the HI-TRAC and results were provided for the different configurations of CRAs and APSRs, respectively, in the MPCs. These results indicate the dose rate on the radial surfaces of the overpack due to the storage of these devices is less than the dose rate from BPRAs (the increase in dose rate on the radial surface due to CRAs and APSRs are virtually negligible). For the surface dose rate at the bottom, the value for the CRA is comparable to or higher than the value from the BPRA. The increase in the bottom dose rates due to the presence of CRAs is on the order of 10-15% (based on bounding configuration 1 in [5.2.17]). The dose rate out the top of the overpack is essentially 0. The latter is due to the fact that CRAs and APSRs do not achieve significant activation in the upper portion of the devices due to the manner in which they are utilized during normal reactor operations. In contrast, the dose rate out the bottom of the overpack is substantial due to these devices. However, these dose rates occur in an area (below the pool lid and transfer doors) which is not normally occupied.

While the evaluations described above are based on conservative assumptions, the conclusions can vary slightly depending on the number of CRAs and their operating conditions.

5.4.5 Effect of Uncertainties

The design basis calculations presented in this chapter are based on a range of conservative assumptions, but do not explicitly account for uncertainties in the methodologies, codes and input parameters, that is, it is assumed that the effect of uncertainties is small compared to the numerous conservatisms in the analyses. To show that this assumption is valid, calculations have previously been performed as "best estimate" calculations and with estimated uncertainties added [5.4.9]. In all scenarios considered (e.g., evaluation of conservatisms in modeling assumptions, uncertainties associated with MCNP as well as the depletion analysis (including input parameters), etc.), the total dose rates long with uncertainties are comparable to, or lower than, the corresponding values from the design basis calculations. This provides further confirmation that the design basis calculations are reasonable and conservative.

Table 5.4.1

FLUX-TO-DOSE CONVERSION FACTORS
(FROM [5.4.1])

Gamma Energy (MeV)	**(rem/hr)/ (photon/cm^2-s)**
0.01	3.96E-06
0.03	5.82E-07
0.05	2.90E-07
0.07	2.58E-07
0.1	2.83E-07
0.15	3.79E-07
0.2	5.01E-07
0.25	6.31E-07
0.3	7.59E-07
0.35	8.78E-07
0.4	9.85E-07
0.45	1.08E-06
0.5	1.17E-06
0.55	1.27E-06
0.6	1.36E-06
0.65	1.44E-06
0.7	1.52E-06
0.8	1.68E-06
1.0	1.98E-06
1.4	2.51E-06
1.8	2.99E-06
2.2	3.42E-06

Table 5.4.1 (continued) FLUX-TO-DOSE CONVERSION FACTORS (FROM [5.4.1])	
Gamma Energy (MeV)	**(rem/hr)/ (photon/cm^2-s)**
2.6	3.82E-06
2.8	4.01E-06
3.25	4.41E-06
3.75	4.83E-06
4.25	5.23E-06
4.75	5.60E-06
5.0	5.80E-06
5.25	6.01E-06
5.75	6.37E-06
6.25	6.74E-06
6.75	7.11E-06
7.5	7.66E-06
9.0	8.77E-06
11.0	1.03E-05
13.0	1.18E-05
15.0	1.33E-05

Table 5.4.1 (continued)

FLUX-TO-DOSE CONVERSION FACTORS
(FROM [5.4.1])

Neutron Energy (MeV)	Quality Factor	(rem/hr)[†]/(n/cm^2-s)
2.5E-8	2.0	3.67E-6
1.0E-7	2.0	3.67E-6
1.0E-6	2.0	4.46E-6
1.0E-5	2.0	4.54E-6
1.0E-4	2.0	4.18E-6
1.0E-3	2.0	3.76E-6
1.0E-2	2.5	3.56E-6
0.1	7.5	2.17E-5
0.5	11.0	9.26E-5
1.0	11.0	1.32E-4
2.5	9.0	1.25E-4
5.0	8.0	1.56E-4
7.0	7.0	1.47E-4
10.0	6.5	1.47E-4
14.0	7.5	2.08E-4
20.0	8.0	2.27E-4

[†] Includes the Quality Factor.

Table 5.4.2

DOSE RATES FOR THE HI-TRAC VW FOR THE FULLY FLOODED MPC CONDITION WITH AN EMPTY NEUTRON SHIELD

MPC-37 DESIGN BASIS ZIRCALOY CLAD FUEL AT 45,000 MWD/MTU AND 4.5-YEAR COOLING

Dose Point Location	Fuel Gammas (mrem/hr)	(n,γ) Gammas (mrem/hr)	^{60}Co Gammas (mrem/hr)	Neutrons (mrem/hr)	Totals (mrem/hr)	Totals with BPRAs (mrem/hr)
ADJACENT TO THE HI-TRAC VW						
1	711	<1	489	67	1268	1268
2	2242	2	<1	319	2563	2563
3	7	<1	128	2	139	210
4	15	<1	227	<1	244	371
5 (bottom lid)	465	<1	1802	79	2346	2346
ONE METER FROM THE HI-TRAC VW						
1	541	<1	61	53	657	657
2	1141	<1	5	116	1263	1264
3	191	<1	75	20	286	326
4	8	<1	127	<1	137	208
5	259	<1	985	20	1266	1266

Notes:

- Refer to Figure 5.1.2 for dose point locations.
- Values are rounded to nearest integer.
- MPC internal water level is 5 inches below the MPC lid.
- The "Fuel Gammas" category includes gammas from the spent fuel, ^{60}Co from the spacer grids, and ^{60}Co from the BPRAs in the active fuel region.

Table 5.4.3

DOSE RATES FOR THE HI-TRAC VW FOR THE FULLY FLOODED MPC CONDITION WITH A FULL NEUTRON SHIELD

MPC-37 DESIGN BASIS ZIRCALOY CLAD FUEL AT 45,000 MWD/MTU AND 4.5-YEAR COOLING

Dose Point Location	Fuel Gammas (mrem/hr)	(n,γ) Gammas (mrem/hr)	^{60}Co Gammas (mrem/hr)	Neutrons (mrem/hr)	Totals (mrem/hr)	Totals with BPRAs (mrem/hr)
ADJACENT TO THE HI-TRAC VW						
1	433	1	301	5	740	740
2	1266	5	<1	27	1298	1298
3	2	<1	69	<1	73	111
4	15	<1	227	<1	244	371
5 (bottom lid)	465	<1	1802	80	2347	2347
ONE METER FROM THE HI-TRAC VW						
1	294	1	34	4	333	334
2	657	2	3	10	671	672
3	95	<1	41	1	138	160
4	8	<1	127	<1	137	208
5	259	<1	985	20	1265	1265

Notes:

- Refer to Figure 5.1.2 for dose point locations.
- Values are rounded to nearest integer.
- MPC internal water level is 5 inches below the MPC lid.
- The "Fuel Gammas" category includes gammas from the spent fuel, ^{60}Co from the spacer grids, and ^{60}Co from the BPRAs in the active fuel region.

Table 5.4.4

DOSE RATES FOR THE HI-TRAC VW FOR THE FULLY FLOODED MPC CONDITION WITH AN EMPTY NEUTRON SHIELD
MPC-89 DESIGN BASIS ZIRCALOY CLAD FUEL AT 45,000 MWD/MTU AND 5-YEAR COOLING

Dose Point Location	Fuel Gammas (mrem/hr)	(n,γ) Gammas (mrem/hr)	^{60}Co Gammas (mrem/hr)	Neutrons (mrem/hr)	Totals (mrem/hr)
ADJACENT TO THE HI-TRAC VW					
1	195	<1	1513	43	1752
2	2435	3	<1	579	3018
3	<1	<1	351	2	355
4	3	<1	217	<1	222
5 (bottom lid)	40	<1	1530	5	1576
ONE METER FROM THE HI-TRAC VW					
1	387	<1	197	69	654
2	1180	<1	12	168	1361
3	118	<1	154	26	299
4	<1	<1	132	<1	135
5	19	<1	864	2	886

Notes:

- Refer to Figure 5.1.2 for dose point locations.
- Values are rounded to nearest integer.
- MPC internal water level is 5 inches below the MPC lid.
- The "Fuel Gammas" category includes gammas from the spent fuel and ^{60}Co from the spacer grids.

Table 5.4.5

DOSE RATES FOR THE HI-TRAC VW FOR THE FULLY FLOODED MPC CONDITION WITH A FULL NEUTRON SHIELD
MPC-89 DESIGN BASIS ZIRCALOY CLAD FUEL AT 45,000 MWD/MTU AND 5-YEAR COOLING

Dose Point Location	Fuel Gammas (mrem/hr)	(n,γ) Gammas (mrem/hr)	^{60}Co Gammas (mrem/hr)	Neutrons (mrem/hr)	Totals (mrem/hr)
ADJACENT TO THE HI-TRAC VW					
1	102	<1	926	2	1031
2	1373	10	<1	47	1431
3	<1	<1	189	<1	192
4	3	<1	217	<1	222
5 (bottom lid)	40	<1	1530	5	1576
ONE METER FROM THE HI-TRAC VW					
1	211	1	115	5	332
2	627	3	7	16	653
3	72	<1	83	1	157
4	<1	<1	132	<1	135
5	19	<1	864	2	886

Notes:

- Refer to Figure 5.1.2 for dose point locations.
- Values are rounded to nearest integer.
- MPC internal water level is 5 inches below the MPC lid.
- The "Fuel Gammas" category includes gammas from the spent fuel and ^{60}Co from the spacer grids.

Table 5.4.6

ANNUAL DOSE AT 300 METERS FROM A SINGLE HI-STORM FW OVERPACK WITH AN MPC-37 WITH DESIGN BASIS ZIRCALOY CLAD FUEL

Dose Component	**45,000 MWD/MTU 4.5-Year Cooling (mrem/yr)**
Fuel gammas	15.8
^{60}Co Gammas	2.2
Neutrons	0.2
Total	18.2

Notes:

- Gammas generated by neutron capture are included with fuel gammas.
- The Co-60 gammas include BPRAs.
- The "Fuel Gammas" category includes gammas from the spent fuel, ^{60}Co from the spacer grids, and ^{60}Co from the BPRAs in the active fuel region.

Table 5.4.7

DOSE VALUES USED IN CALCULATING ANNUAL DOSE FROM VARIOUS HI-STORM FW ISFSI CONFIGURATIONS
45,000 MWD/MTU AND 4.5-YEAR COOLING ZIRCALOY CLAD FUEL

Distance	**A Side of Overpack (mrem/yr)**	**B Top of Overpack (mrem/yr)**	**C Side of Shielded Overpack (mrem/yr)**
100 meters	396.0	44.0	79.2
200 meters	61.7	6.9	12.3
300 meters	16.4	1.8	3.3
400 meters	5.3	0.6	1.1
500 meters	2.0	0.2	0.4
600 meters	0.8	0.1	0.2

Notes:

- 8760 hour annual occupancy is assumed.
- Values are rounded to nearest integer where appropriate.

Table 5.4.8

DOSE RATES DUE TO BPRAs AND TPDs FROM THE HI-TRAC VW FOR NORMAL CONDITIONS

Dose Point Location	BPRAs (mrem/hr)	TPDs (mrem/hr)
ADJACENT TO THE HI-TRAC VW		
1	159.09	0.0
2	509.04	0.0
3	192.78	165.31
4	304.15	275.53
5	137.27	0.0
ONE METER FROM THE HI-TRAC VW		
1	122.06	0.40
2	240.70	3.10
3	128.50	86.95
4	174.25	153.49
5	63.13	0.0

Notes:

- Refer to Figure 5.1.2 for dose locations.
- Dose rates are based on no water within the MPC, an empty annulus, and a water jacket full of water. For the majority of the duration that the HI-TRAC bottom lid is installed, the MPC cavity will be flooded with water. The water within the MPC greatly reduces the dose rate
- Includes the BPRAs from both the active and non-active region.

5.5 REGULATORY COMPLIANCE

Chapters 1 and 2 and this chapter of this SAR describe in detail the shielding structures, systems, and components (SSCs) important to safety.

The shielding-significant SSCs important to safety have been evaluated in this chapter and their impact on personnel and public health and safety resulting from operation of an independent spent fuel storage installation (ISFSI) utilizing the HI-STORM FW system has been evaluated.

It has been shown that the design of the shielding system of the HI-STORM FW system is in compliance with 10CFR72 and that the applicable design and acceptance criteria including 10CFR20 have been satisfied. Thus, this shielding evaluation provides reasonable assurance that the HI-STORM FW system will allow safe storage of spent fuel in full conformance with 10CFR72.

5.6 REFERENCES

[5.1.1] LA-UR-03-1987, MCNP — A General Monte Carlo N-Particle Transport Code, Version 5, April 24, 2003 (Revised 10/3/05).

[5.1.2] I.C. Gauld, O.W. Hermann, "SAS2: A Coupled One-Dimensional Depletion and Shielding Analysis Module," ORNL/TM-2005/39, Version 5.1, Vol. I, Book 3, Sect. S2, Oak Ridge National Laboratory, November 2006.

[5.1.3] I.C. Gauld, O.W. Hermann, R.M. Westfall, "ORIGEN-S: SCALE System Module to Calculate Fuel Depletion, Actinide Transmutation, Fission Product Buildup and Decay, and Associated Radiation Source Terms," ORNL/TM-2005/39, Version 5.1, Vol. II, Book 1, Sect. F7, Oak Ridge National Laboratory, November 2006.

[5.2.1] NUREG-1536, SRP for Dry Cask Storage Systems, USNRC, Washington, DC, January 1997.

[5.2.2] A.G. Croff, M.A. Bjerke, G.W. Morrison, L.M. Petrie, "Revised Uranium-Plutonium Cycle PWR and BWR Models for the ORIGEN Computer Code," ORNL/TM-6051, Oak Ridge National Laboratory, September 1978.

[5.2.3] A. Luksic, "Spent Fuel Assembly Hardware: Characterization and 10CFR 61 Classification for Waste Disposal," PNL-6906-vol. 1, Pacific Northwest Laboratory, June 1989.

[5.2.4] J.W. Roddy et al., "Physical and Decay Characteristics of Commercial LWR Spent Fuel," ORNL/TM-9591/V1&R1, Oak Ridge National Laboratory, January 1996.

[5.2.5] "Characteristics of Spent Fuel, High Level Waste, and Other Radioactive Wastes Which May Require Long-Term Isolation," DOE/RW-0184, U.S. Department of Energy, December 1987.

[5.2.6] Not Used.

[5.2.7] "Characteristics Database System LWR Assemblies Database," DOE/RW-0184-R1, U.S. Department of Energy, July 1992.

[5.2.8] O. W. Hermann, et al., "Validation of the Scale System for PWR Spent Fuel Isotopic Composition Analyses," ORNL/TM-12667, Oak Ridge National Laboratory, March 1995.

[5.2.9] M. D. DeHart and O. W. Hermann, "An Extension of the Validation of SCALE (SAS2H) Isotopic Predictions for PWR Spent Fuel," ORNL/TM-13317, Oak Ridge National Laboratory, September 1996.

[5.2.10] O. W. Hermann and M. D. DeHart, "Validation of SCALE (SAS2H) Isotopic Predictions for BWR Spent Fuel," ORNL/TM-13315, Oak Ridge National Laboratory, September 1998.

[5.2.11] "Summary Report of SNF Isotopic Comparisons for the Disposal Criticality Analysis Methodology," B00000000-01717-5705-00077 REV 00, CRWMS M&O, September 1997.

[5.2.12] "Isotopic and Criticality Validation of PWR Actinide-Only Burnup Credit," DOE/RW-0497, U.S. Department of Energy, May 1997.

[5.2.13] B. D. Murphy, "Prediction of the Isotopic Composition of UO_2 Fuel from a BWR: Analysis of the DU1 Sample from the Dodewaard Reactor," ORNL/TM-13687, Oak Ridge National Laboratory, October 1998.

[5.2.14] O. W. Hermann, et al., "Technical Support for a Proposed Decay Heat Guide Using SAS2H/ORIGEN-S Data," NUREG/CR-5625, ORNL-6698, Oak Ridge National Laboratory, September 1994.

[5.2.15] C. E. Sanders, I. C. Gauld, "Isotopic Analysis of High-Burnup PWR Spent Fuel Samples from the Takahama-3 Reactor," NUREG/CR-6798, ORNL/TM-2001/259, Oak Ridge National Laboratory, January 2003.

[5.2.16] Not Used.

[5.2.17] HI-2002444, Rev. 7, "Final Safety Analysis Report for the HI-STORM 100 Cask System", USNRC Docket 72-1014.

[5.4.1] "American National Standard Neutron and Gamma-Ray Flux-to-Dose Rate Factors", ANSI/ANS-6.1.1-1977.

[5.4.2] D. J. Whalen, et al., "MCNP: Photon Benchmark Problems," LA-12196, Los Alamos National Laboratory, September 1991.

[5.4.3] D. J. Whalen, et al., "MCNP: Neutron Benchmark Problems," LA-12212, Los Alamos National Laboratory, November 1991.

[5.4.4] J. C. Wagner, et al., "MCNP: Criticality Safety Benchmark Problems," LA-12415, Los Alamos National Laboratory, October 1992.

[5.4.5] S. E. Turner, "Uncertainty Analysis - Axial Burnup Distribution Effects," presented in "Proceedings of a Workshop on the Use of Burnup Credit in Spent Fuel Transport Casks," SAND-89-0018, Sandia National Laboratory, Oct. 1989.

[5.4.6] Commonwealth Edison Company, Letter No. NFS-BND-95-083, Chicago, Illinois.

[5.4.7] B.L. Broadhead, "Recommendations for Shielding Evaluations for Transport and Storage Packages," NUREG/CR-6802 (ORNL/TM-2002/31), Oak Ridge National Laboratory, May 2003.

[5.4.8] HI-2012610, Rev. 3, "Final Safety Analysis Report for the HI-STAR 100 Cask System", USNRC Docket 72-1008.

[5.4.9] HI-2073681, Rev. 3, "Safety Analysis Report on the HI-STAR 180 Package", USNRC Docket 71-9325.

APPENDIX 5.A

SAMPLE INPUT FILES FOR SAS2H, ORIGEN-S, AND MCNP

SAS2H SAMPLE INPUT FILE

(b)(4)

(b)(4)

ORIGEN-S SAMPLE INPUT FILE

(b)(4)

(b)(4)

(b)(4)

(b)(4)

(b)(4)

(b)(4)

(b)(4)

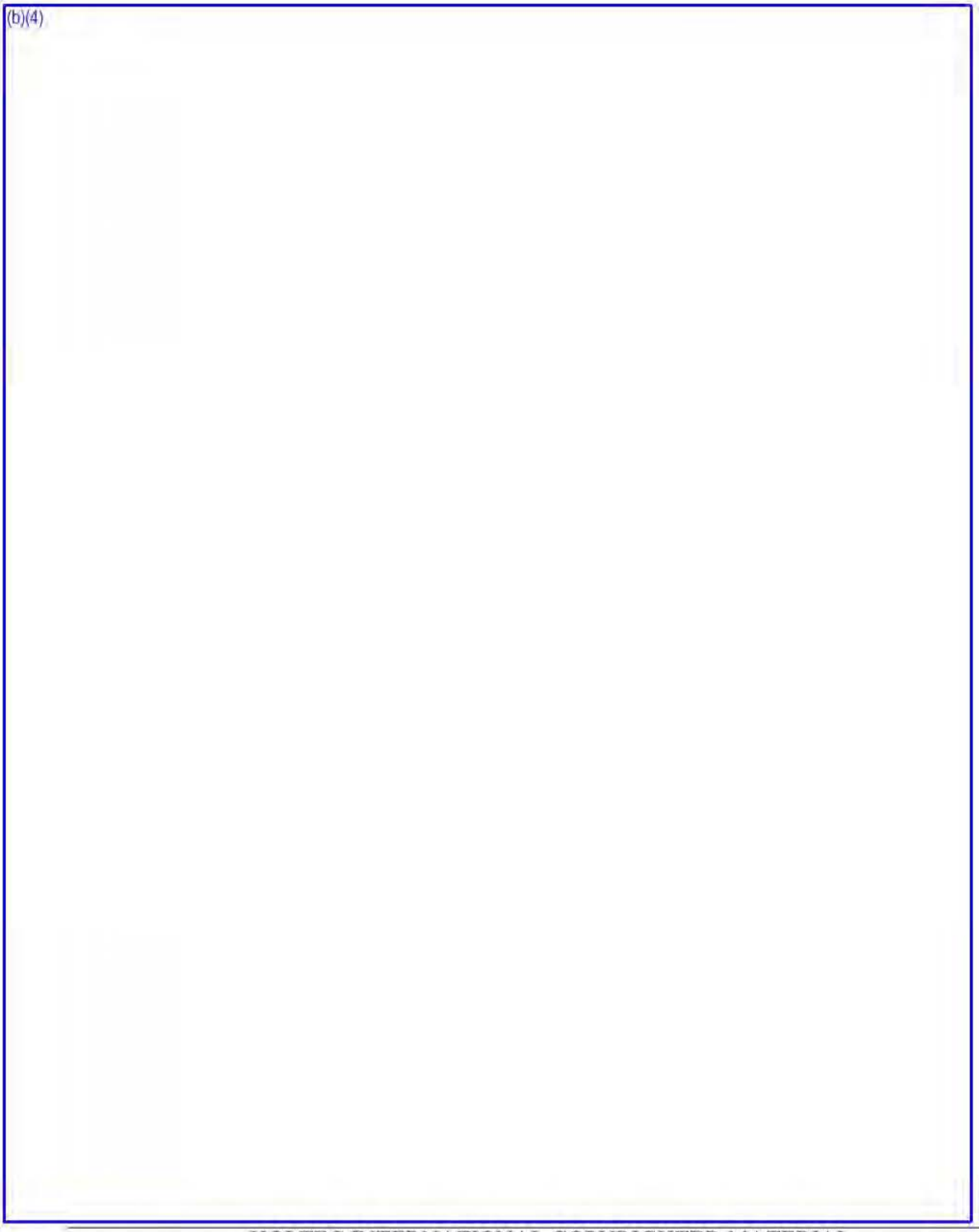

(b)(4)

(b)(4)

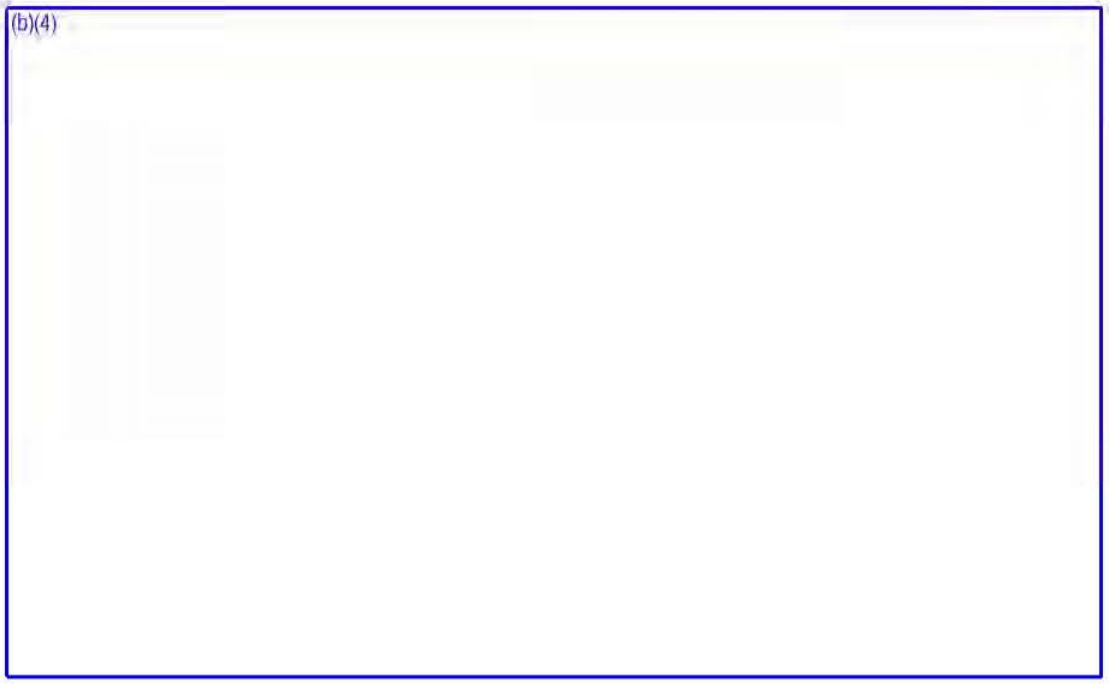

MCNP SAMPLE INPUT FILE

(b)(4)

(b)(4)

(b)(4)

(b)(4)

(b)(4)

(b)(4)

(b)(4)

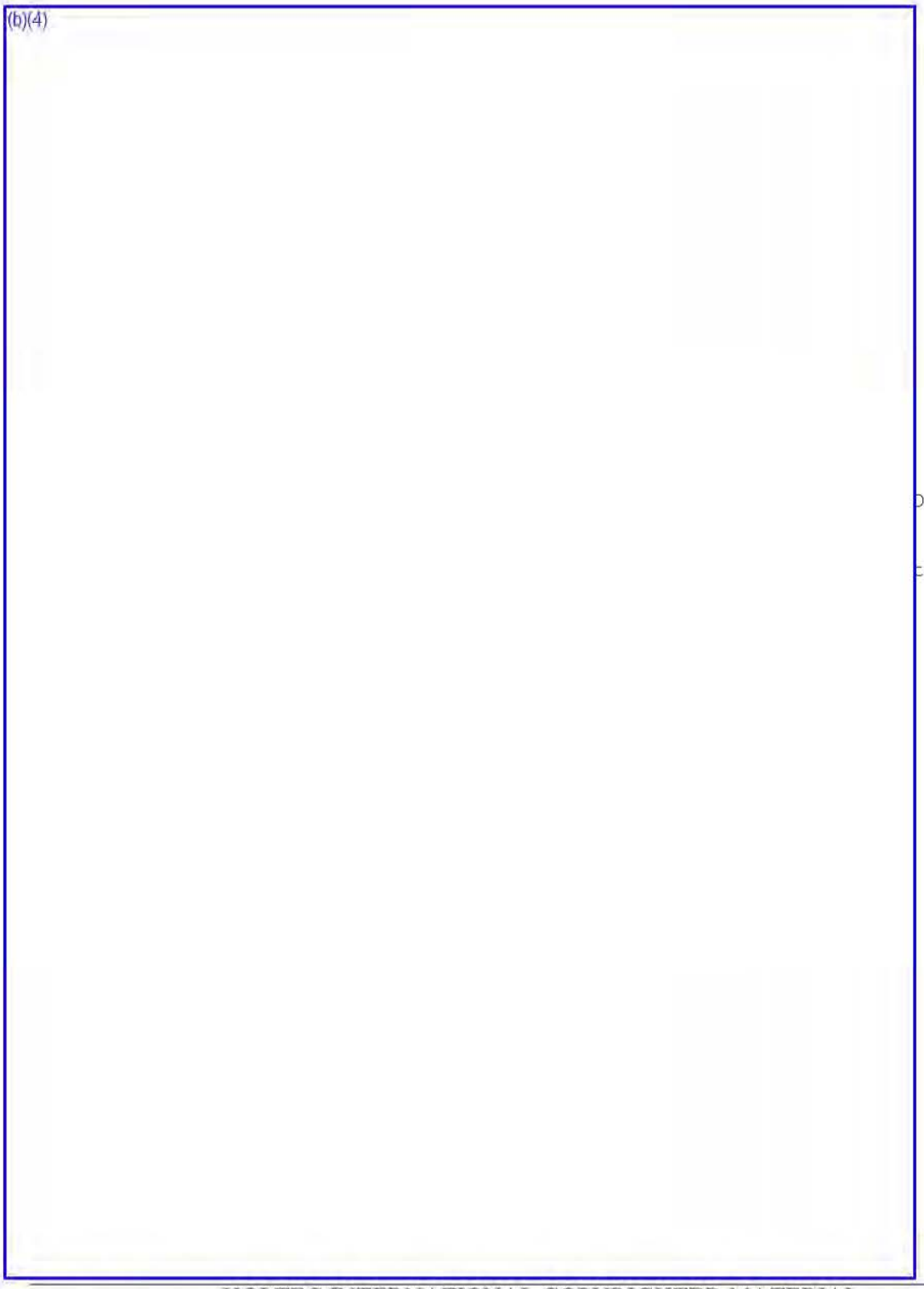

(b)(4)

(b)(4)

(b)(4)

(b)(4)

(b)(4)

(b)(4)

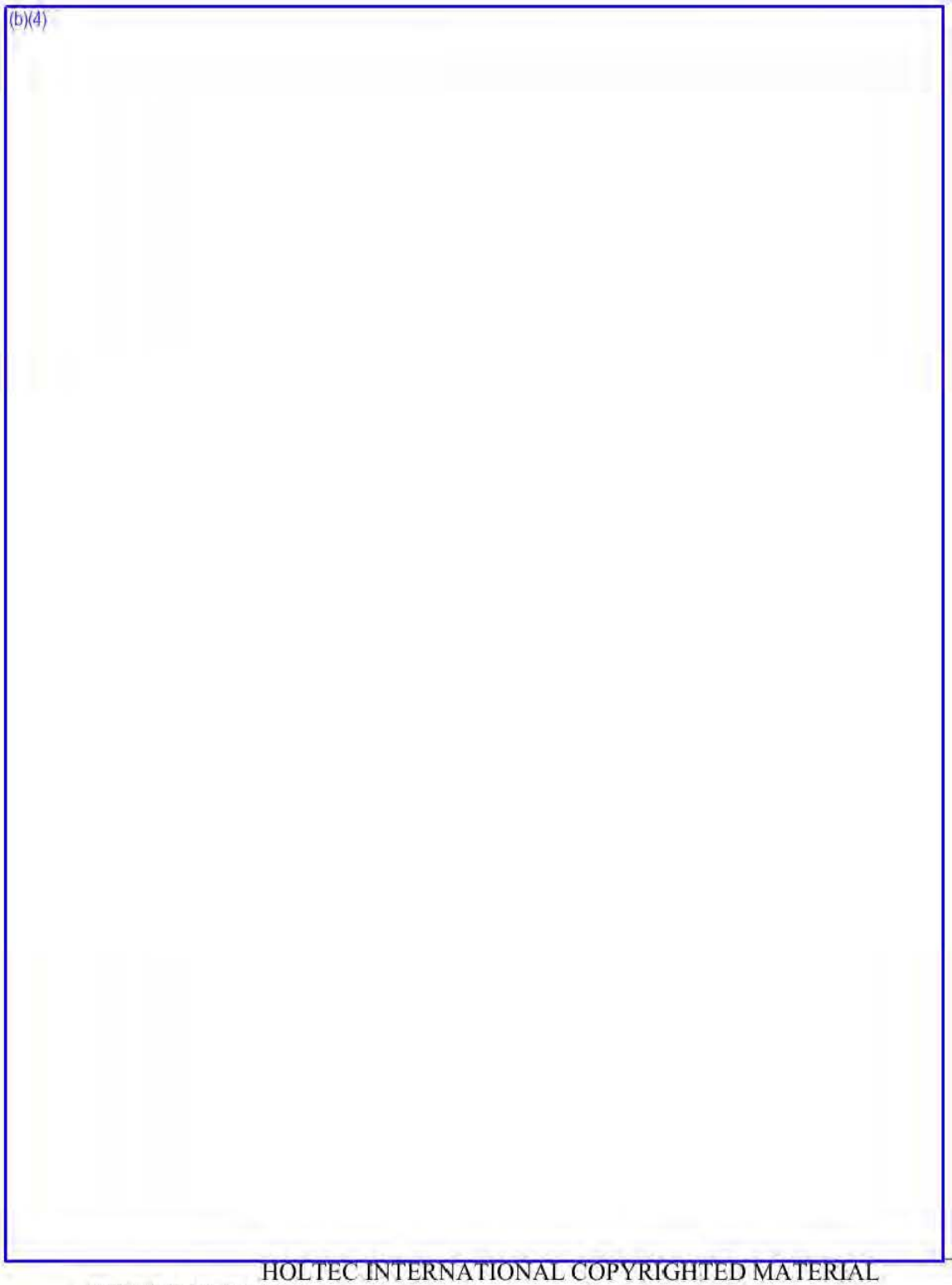

(b)(4)

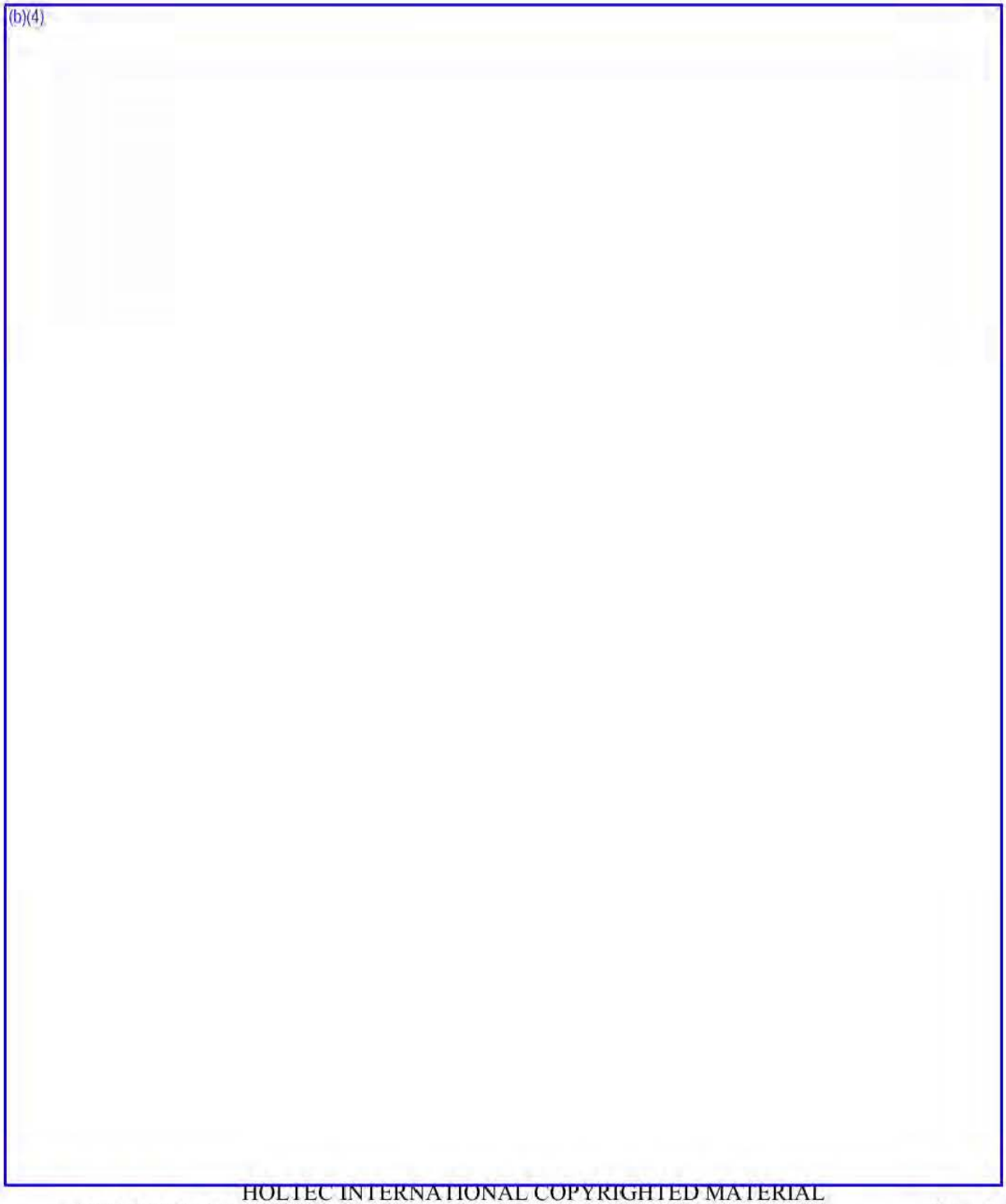

(b)(4)

(b)(4)

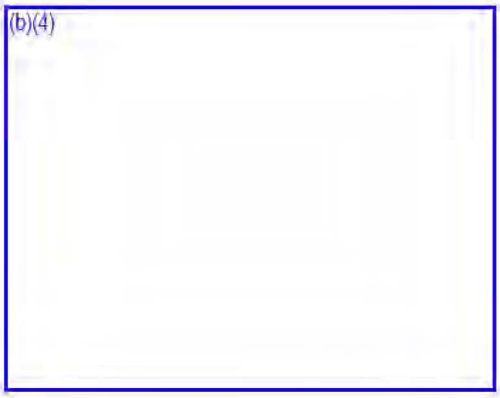

CHAPTER 6†: CRITICALITY EVALUATION

6.0 INTRODUCTION

This chapter documents the criticality evaluation of the HI-STORM FW system for the storage of spent nuclear fuel in accordance with 10CFR72.124 [6.1.2]. The evaluation shows that the maximum k_{eff} value, including all applicable biases and uncertainties is below 0.95 for all normal, off-normal and accident conditions. This demonstrates that the HI-STORM FW system meets the criticality safety requirements of 10CFR72 [6.1.2] and the Standard Review Plan for Dry Cask Storage Systems (NUREG-1536) [6.1.1].

In addition, this chapter describes the HI-STORM FW system design structures and components important to criticality safety and defines the limiting fuel characteristics in sufficient detail to provide a sufficient basis for the evaluation of the package.

Note that the analysis methodologies and modeling assumptions are identical to those utilized in the licensing of the HI-STORM 100 system in Docket No. 72-1014 ([6.0.1], Chapter 6), except for the following:

- A newer version of the Monte Carlo code MCNP, namely MCNP5, is used, together with the corresponding cross-sections. The benchmark calculations were updated accordingly.

The safety analyses summarized in this chapter demonstrate acceptable margins to the allowable limits under all design basis loading conditions and operational modes. Minor changes to the design parameters that inevitably occur during the product's life cycle which are treated within the purview of 10CFR72.48 and are ascertained to have an insignificant effect on the computed safety factors may not prompt a formal reanalysis and revision of the results and associated data in the tables of this chapter unless the cumulative effect of all such unquantified changes on the reduction of any of the computed safety margins cannot be deemed to be insignificant. For purposes of this determination, an insignificant loss of safety margin with reference to an

---

† This chapter has been prepared in the format and section organization set forth in Regulatory Guide 3.61. However, the material content of this chapter also fulfills the requirements of NUREG-1536. Pagination and numbering of sections, figures, and tables are consistent with the convention set down in Chapter 1, Section 1.0, herein. Finally, all terms-of-art used in this chapter are consistent with the terminology of the Glossary and component nomenclature of the Bill-of-Materials (Section 1.5).

Evaluations and results presented in this chapter are supported by documented calculation package(s) [6.0.2].

acceptance criterion is defined as the estimated reduction that is no more than one order of magnitude below the available margin reported in the FSAR. To ensure rigorous configuration control, the information in the Licensing drawings in Section 1.5 should be treated as the authoritative source for numerical analysis at all times. Reliance on the input data and associated results in this chapter for additional mathematical computations may not be appropriate as they serve the sole purpose of establishing safety compliance in accordance with the acceptance criteria set down in Chapter 2 and in this chapter.

6.1 DISCUSSION AND RESULTS

In conformance with the principles established in NUREG-1536 [6.1.1] and 10CFR72.124 [6.1.2], the results in this chapter demonstrate that the effective multiplication factor (k_{eff}) of the HI-STORM FW system, including all biases and uncertainties evaluated with a 95% probability at the 95% confidence level, does not exceed 0.95 under all credible normal, off-normal, and accident conditions. Moreover, the results demonstrate that the HI-STORM FW system is designed and maintained such that at least two unlikely, independent, and concurrent or sequential changes must occur to the conditions essential to criticality safety before a nuclear criticality accident is possible. These criteria provide a large subcritical margin, sufficient to assure the criticality safety of the HI-STORM FW system when fully loaded with fuel of the highest permissible reactivity.

Criticality safety of the HI-STORM FW system depends on the following four principal design parameters:

1. The inherent geometry of the fuel basket designs within the MPC;

2. The fuel basket structure which is made entirely of the Metamic-HT neutron absorber material;

3. An administrative limit on the maximum enrichment for PWR fuel and maximum planar-average enrichment for BWR fuel; and

4. An administrative limit on the minimum soluble boron concentration in the water for loading/unloading fuel in the PWR fuel basket.

The off-normal and accident conditions defined in Chapter 2 and considered in Chapter 12 have no adverse effect on the design parameters important to criticality safety, except for the non-mechanistic tip-over event, which could result in limited plastic deformation of the basket. However, a bounding basket deformation is already included in the criticality models for normal conditions, and thus, from the criticality safety standpoint, the off-normal and accident conditions are identical to those for normal conditions.

The HI-STORM FW system is designed such that the fixed neutron absorber will remain effective for a storage period greater than 60 years, and there are no credible mechanisms that would cause its loss or a diminution of its effectiveness (see Chapter 8, specifically Section 8.9, and Section 10.1.6.3 for further information on the qualification and testing of the neutron absorber material). Therefore, in accordance with 10CFR72.124(b), there is no need to provide a surveillance or monitoring program to verify the continued efficacy of the neutron absorber.

Criticality safety of the HI-STORM FW system does not rely on the use of any of the following aids to the reduction of reactivity present in the storage system:

- burnup of fuel
- fuel-related burnable neutron absorbers
- more than 90 percent of the B-10 content for the Metamic-HT fixed neutron absorber undergirded by comprehensive tests as described in Subsection 10.1.6.3.

The HI-STORM FW system consists of the HI-STORM FW storage cask, the HI-TRAC VW transfer cask and Multi-Purpose-Canisters (MPCs) for PWR and BWR fuel (see Chapter 1, Table 1.0.1). Both the HI-TRAC VW transfer cask and the HI-STORM FW storage cask accommodate the interchangeable MPC designs. The HI-STORM FW storage cask uses concrete as a shield for both gamma and neutron radiation, while the HI-TRAC VW uses lead and steel for gamma radiation and a water-filled jacket for neutron shielding. The design details can be found in the drawing packages in Section 1.5.

While the MPCs are in the HI-STORM FW cask during storage, they are internally dry (no moderator), and thus, the reactivity is very low ($k_{eff} \sim 0.6$). However, the MPCs are flooded for loading and unloading operations in the HI-TRAC VW cask, which represents the limiting case in terms of reactivity. Therefore, the majority of the analyses have been performed with the MPCs in a HI-TRAC VW cask, and only selected cases have been performed for the HI-STORM FW cask.

Confirmation of the criticality safety of the HI-STORM FW system was accomplished with the three-dimensional Monte Carlo code MCNP5 [6.1.4]. K-factors for one-sided statistical tolerance limits with 95% probability at the 95% confidence level were obtained from the National Bureau of Standards (now NIST) Handbook 91 [6.1.5].

To assess the reactivity effects due to temperature changes, CASMO-4, a two-dimensional transport theory code [6.1.6] for fuel assemblies was used. CASMO-4 was not used for quantitative information, but only to qualitatively indicate the direction and approximate magnitude of the reactivity effects.

Benchmark calculations were made to compare the primary code package (MCNP5) with experimental data, using critical experiments selected to encompass, insofar as practical, the design parameters of the HI-STORM FW system. The most important parameters are (1) the enrichment, (2) cell spacing, (3) the ^{10}B loading of the neutron absorber panels, and (4) the soluble boron concentration in the water (for PWR fuel). The critical experiment benchmarking work is summarized in Appendix 6.A.

To assure the true reactivity will always be less than the calculated reactivity, the following conservative design criteria and assumptions were made:

- The MPCs are assumed to contain the most reactive fresh fuel authorized to be loaded into a specific basket design.

- No credit for fuel burnup is assumed, either in depleting the quantity of fissile nuclides or in producing fission product.

- The fuel stack density is assumed to be at 97.5% of the theoretical density for all criticality analyses. This is a conservative value, since it corresponds to a very high pellet density of 99% or more of the theoretical density. Note that this difference between stack and pellet density is due to the necessary dishing and chamfering of the pellets.

- No credit is taken for the ^{234}U and ^{236}U in the fuel.

- When flooded, the moderator is assumed to be water, with or without soluble boron, at a temperature and density corresponding to the highest reactivity within the expected operating range.

- When credit is taken for soluble boron, a ^{10}B content of 18.0 wt% in boron is assumed.

- Neutron absorption in minor structural members is neglected, i.e., spacer grids are replaced by water. This is conservative since studies presented in Section 6.2.1 show that all assemblies are undermoderated, and that the reduction in the amount of (borated or unborated) water within the fuel assembly always results in a reduction of the reactivity. The presence of any other structural material, which would reduce the amount of water, is therefore bounded by those studies, and neglecting this material is conservative. Additionally, the potential neutron absorption of those materials is neglected.

- Consistent with NUREG-1536, the worst hypothetical combination of tolerances (most conservative values within the range of acceptable values), as identified in Section 6.3, is assumed.

- When flooded, the fuel rod pellet-to-clad gap regions are assumed to be flooded with pure unborated water.

- Planar-averaged enrichments are assumed for BWR fuel. Analyses are presented that demonstrate that the use of planar-averaged enrichments is appropriate.

- Consistent with NUREG-1536, fuel-related burnable neutron absorbers, such as the Gadolinia normally used in BWR fuel and IFBA normally used in PWR fuel, are neglected.

- For evaluation of the bias and bias uncertainty, two approaches are utilized. One where the results of the benchmark calculations are used directly and one where benchmark calculations that result in a k_{eff} greater than 1.0 are conservatively truncated to 1.0000. Consistent with NUREG-1536, the larger of the combined bias and bias uncertainty of the two approaches is used.

- The water reflector above and below the fuel is assumed to be unborated water, even if borated water is used in the fuel region.

- For fuel assemblies that contain low-enriched axial blankets, the governing enrichment is that of the highest planar average, and the blankets are not included in determining the average enrichment.

- Regarding the position of assemblies in the basket, configurations with centered and eccentric positioning of assemblies in the fuel storage locations are considered.

- For undamaged fuel assemblies, as defined in the Glossary, all fuel rod positions are assumed to contain a fuel rod. To qualify assemblies with missing fuel rods, those missing fuel rods must be replaced with dummy rods that displace a volume of water that is equal to, or larger than, that displaced by the original rods.

- For DFCs with damaged fuel or fuel debris, a large ID is used. This is conservative, since it maximizes the area of the optimum moderated fuel.

The design basis criticality safety calculations are performed for a single internally flooded HI-TRAC VW transfer cask with full water reflection on all sides (limiting cases for the HI-STORM FW system), for fuel assemblies listed in Chapter 2, are conservatively evaluated for the worst combination of manufacturing tolerances (as identified in Section 6.3), and include the calculational bias, uncertainties, and calculational statistics. In addition, a few results for single internally dry (no moderator) HI-STORM FW storage casks with full water reflection on all external surfaces of the overpack, including the annulus region between the MPC and overpack, are performed to confirm the low reactivity of the HI-STORM FW system in storage.

Note that throughout this chapter reactivity results are stated as maximum neutron multiplication factor values (k_{eff}) conservatively evaluated for the worst combination of manufacturing tolerances (as identified in Section 6.3), and including the calculational bias, uncertainties, and calculational statistics, unless otherwise noted.

For undamaged fuel, and for each of the MPC designs under flooded conditions (HI-TRAC VW), minimum soluble boron concentration (if applicable) and fuel assembly classes[††], Tables 6.1.1, 6.1.2 and 6.1.6 list the bounding maximum k_{eff} value, and the associated maximum allowable

[††] The assembly classes for BWR and PWR fuel are defined in Section 6.2.

enrichment. Tables 6.1.1 and 6.1.2 provide the information for undamaged fuel without known or suspected cladding defects larger than pinhole leaks or hairline cracks, while Table 6.1.6 provides the information for low-enriched, channeled BWR undamaged fuel without known or suspected grossly breached fuel rods. The maximum allowed enrichments and the minimum soluble boron concentrations are also cited in Subsection 2.1.

For MPCs in the HI-STORM FW under dry conditions, results are listed in Table 6.1.3 for selected assembly classes.

For MPCs loaded with a combination of undamaged and damaged fuel assemblies under flooded conditions, results are listed in Tables 6.1.4 and 6.1.5. For each of the MPC designs, the tables indicate the maximum number of DFCs and list the fuel assembly classes, the bounding maximum k_{eff} value, the associated maximum allowable enrichment, and if applicable the minimum soluble boron concentration. Allowed enrichments are also cited in Subsection 2.1.

These results confirm that the maximum k_{eff} values for the HI-STORM FW system are below the limiting design criteria ($k_{eff} < 0.95$) when fully flooded and loaded with any of the candidate fuel assemblies and basket configurations. Analyses for the various conditions of flooding that support the conclusion that the fully flooded condition corresponds to the highest reactivity, and thus is most limiting, are presented in Section 6.4. The capability of the HI-STORM FW system to safely accommodate damaged fuel and fuel debris is demonstrated in Subsection 6.4.4. The capability of the HI-STORM FW to accommodate low enriched, channeled BWR fuel as undamaged fuel demonstrated in Subsection 6.4.9.

Accident conditions have also been considered and no credible accident has been identified that would result in exceeding the design criteria limit on reactivity. After the MPC is loaded with spent fuel, it is seal-welded and cannot be internally flooded. The HI-STORM FW System for storage is dry (no moderator) and the reactivity is very low. For arrays of HI-STORM FW storage casks, the radiation shielding and the physical separation between overpacks due to the large diameter and cask pitch preclude any significant neutronic coupling between the casks.

For PWR fuel in the MPC-37, soluble boron in the water is credited. There is a strict administrative control on the soluble boron concentration during loading and unloading of the MPC, consisting of frequent and independent measurements (For details see Subsections 9.2.2, 9.2.3, 9.2.4, and 9.4.3 and the bases for LCO 3.3.1 in Chapter 13). An accidental loss of soluble boron is therefore not credible and hence not considered.

TABLE 6.1.1

BOUNDING MAXIMUM k_{eff} VALUES FOR EACH ASSEMBLY CLASS IN THE MPC-37 (HI-TRAC VW)

Fuel Assembly Class	4.0 wt% ^{235}U Maximum Enrichment†		5.0 wt% ^{235}U Maximum Enrichment†	
	Minimum Soluble Boron Concentration (ppm)	Maximum k_{eff}	Minimum Soluble Boron Concentration (ppm)	Maximum k_{eff}
14x14A	1000	0.8946	1500	0.8983
14x14B	1000	0.9213	1500	0.9282
14x14C	1000	0.9211	1500	0.9277
15x15B	1500	0.9129	2000	0.9311
15x15C	1500	0.9029	2000	0.9188
15x15D	1500	0.9223	2000	0.9421
15x15E	1500	0.9206	2000	0.9410
15x15F	1500	0.9244	2000	0.9455
15x15H	1500	0.9142	2000	0.9325
15x15I	1500	0.9155	2000	0.9362
16x16A	1000	0.9275	1500	0.9366
16x16A[DFC][1]	1000	0.9400	1600	0.9404
16x16B	1000	0.9258	1500	0.9334
16x16C	1000	0.9099	1500	0.9187
17x17A	1500	0.9009	2000	0.9194
17x17B	1500	0.9181	2000	0.9380
17x17C	1500	0.9222	2000	0.9424
17x17D	1500	0.9183	2000	0.9384
17x17E	1500	0.9203	2000	0.9392

† For maximum allowable enrichments between 4.0 wt% ^{235}U and 5.0 wt% ^{235}U, the minimum soluble boron concentration may be calculated by linear interpolation between the minimum soluble boron concentrations specified for each assembly class.

[1] Intact Fuel Assembly Class 16x16A loaded in DFCs in all 37 cell locations, if permitted by the certificate of compliance.

TABLE 6.1.2

BOUNDING MAXIMUM k_{eff} VALUES FOR EACH ASSEMBLY CLASS IN THE MPC-89 (HI-TRAC VW)

Fuel Assembly Class	**Maximum Allowable Planar-Average Enrichment (wt% ^{235}U)**	**Maximum k_{eff}**
7x7B	4.8	0.9317
8x8B	4.8	0.9369
8x8C	4.8	0.9399
8x8D	4.8	0.9380
8x8E	4.8	0.9281
8x8F	4.5	0.9328
9x9A	4.8	0.9421
9x9B	4.8	0.9410
9x9C	4.8	0.9338
9x9D	4.8	0.9342
9x9E/F	4.5	0.9346
9x9G	4.8	0.9307
10x10A	4.8	0.9435
10x10B	4.8	0.9417
10x10C	4.8	0.9389
10x10F	4.7	0.9440
10x10G	4.6	0.9466

TABLE 6.1.3

REPRESENTATIVE k_{eff} VALUES FOR MPC-37 AND MPC-89 IN THE HI-STORM FW OVERPACK

MPC	**Fuel Assembly Class**	**Maximum Allowable Planar-Average Enrichment (wt% ^{235}U)**	**Maximum k_{eff}**
MPC-37	17x17B	5.0	0.6076
MPC-89	10x10A	4.8	0.3986

TABLE 6.1.4

BOUNDING MAXIMUM k_{eff} VALUES FOR THE MPC-37
WITH UP TO 12 DFCs

Fuel Assembly Class of Undamaged Fuel	**4.0 wt% ^{235}U Maximum Enrichment for Undamaged Fuel and Damaged Fuel/Fuel Debris †**		**5.0 wt% ^{235}U Maximum Enrichment for Undamaged Fuel and Damaged Fuel/Fuel Debris †**	
	Minimum Soluble Boron Concentration (ppm)	**Maximum k_{eff}**	**Minimum Soluble Boron Concentration (ppm)**	**Maximum k_{eff}**
All 14x14, 16x16A††	1300	0.9155	1800	0.9305
All 15x15, all 17x17	1800	0.9032	2300	0.9276

† For maximum allowable enrichments between 4.0 wt% ^{235}U and 5.0 wt% ^{235}U, the minimum soluble boron concentration may be calculated by linear interpolation between the minimum soluble boron concentrations specified for each assembly class.

†† For assembly class 16x16A intact fuel can be loaded with or without DFCs, if permitted in the certificate of compliance.

TABLE 6.1.5

BOUNDING MAXIMUM k_{eff} VALUES FOR THE MPC-89
WITH UP TO 16 DFCs

Fuel Assembly Class	**Maximum Allowable Planar-Average Enrichment (wt% ^{235}U)**	**Maximum k_{eff}**
All BWR Classes except 8x8F, 9x9E/F, 10x10F and 10x10G	4.8	0.9464
8x8F, 9x9E/F and 10x10G	4.0	0.9299
10x10F	4.6	0.9428

TABLE 6.1.6

BOUNDING MAXIMUM k_{eff} VALUES FOR THE MPC-89
WITH LOW ENRICHED, CHANNELED BWR FUEL

Fuel Assembly Class	**Maximum Allowable Planar-Average Enrichment (wt% ^{235}U)**	**Maximum k_{eff}**
All BWR Classes	3.3	0.9325

6.2 SPENT FUEL LOADING

Due to the large number of minor variations in the fuel assembly dimensions, the use of explicit dimensions in defining the authorized contents could limit or complicate the applicability of the HI-STORM FW system. To resolve this limitation, a number of fuel assembly classes for both fuel types (PWR and BWR) are defined based on bounding fuel dimensions. The results of parametric studies justify using those bounding fuel dimensions for defining the authorized contents.

6.2.1 Definition of Assembly Classes

For each array size the fuel assemblies have been subdivided into a number of defined classes, where a class is defined in terms of (1) the number of fuel rods; (2) pitch; and (3) number and locations of guide tubes (PWR) or water rods (BWR). The assembly classes for PWR and BWR fuel are defined in Chapter 2, Tables 2.1.2 and 2.1.3, respectively. It should be noted that these assembly classes are consistent with the class designations in the HI-STORM 100 FSAR (Docket No. 72-1014). Specifically, assembly classes with the same identifier refer to the same set of limiting dimensions. However, some classes have been removed and others have been added compared to the HI-STORM 100.

In HI-STORM 100 FSAR (Docket No. 72-1014), extensive analyses of fuel dimensional variations have been performed. These calculations demonstrate that the maximum reactivity corresponds to:

- maximum active fuel length,
- maximum fuel pellet diameter,
- maximum fuel rod pitch,
- minimum cladding outside diameter (OD),
- maximum cladding inside diameter (ID),
- minimum guide tube/water rod thickness, and
- maximum channel thickness (for BWR assemblies only).

The reason that those are bounding dimensions, i.e. that they result in maximum reactivity is directly based on, and can be directly derived from the three main characteristics affecting reactivity, namely 1) characteristics of the fission process; 2) the characteristics of the fuel assemblies and 3) the characteristics of the neutron absorber in the basket. These affect the reactivity as follows:

- The neutrons generated by fission are fast neutrons while the neutrons that initiate the fission need to be thermal neutrons. A moderator (water) is therefore necessary for the nuclear chain reaction to continue.

- Fuel assemblies are predominantly characterized by the amount of fuel and the fuel-to-water (moderator) ratio. Increasing the amount of fuel, or the enrichment of the fuel, will increase the amount of fissile material, and therefore increase reactivity. Regarding the fuel-to-water ratio, it is important to note that commercial PWR and BWR assemblies are undermoderated, i.e. they do not contain enough water for a maximum possible reactivity.
- The neutron poison in the basket walls uses B-10, which is an absorber of thermal neutrons. This poison therefore also needs water (moderator) to be effective. This places a specific importance on the amount of water between the outer rows of the fuel assemblies and the basket cell walls. Note that this explains some of the differences in reactivity between the different assembly types in the same basket, even for the same enrichment, where assemblies with a smaller cross section, i.e. which have more water between the periphery of the assembly and the surrounding wall, generally have a lower reactivity.

Based on these characteristics, the following conclusions can be made:

- Since fuel assemblies are undermoderated, any changes in geometry inside the fuel assembly that increases the amount of water while maintaining the amount of fuel are expected to increase reactivity. This explains why reducing the cladding or guide tube/water rod thicknesses, or increasing the fuel rod pitch results in an increase in reactivity.
- Increasing the active length will increase the amount of fuel while maintaining the fuel-to-water ratio, and therefore increase reactivity.
- The channel of the BWR assembly is a structure located outside of the rod array. It therefore does not affect the water-to-fuel ratio within the assembly. However, it reduces the amount of water between the assembly and the neutron poison, therefore reducing the effective thermalization for the poison. Therefore, an increase of the channel wall thickness will increase reactivity.
- In respect to the effect of the fuel pellet diameter, several compensatory effects need to be considered. Increasing the diameter will tend to increase the reactivity due to the increase in the fuel amount. However, it will also change the fuel-to-water-ratio, and will therefore make the fuel more undermoderated, which in turn tends to reduce reactivity. The effect of this change in moderation may depend on the condition of the pellet-to-clad gap. Assuming an empty pellet-to clad gap, which would be consistent with undamaged fuel rods, the change in moderation is small, and the net effect is an increase in reactivity, since the effect of the increase in the fissionable material dominates. In this case, the maximum pellet diameter is more reactive. When the pellet-to-clad gap is conservatively flooded, as recommended by NUREG 1536 (see section 6.4.2.3), a reduction of the fuel pellet diameter will also result in an increase in the amount of water, i.e. have a double effect on the water-to-fuel ratio. In this case, it is possible that a slight reduction may result in no reduction or even an increase in reactivity. However, this is caused by a further amplification of the conservative assumption of the flooded pellet-to-clad gap, not by a positive increase in reactivity from the reduction in fuel (which would be counter-

intuitive). Therefore, in order not to overstate the conservative effect of the flooded fuel-to-clad gap, the calculations for the variation of the fuel pellet diameter are performed for a flooded gap of constant thickness by also changing the clad ID.

Since all assemblies have the same principal design, i.e. consist of bundles of cladded fuel rods, most of them with embedded guide/instrument tubes or water rods or channels, the above conclusions apply to all of them, and the bounding dimensions are therefore also common to all fuel assemblies analyzed here. Nevertheless, to clearly demonstrate that the main assumption is true, i.e. that all assemblies are undermoderated, a study was performed for all assembly types where the pellet-to-clad gap is empty instead of being flooded (a conservative assumption for the design basis calculations, see Section 6.4.2.3) The results are listed in Table 6.2.3, in comparison with the results of the reference cases with the flooded gap from Section 6.1 for those assembly types. In all cases, the reactivity is reduced compared to the reference case. This verifies that all assembly types considered here are in fact undermoderated, and therefore validates the main assumption stated above. All assembly types are therefore behaving in a similar fashion, and the bounding dimensions are therefore applicable to all assembly types. This discussion and the corresponding conclusions not only affect fuel behavior, but also other moderation effects, and is therefore further referenced in Section 6.3.1 and 6.4.2

As a result, the authorized contents in Subsection 2.1 are defined in terms of those bounding assembly parameters for each class.

Nevertheless, to further demonstrate that the aforementioned characteristics are in fact bounding for the HI-STORM FW, parametric studies were performed on reference PWR and BWR assemblies, namely PWR assembly class 17x17B and BWR assembly class 10x10A. The results of these studies are shown in Table 6.2.1 and 6.2.2, and verify the bounding parameters listed above. Note that in the studies presented in Tables 6.2.1 and 6.2.2, the fuel pellet diameter and cladding inner diameter are changed together. This is to keep the cladding-to-pellet gap, which is conservatively flooded with pure water in all cases (see Section 6.4.2.3), at a constant thickness, to ensure the studies evaluate the fuel parameters rather than the moderation conditions, as discussed above.

In addition to those dimensions, additional fuel assembly characteristics important to criticality control are the location of guide tubes, water rods, part length rods, and rods with differing dimensions (classes 9x9E/F only). These are identified in the assembly cross sections provided in Appendix 6.B, Section B.4.

In all cases, the gadolinia (Gd_2O_3) normally incorporated in BWR fuel, and Integral Fuel Burnable Absorbers (IFBA) used in PWR fuel was conservatively neglected.
Some assembly classes contain partial length rods. There are differences in location of those partial length rods within the assembly that influence how those rods affect reactivity: Assembly classes 9x9A, 10x10A, 10x10B and 10x10F have partial length rods that are completely surrounded by full length rods, whereas assembly class 10x10G has those partial length rods on the periphery of the assembly or facing the water gap, where they directly only face two full

length rods (see Appendix 6.B, Section B.4). To determine a bounding configuration for those assembly classes where partial length rods are completely surrounded by full length rods, calculations are listed in Table 6.2.2 for the actual (real) assembly configuration and for the axial segments (assumed to be full length) with and without the partial length rods. The results show that the configurations with only the full length rods present, i.e. where the partial length rods are assumed completely absent from the assembly, is bounding. This is an expected outcome, since LWR assemblies are typically undermoderated, therefore reducing the fuel-to-water-ratio within the rod array tends to increase reactivity. Consequently, all assembly classes that contain partial length rods surrounded by full-length rods are analyzed with the partial length rods absent. For assembly class 10x10G, calculations with different assumptions for the length of the part-length rods are presented in Table 6.2.7, and show that reducing the length of the part length rods reduces reactivity. This means that the reduction in the fuel amount is more dominating than the change in moderation for this configuration. For this class, all rods therefore are assumed full length. Note that in neither of the cases is the configuration with the actual part length rods bounding. The specification of the authorized contents has therefore no minimum requirement for the active fuel length of the partial length rods.

BWR assemblies are specified in Table 2.1.3 with a maximum planar-average enrichment. The analyses presented in this chapter use a uniform enrichment, equal to the maximum planar-average. Analyses presented in the HI-STORM FSAR ([6.0.1], Chapter 6, Appendix 6.B) show that this is a conservative approach, i.e. that a uniform enrichment bounds the planar-average enrichment in terms of the maximum k_{eff}. To verify that this is applicable to the HI-STORM FW, those calculations were re-performed in the MPC-89. The results are presented in Table 6.2.4, and show that, as expected, the planar average enrichments bound or are statistically equivalent to the distributed enrichment in the HI-STORM FW as they do in the HI-STORM 100. To confirm that this is also true for the higher enrichments analyzed here, additional calculations were performed and are presented in Table 6.2.2 in comparison with the results for the uniform enrichment. Since the maximum planar-average enrichment of 4.8 wt% ^{235}U is above the actual enrichments of those assemblies, actual (as-built) enrichment distributions are not available. Therefore, several bounding cases are analyzed. Note that since the maximum planar-average enrichment of 4.8 wt% ^{235}U is close to the maximum rod enrichment of 5.0 wt% ^{235}U, the potential enrichment variations within the cross section are somewhat limited. To maximize the differences in enrichment under these conditions, the analyzed cases assume that about 50% of the rods in the cross section are at an enrichment of 5.0 wt% ^{235}U, while the balance of the rods are at an enrichment of about 4.6 wt%, resulting in an average of 4.8 wt%. Calculations are performed for cross sections where all full-length and part-length, or only all full-length rods are present. For each case, two conditions are analyzed that places the different enrichment in areas with different local fuel-to-water ratios. Specifically, one condition places the higher enriched rods in locations where they are more surrounded by other rods, whereas the other condition places them in locations where they are more surrounded by water, such as near the water-rods or the periphery of the assembly. The results are also included in table 6.2.2 and show that in all cases, the maximum k_{eff} calculated for the distributed enrichments are statistically equivalent to or below those for the uniform enrichments. Therefore, modeling BWR assemblies with distributed enrichments using a uniform enrichment equal to the planar-average value is

acceptable and conservative. The assumed enrichment distributions analyzed are shown in Appendix 6.B.

Note that for some BWR fuel assembly classes, the Zircaloy water rod tubes are artificially replaced by water in the bounding cases to remove the requirement for water rod thickness from the specification of the authorized contents. For these cases, the bounding water rod thickness is listed as zero.

Two BWR classes (8x8B and 8x8D) are specified with slight variation in the number of fuel and/or water rods (see Section 6.B.4). The results listed in Section 6.1 utilize the minimum number of fuel rods, i.e. maximizing the water-to-fuel ratio. To show that this is appropriate and bounding, calculations were also performed with the alternative configurations, and are presented in Table 6.2.5. The results show that the reference conditions used for the calculations documented in Section 6.1 are in fact bounding.

For BWR assembly class 9x9E/F, two patterns of water rods were analyzed (see Section 6.B.4). The comparison is also presented in Table 6.2.5 and shows that the condition with the larger water rod spacing is bounding.

For PWR assembly class 15x15I (see Section 6.B.4), calculations with and without guide rods were performed. The comparison is also presented in Table 6.2.5. The case without the guide rods is used as the design basis case for this assembly type, therefore, no specific restrictions on the location and number of guide rods exists. The 15x15I fuel assembly class also includes versions with reduced number of fuel rods in specific locations, specifically; two versions with 212 fuel rods and one version with 208 fuel rods (see Section 6.B.4 for the specific fuel cross-sections). The missing fuel rods can be replaced with water or guide tubes. The comparison for the reduced number of fuel rods in 15x15I fuel class is shown in Table 6.2.5.

Typically, PWR fuel assemblies are designed with solid fuel pellets throughout the entire active fuel length. However, some PWR assemblies contain annular fuel pellets in the top and bottom 6 to 8 inches of the active fuel length. This changes the fuel to water ratio in these areas, which could have an effect on reactivity. However, the top and bottom of the active length are areas with high neutron leakage, and changes in these areas typically have no significant effect on reactivity. Studies with up to 12 inches of annular pellets at the top and bottom performed for the HI-STORM FW with various pellet IDs (see Table 6.2.6) confirm this, i.e., shown no significant reactivity effects, even if the annular region of the pellet is flooded with pure water. All calculations for PWR fuel assemblies are therefore performed with solid fuel pellets along the entire length of the active fuel region, and the results are directly applicable to those PWR assemblies with annular fuel pellets. This is consistent with the HI-STORM 100, where the same analyzed conditions are analyzed and qualified.

TABLE 6.2.1

REACTIVITY EFFECT OF ASSEMBLY PARAMETER VARIATIONS in PWR Fuel in the MPC-37 with 2000 ppm soluble boron concentration
(all dimensions are in inches)

Fuel Assembly/ Parameter Variation	reactivity effect	Maximum k_{eff}	standard deviation
17x17B (5.0 wt% Enrichment)	Reference	0.9374	0.0004
increase pellet OD and clad ID (+0.004)	0.0052	0.9426	0.0003
decrease pellet OD and Clad ID (-0.004)	-0.0058	0.9316	0.0004
increase clad OD (+0.004)	-0.0014	0.9360	0.0004
decrease clad OD (-0.004)	0.0017	0.9391	0.0004
increase guide tube thickness (+0.004)	-0.0001	0.9373	0.0004
decrease guide tube thickness (-0.004)	0.0004	0.9378	0.0003
remove guide tubes (i.e., replace the guide tubes with water)	0.0009	0.9383	0.0004
reduced active length (100 Inches)	-0.0020	0.9354	0.0004
increase rod pitch (+0.004)	0.0019	0.9393	0.0004
reduce rod pitch (-0.004)	-0.0017	0.9357	0.0004

TABLE 6.2.2

REACTIVITY EFFECT OF ASSEMBLY PARAMETER VARIATIONS for BWR Fuel in the MPC-89
(all dimensions are in inches)

Fuel Assembly/ Parameter Variation	reactivity effect	Maximum k_{eff}	standard deviation
10x10A (Reference, full-length rods only)	Reference	0.9429	0.0004
increase pellet OD and Clad ID (+0.004)	0.0037	0.9466	0.0004
decrease pellet OD and Clad ID (-0.004)	-0.0042	0.9387	0.0004
increase clad OD (+0.004)	-0.0021	0.9408	0.0003
decrease clad OD (-0.004)	0.0032	0.9461	0.0004
increase water rod thickness (+0.004)	0.0002	0.9431	0.0004
decrease water rod thickness (-0.004)	0.0009	0.9438	0.0004
remove water rods (i.e., replace the water rod tubes with water)	0.0031	0.9460	0.0004
reduced active length (100 Inches)	-0.0026	0.9403	0.0004
remove channel	-0.0113	0.9316	0.0003
increase channel thickness (+0.020)	0.0007	0.9436	0.0003
full-length and part-length rods (real assembly)	-0.0054	0.9375	0.0004
part-length rods extended to full-length	-0.0102	0.9327	0.0004
increased rod pitch (+0.004)	0.0050	0.9479	0.0004
reduced rod pitch (-0.004)	-0.0043	0.9386	0.0003
distributed enrichment, Case 1	-0.0011	0.9418	0.0003
distributed enrichment, Case 2	+0.0004	0.9433	0.0003
distributed enrichment, Case 3	-0.0099	0.9330	0.0004
distributed enrichment, Case 4	-0.0121	0.9308	0.0003

TABLE 6.2.3

EFFECT OF THE FLOODING OF THE PELLET-TO-CLAD GAP

Fuel Assembly Class	Maximum k_{eff} at 5.0 wt% ^{235}U Maximum Enrichment		
	Flooded Pellet-to-Clad Gap	Empty Pellet-to-Clad Gap	Difference
14x14A	0.8983	0.8962	-0.0021
14x14B	0.9282	0.9235	-0.0047
14x14C	0.9277	0.9237	-0.0038
15x15B	0.9311	0.9284	-0.0027
15x15C	0.9188	0.9164	-0.0024
15x15D	0.9421	0.9386	-0.0035
15x15E	0.9410	0.9371	-0.0039
15x15F	0.9455	0.9408	-0.0047
15x15H	0.9325	0.9300	-0.0025
15x15I	0.9357	0.9305	-0.0052
16x16A	0.9366	0.9284	-0.0082
16x16A[DFC]	0.9400	0.9340	-0.0060
16x16B	0.9334	0.9297	-0.0037
16x16C	0.9187	0.9144	-0.0043
17x17A	0.9194	0.9160	-0.0034
17x17B	0.9380	0.9335	-0.0045
17x17C	0.9424	0.9375	-0.0049
17x17D	0.9384	0.9323	-0.0061
17x17E	0.9392	0.9346	-0.0046

TABLE 6.2.3 (continued)

EFFECT OF THE FLOODING OF THE PELLET-TO-CLAD GAP

Fuel Assembly Class	Maximum k_{eff}		
	Flooded Pellet-to-Clad Gap	Empty Pellet-to-Clad Gap	Difference
7x7B	0.9317	0.9261	-0.0056
8x8B	0.9369	0.9318	-0.0051
8x8C	0.9399	0.9331	-0.0068
8x8D	0.9380	0.9334	-0.0046
8x8E	0.9281	0.9230	-0.0051
8x8F	0.9328	0.9275	-0.0053
9x9A	0.9421	0.9370	-0.0051
9x9B	0.9410	0.9292	-0.0118
9x9C	0.9338	0.9290	-0.0048
9x9D	0.9342	0.9294	-0.0048
9x9E/F	0.9346	0.9261	-0.0085
9x9G	0.9307	0.9250	-0.0057
10x10A	0.9435	0.9391	-0.0044
10x10B	0.9417	0.9317	-0.0100
10x10C	0.9389	0.9333	-0.0056
10x10F	0.9440	0.9395	-0.0045
10x10G	0.9466	0.9408	-0.0058

Table 6.2.4

COMPARISON CALCULATIONS FOR BWR FUEL WITH AVERAGE AND DISTRIBUTED ENRICHMENTS

Case	Planar Average Enrichment (wt%)	Peak Rod Enrichment (wt%)	Maximum k_{eff}	
			Planar Average Enrichment (wt%)	Peak Rod Enrichment (wt%)
8x8C	3.01	3.80	0.8358	0.8309
8x8C	3.934	4.9	0.8975	0.8899
8x8D	3.42	3.95	0.8628	0.8636
8x8D	3.78	4.40	0.8862	0.8855
8x8D	3.90	4.90	0.8934	0.8913
9x9B	4.34	4.71	0.9195	0.9179
9x9D	3.35	4.34	0.8575	0.8456
Hypothetical #1 (48 outer rods of 3.967%E, 14 inner rods of 5.0%)	4.20	5.00	0.9104	0.9102
Hypothetical #2 (48 outer rods of 4.354%E, 14 inner rods of 5.0%)	4.50	5.00	0.9258	0.9247

Table 6.2.5

VARIATIONS OF NUMBER OF FUEL AND/OR WATER RODS FOR ASSEMBLY CLASSES 8x8B AND 8x8D (see Appendix B)

Case	**Maximum k_{eff}**
Assembly Class 8x8B	
63 Fuel Rods (Reference)	0.9369
64 Fuel Rods	0.9342
Assembly Class 8x8D	
60 Fuel Rods, no water rods modeled (Reference)	0.9380
60 Fuel Rods, 2 larger, 2 smaller water rods	0.9362
60 Fuel Rods, 4 larger water rods	0.9347
60 Fuel Rods, 4 smaller water rods	0.9359
60 Fuel Rods, 1 large water rods	0.9343
61 Fuel Rods, 3 water rods	0.9354

VARIATION OF WATER ROD LOCATIONS FOR ASSEMBLY CLASS 9x9E/F (see Appendix B)

Case	**Maximum k_{eff}**
Adjacent Water Rods (Reference)	0.9346
Water Rods separated by a Fuel Rod	0.9313

VARIATION OF GUIDE RODS FOR ASSEMBLY CLASS 15x15I (see Appendix B)

Case	**Maximum k_{eff}**
No Guide Rods (Reference)	0.9362
8 Guide Rods	0.9259

Table 6.2.5 (continued)

BOUNDING MAXIMUM k_{eff} FOR REDUCED NUMBER OF FUEL RODS FOR ASSEMBLY CLASS 15x15I (see Appendix B)

Fuel Assembly Class **15x15I**	**4.0 wt% ^{235}U Maximum Enrichment**		**5.0 wt% ^{235}U Maximum Enrichment**	
	Minimum Soluble Boron Concentration (ppm)	**Maximum k_{eff}**	**Minimum Soluble Boron Concentration (ppm)**	**Maximum k_{eff}**
15x15I(Reference) 216 Fuel Rods	1500	0.9155	2000	0.9362
15x15I-1 212 Fuel Rods	1500	0.9131	2000	0.9330
15x15I-2 212 Fuel Rods	1500	0.9115	2000	0.9317
15x15I-3 208 Fuel Rods	1500	0.9101	2000	0.9290

Table 6.2.6

EFFECT OF ANNULAR PELLETS IN THE TOP AND BOTTOM 12 INCHES OF THE ACTIVE REGION

Diameter of Annulus in Pellets	**Maximum k_{eff}**
Assembly Class 17x17B, 5% Enrichment, Undamaged Fuel	
None (Reference)	0.9380
0.1 Inches	0.9382
0.2 Inches	0.9379
0.3 Inches	0.9371
0.4 Inches	0.9371
0.5 Inches	0.9363
0.6 Inches	0.9368
Assembly Class 16x16A, 5% Enrichment, Damaged and Undamaged Fuel	
None (Reference)	0.9163
0.2 Inches	0.9162
Assembly Class 15x15F, 5% Enrichment, Damaged and Undamaged Fuel	
None (Reference)	0.9276
0.2 Inches	0.9266

Table 6.2.7

EFFECT OF PARTIAL LENGTH RODS FOR ASSEMBLY CLASS 10x10G

Length of Partial Length Rods as a Percentage of Full Length Rods	**Maximum k_{eff}**
100%	0.9466
75%	0.9455
50%	0.9404
25%	0.9286
0%	0.9208

6.3 MODEL SPECIFICATION

6.3.1 Description of Calculational Model

Figures 6.3.1 through 6.3.5 show representative cross sections of the criticality models for the two baskets. Figures 6.3.1 and 6.3.2 show a single cell from each of the two baskets. Figures 6.3.3 and 6.3.4 show the entire MPC-37 and MPC-89 basket, respectively. Figure 6.3.5 shows a sketch of the calculational model in the axial direction.

Full three-dimensional calculational models were used for all calculations. The calculational models explicitly define the fuel rods and cladding, the guide tubes, water rods and the channel (for the BWR assembly), the neutron absorber walls of the basket cells, and the surrounding MPC shell and overpack. For the flooded condition (loading and unloading), pure, unborated water was assumed to be present in the fuel rod pellet-to-clad gaps, since this represents the bounding condition as demonstrated in Section 6.4.2.3. Appendix 6.B provides sample input files for typical MPC basket designs

Note that the water thickness above and below the fuel is modeled as unborated water, even when borated water is present in the fuel region.

The discussion provided in Section 6.2.1 regarding the principal characteristics of fuel poison is also important for the various studies presented in this section, and supports the fact that those studies only need to be performed for a single BWR and PWR assembly type, and that the results of those studies are then generally applicable to all assembly types. The studies and the relationship to the discussion in Section 6.2.1 are listed below. Note that this approach is consistent with that used for the HI-STORM 100.

Basket Manufacturing Tolerance: The two aspects of the basket tolerance that are evaluated are the cell wall thickness and the cell ID. The reduced cell wall thickness results in a reduced amount of poison (since the material composition of the wall is fixed), and therefore in an increase in reactivity. The reduced cell ID reduces amount of water between the fuel the poison, and therefore the effectiveness of the poison material. Both effects are simply a function of the geometry, and are independent of the fuel type.

Panel Gaps: Similar to the basket manufacturing tolerance for the cell wall thickness, this tolerance has a small effect on the overall poison amount of the basket, which would affect the reactivity of the system independent of the fuel type.

Eccentric positioning (see Section 6.3.3): When a fuel assembly is located in the center of a basket cell, it is surrounded by equal amounts of water on all sides, and hence the thermalization of the neutrons that occur between the assembly and the poison in the cell wall, and hence the effectiveness of the poison, is also equal on all sides. For an eccentric positioning, the

effectiveness of the poison is now reduced on those sides where the assembly is located close to the cell walls, and increased on the opposite sides. This creates a compensatory situation for a single cell, where the net effect is not immediately clear. However, for the entire basket, and for the condition where all assemblies are located closest to the center of the basket, the four assemblies at the center of the basket are now located close to each other, separated by poison plates with a reduced effectiveness since they are not surrounded by water on any side. This now becomes the dominating condition is terms of reactivity increase. This effect is also applicable to all assembly types, since those assemblies are all located close to the center of the basket, i.e. the eccentric position with all assemblies moved towards the center will be bounding regardless of the assembly type.

Wall thicknesses of DFCs: DFCs are used for damaged fuel and fuel debris in selected locations of the basket, but are also permitted to be used for intact fuel of the array/type 16x16A. Generally, DFCs are thin-walled containers, in order to minimize the additional weight to be supported by the basket. For damaged fuel and fuel debris calculations, a wall thickness of 0.025" is used, and studies with larger wall thicknesses show an insignificant effect. However, when DFCs are also used for intact assemblies of the 16x16A array/type, it is shown that there is a noticeable effect when a thicker wall is modeled. Consequently, for DFCs for intact 16x16A fuel, a conservative DFC wall thickness of 0.075" is used to provide manufacturing flexibility. Note that this already a rather thick wall, the same as typically used for storage racks in spent fuel pools, and would therefore present a practical upper limit for any DFC design.

The basket geometry can vary due to manufacturing tolerances and due to potential deflections of basket walls as the result of accident conditions. The basket tolerances are defined on the drawings in Chapter 1. The structural acceptance criteria for the basket during accident conditions is that the permanent deflection of the basket panels is limited to a fraction of 0.005 (0.5%) of the panel width (see Chapter 3). The analyses in Chapter 3 demonstrate that permanent deformations of the basket walls during accident conditions are far below this limit. In fact, the analyses show that the vast majority of the basket panels remain elastic during and after an accident, and therefore show no permanent deflection whatsoever, and that any deformation is limited to small localized areas. Nevertheless, it is conservatively assumed that 2 adjacent cell walls in each cell are deflected to the maximum extent possible over their entire length and width, i.e. that the cell ID is reduced by 0.5% of the cell width, or 0.045" for the MPC-37 cells and 0.030" for the MPC-89 cells. Stated differently, the minimum cell ID based on tolerances was further reduced by the amounts stated above for all cells in each basket to account for the potential deflections of basket walls during accident conditions. Assuming that all cell sizes are reduced is a simplifying, but very conservative assumption, since cell walls are shared between neighboring cells, so while the deflection of a basket wall would reduce the cell size on one side, it necessarily increases that on the other side of the wall. MCNP5 was used to determine the manufacturing tolerances and deflections that produced the most adverse effect on criticality. After the reactivity effect (positive effect with an increase in reactivity; or negative effect with a decrease in reactivity) of the manufacturing tolerances was determined, the criticality analyses were performed using the worst case conditions in the direction which would increase reactivity.

For simplification, the same worst case conditions are used for both normal and accident conditions. For all calculations, fuel assemblies were assumed to be eccentrically located in the cells, since this results in higher reactivities (see Section 6.3.3). Maximum k_{eff} results (including the bias, uncertainties, or calculational statistics), along with the selected dimensions, for a number of dimensional combinations are shown in Table 6.3.2 for both baskets. The cell ID is evaluated for minimum (tolerance only), minimum with deformation, nominal and an increased value. The wall thickness is evaluated for nominal and minimum values.

Based on the calculations, the conservative dimensional assumptions listed in Table 6.3.3 were determined for the basket designs. Because the reactivity effect (positive or negative) of the manufacturing tolerances is not assembly dependent, these dimensional assumptions were employed for all criticality analyses.

The basket is manufactured from individual slotted panels. The panels are expected to be in direct contact with each other (see Drawings in Chapter 1). However, to show that small gaps between panels would have essentially no effect on criticality, calculations are performed with a postulated 0.06" gap between panels, repeated in the axial direction every 10" in all panels. Since it is expected that the effect of these gaps would be small, these calculations were performed with a larger number of particles per cycle, larger number of inactive cycles, and a larger total number of cycles to improve the statistics of each run, so the real reactivity effect could be better separated from the statistical "noise". The results are summarized in Tables 6.3.6 and show that the METAMIC gap has a very small effect. Therefore, all calculations are performed without any gaps between panels.

Variations of water temperature in the cask were analyzed using CASMO-4. The analyses were performed for the assembly class 10x10A in the MPC-89, and for the assembly class 17x17B with 2000 ppm soluble boron in the water in the MPC-37. These are the same assemblies and conditions used for the fuel dimension studies in Section 6.2, and shown there to be representative of all assemblies qualified for those baskets. The results are presented in Table 6.3.1, and show that the minimum water temperature (corresponding to a maximum water density) are bounding. This condition is therefore used in all further calculations. This is expected since an increased temperature results in a reduced water density, a condition that is shown in Section 6.4 to result in reduced reactivities.

Calculations documented in Chapter 3 show that the baskets stay within the applicable structural limits during all normal and accident conditions. Furthermore, the neutron poison material is an integral and non-removable part of the basket material, and its presence is therefore not affected by the accident conditions. Except for the potential deflection of the basket walls that is already considered in the criticality models, damage to the cask under accident conditions is limited to possible loss of the water in the water jacket of he HI-TRAC VW. However, this condition is already considered in the calculational models. Other parameters important to criticality safety are fuel type and enrichment, which are not affected by the hypothetical accident conditions. The calculational models of the cask and basket for the accident conditions are therefore identical to

the models for normal conditions, and no separate models need to be developed for accident conditions.

6.3.2 Cask Regional Densities

Composition of the various components of the principal designs of the HI-STORM FW system are listed in Table 6.3.4. The cross section set for each nuclide is listed in Table 6.3.8, and is consistent with the cross section sets used in the benchmarking calculations documented in Appendix A. Note that these are the default cross sections chosen by the code.

The HI-STORM FW system is designed such that the fixed neutron absorber will remain effective for a storage period greater than 60 years, and there are no credible means to lose it.

The continued efficacy of the fixed neutron absorber is assured by acceptance testing, documented in Subsection 10.1.6.3, to validate the ^{10}B (poison) concentration in the fixed neutron absorber. To demonstrate that the neutron flux from the irradiated fuel results in a negligible depletion of the poison material over the storage period, an evaluation of the number of neutrons absorbed in the ^{10}B was performed. The calculation conservatively assumed a constant neutron source for 60 years equal to the initial source for the design basis fuel, as determined in Section 5.2, and shows that the fraction of ^{10}B atoms destroyed is less than 10^{-7} in 60 years. Thus, the reduction in ^{10}B concentration in the fixed neutron absorber by neutron absorption is negligible. Therefore, in accordance with 10CFR72.124(b), there is no need to provide a surveillance or monitoring program to verify the continued efficacy of the neutron absorber.

6.3.3 Eccentric Positioning of Assemblies in Fuel Storage Cells

The potential reactivity effect of eccentric positioning of assemblies in the fuel storage locations is accounted for in a conservatively bounding fashion, as described further in this subsection The calculations in this subsection serve to identify the eccentric positioning of assemblies in the fuel storage locations, which results in a higher maximum k_{eff} value than the centered positioning. For the cases where the eccentric positioning results in a higher maximum k_{eff} value, the eccentric positioning is used for all corresponding cases reported in the summary tables in Section 6.1 and the results tables in Section 6.4.

To conservatively account for eccentric fuel positioning in the fuel storage cells, three different configurations are analyzed, and the results are compared to determine the bounding configuration:

- Cell Center Configuration: All assemblies centered in their fuel storage cell;
- Basket Center Configuration: All assemblies in the basket are moved as close to the center of the basket as permitted by the basket geometry; and

- Basket Periphery Configuration: All assemblies in the basket are moved furthest away from the basket center, and as close to the periphery of the basket as possible.

It should be noted that the two eccentric configurations are hypothetical, since there is no known physical phenomenon that could move all assemblies within a basket consistently to the center or periphery. However, since the configurations listed above bound all credible configurations, they are conservatively used in the analyses.

In Table 6.3.5, results are presented for all representative conditions. The table shows the maximum k_{eff} value for centered and the two eccentric configurations for each condition, and the difference in k_{eff} between the centered and eccentric positioning. In all cases, moving the assemblies and DFCs to the periphery of the basket results in a reduction in reactivity, compared to the cell centered position, and moving the assemblies and DFCs towards the center results in an increase in reactivity, compared to the cell centered position. All calculations are therefore performed with assemblies/DFCs moved towards the center of the basket.

TABLE 6.3.1

CASMO-4 CALCULATIONS FOR EFFECT OF TEMPERATURE

Change in Nominal Parameter	Δk Maximum Tolerance		Action/Modeling Assumption
	MPC-37, 17x17B, 5.0 wt%, Borated Water with 2000 ppm Soluble Boron	MPC-89, 10x10A, 4.8 wt%, Fresh Water	
Increase in Temperature			Assume 20°C
20°C	Ref.	Ref.	
40°C	-0.0008	-0.0035	
70°C	-0.0023	-0.0100	
100°C	-0.0042	-0.0180	
10% Void in Moderator			Assume no void
20°C with no void	Ref.	Ref.	
20°C	-0.0036	-0.0282	
100°C	-0.0096	-0.0463	

TABLE 6.3.2

EVALUATION OF BASKET MANUFACTURING TOLERANCES

Box I.D.	**Box Wall Thickness**	**Maximum k_{eff}**
MPC-37 (17x17B, 5.0% Enrichment)		
nominal (8.94")	nominal (0.59")	0.9332
nominal (8.94")	minimum (0.57”)	0.9346
increased (8.96")	minimum (0.57”)	0.9350
minimum (8.92")	minimum (0.57”)	0.9352
minimum, including deformation (8.875")	minimum (0.57”)	0.9374
MPC-89 (10x10A 4.8% Enrichment)		
nominal (6.01")	nominal (0.40")	0.9365
nominal (6.01")	minimum (0.38”)	0.9403
increased (6.03")	minimum (0.38”)	0.9396
minimum (5.99")	minimum (0.38”)	0.9417
minimum, including deformation (5.96")	minimum (0.38”)	0.9428

TABLE 6.3.3

BASKET DIMENSIONAL ASSUMPTIONS

Basket Type	Box I.D.	Box Wall Thickness
MPC-37	minimum, including deformation(8.875")	minimum (0.57")
MPC-89	minimum, including deformation (5.96")	minimum (0.38")

TABLE 6.3.4

COMPOSITION OF THE MAJOR COMPONENTS OF THE HI-STORM FW SYSTEM

UO_2, DENSITY 10.686 g/cm^3 (97.5% of theoretical density of 10.96 g/cm^3)					
Nuclide	**Wgt. Fraction, 4.0 wt%**	**Wgt. Fraction, 4.5 wt%**	**Wgt. Fraction, 4.7 wt%**	**Wgt. Fraction, 4.8 wt%**	**Wgt. Fraction, 5.0 wt%**
8016	0.1185	0.1185	0.1185	0.1185	0.1185
92235	0.03526	0.03967	0.04143	0.04231	0.04408
92238	0.84624	0.84183	0.84007	0.83919	0.83742

WATER (unborated and borated), DENSITY 1.0 g/cm^3							
Nuclide	**Wgt. Fraction, 0 ppm**	**Wgt. Fraction, 1000 ppm**	**Wgt. Fraction, 1300 ppm**	**Wgt. Fraction, 1500 ppm**	**Wgt. Fraction, 1800 ppm**	**Wgt. Fraction, 2000 ppm**	**Wgt. Fraction, 2300 ppm**
5010	0.000E+00	1.800E-04	2.340E-04	2.700E-04	3.240E-04	3.600E-04	4.140E-04
5011	0.000E+00	8.200E-04	1.066E-03	1.230E-03	1.476E-03	1.640E-03	1.886E-03
1002	0.11190	0.11179	0.11175	0.11173	0.11170	0.11167	0.11164
8016	0.88810	0.88721	0.88695	0.88677	0.88650	0.88633	0.88606

METAMIC HT, 9% B_4C, DENSITY 2.6 g/cm^3	
Nuclide	**Wgt. Fraction**
13027	0.91
6000	0.01956
5010	0.01289
5011	0.05755

TABLE 6.3.4 (continued)

COMPOSITION OF THE MAJOR COMPONENTS OF THE HI-STORM FW SYSTEM

ZR CLAD, DENSITY 6.55 g/cm^3	
Nuclide	**Wgt. Fraction**
40000	1.0
STAINLESS STEEL, DENSITY 7.84 g/cm^3	
Nuclide	**Wgt. Fraction**
24000	0.190
25055	0.020
26000	0.695
28000	0.095
ALUMINUM, DENSITY 2.7 g/cm^3	
Nuclide	**Wgt. Fraction**
13027	1.0
CONCRETE, DENSITY 2.35 g/cm^3	
Nuclide	**Wgt. Fraction**
1001	0.006
8016	0.500
11000	0.017
13027	0.048
14000	0.315
19000	0.019
20000	0.083
26000	0.012
LEAD, DENSITY 11.34 g/cm^3	
Nuclide	**Wgt. Fraction**
82000	1.0

TABLE 6.3.5

REACTIVITY EFFECTS OF ECCENTRIC POSITIONING OF CONTENT
(FUEL ASSEMBLIES AND DFCs) IN BASKET CELLS

CASE	Contents centered (Reference)	Content moved towards center of basket		Content moved towards basket periphery	
	Maximum k_{eff}	Maximum k_{eff}	k_{eff} Difference to Reference	Maximum k_{eff}	k_{eff} Difference to Reference
MPC-37, Undamaged Fuel	0.9327	0.9380	0.0053	0.9143	-0.0184
MPC-37, Undamaged Fuel and Damaged Fuel/Fuel Debris (12 DFCs)	0.9260	0.9276	0.0016	0.9158	-0.0102
MPC-89, Undamaged Fuel	0.9369	0.9435	0.0066	0.9211	-0.0158
MPC-89, Undamaged Fuel and Damaged Fuel/Fuel Debris (16 DFCs)	0.9415	0.9451	0.0036	0.9301	-0.0114

TABLE 6.3.6

REACTIVITY EFFECTS GAPS IN BASKET CELL PLATES

Gaps in Metamic-HT	**MPC-37 (17x17B, 5.0% ENRICHMENT)**	**MPC-89 (10x10A, 4.8% ENRICHMENT)**
None	0.9380	0.9435
0.06” every 10”	0.9382	0.9439

TABLE 6.3.7

RADIAL AND AXIAL DIMENSIONS OF THE HI-TRAC VW IN THE MCNP MODELS

Component / Material	Thickness (Inches)
Radial Direction (Inside to Outside)	
MPC Shell (Steel)	0.5
Water between MPC and HI-TRAC VW	0.125
HI-TRAC VW Shell (Steel)	0.75
HI-TRAC VW Lead	2.75
HI-TRAC VW Shell (Steel)	0.75
HI-TRAC VW Water Jacket	4.75
HI-TRAC VW Shell (Steel)	0.5
External Water Reflector	12
Axial Direction (Bottom to Top)	
External Water Reflector	12
HI-TRAC VW Bottom Lid (Steel)	5.5
MPC Base Plate (Steel)	3
Water	2
Active Fuel Region	150
Water	6
MPC Lid (Steel)	9
External Water Reflector	12

TABLE 6.3.8

MCNP CROSS SECTION SETS USED IN THE ANALYSES

Nuclide	MCNP Cross Section Set [6.1.4]
1001	62c
5010	66c
5011	66c
6000	66c
8016	62c
13027	62c
24000	50c
25055	62c
26000	55c
28000	50c
40000	66c
82000	50c
92235	69c
92238	69c

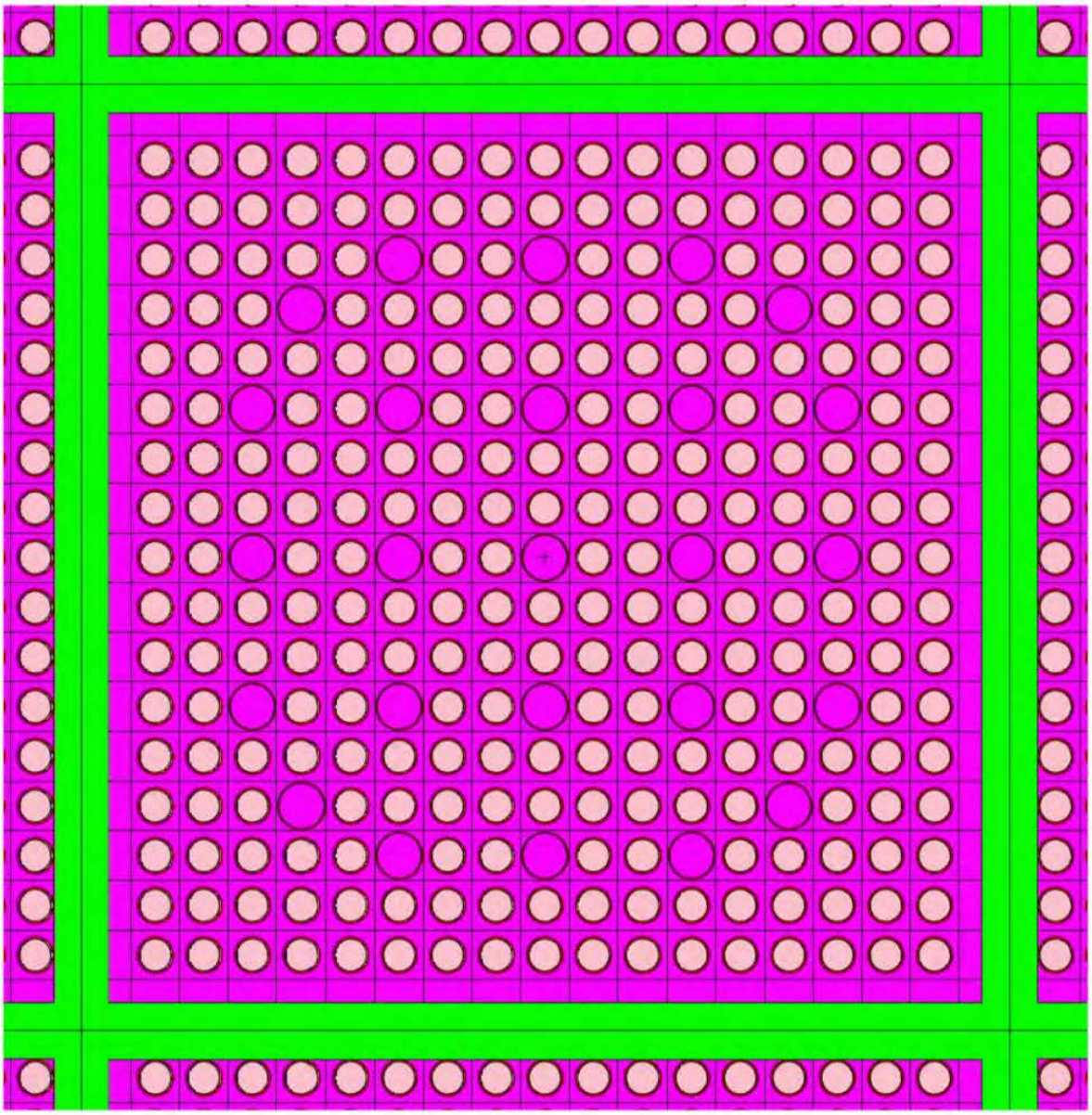

Figure generated directly from MCNP input file using the MCNP plot function. For Cell ID and Cell Wall Thickness see Table 6.3.3. For true dimensions see the drawings in Chapter 1.

Figure 6.3.1: Typical Cell of the Calculational Model (planar cross-section) with representative fuel in the MPC-37

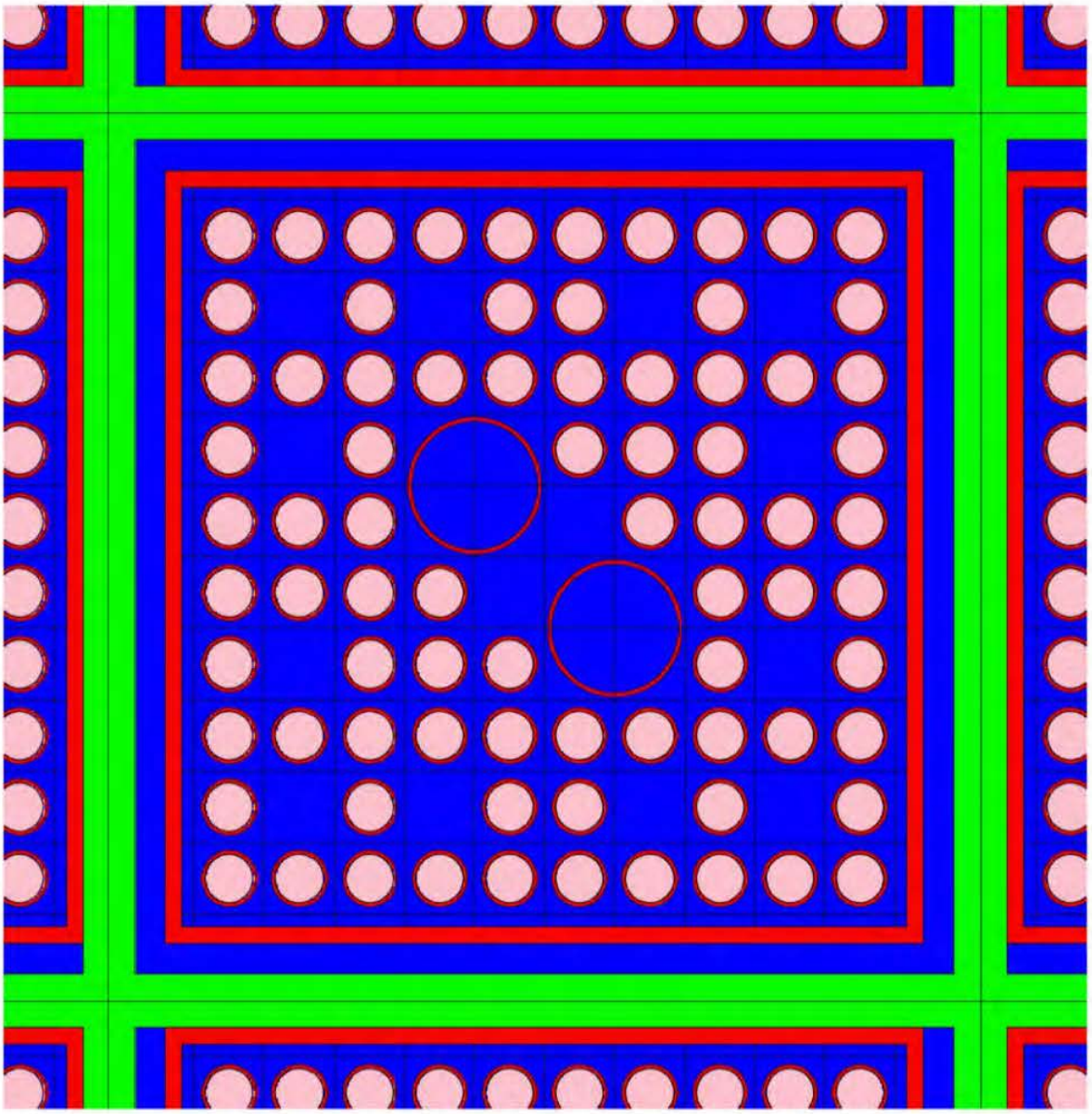

Figure generated directly from MCNP input file using the MCNP plot function. For Cell ID and Cell Wall Thickness see Table 6.3.3. For true dimensions see the drawings in Chapter 1.

Figure 6.3.2: Typical Cell of the Calculational Model (planar cross-section) with representative fuel in the MPC-89

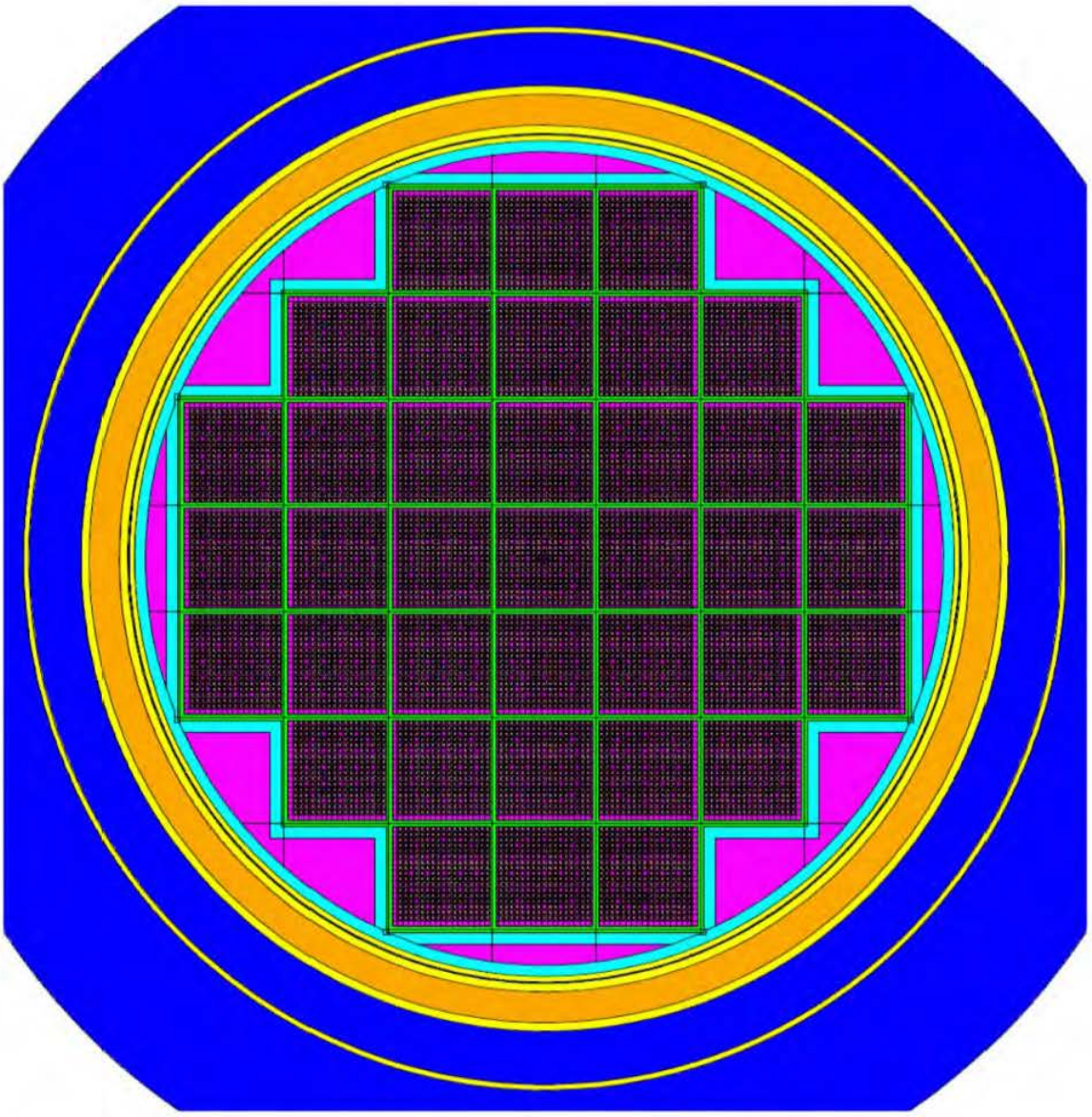

Figure generated directly from MCNP input file using the MCNP plot function. For radial dimensions of the HI-TRAC VW used in the analyses see Table 6.3.7. For true dimensions see the drawings in Chapter 1.

Figure 6.3.3: Calculational Model (planar cross-section) of the MPC-37

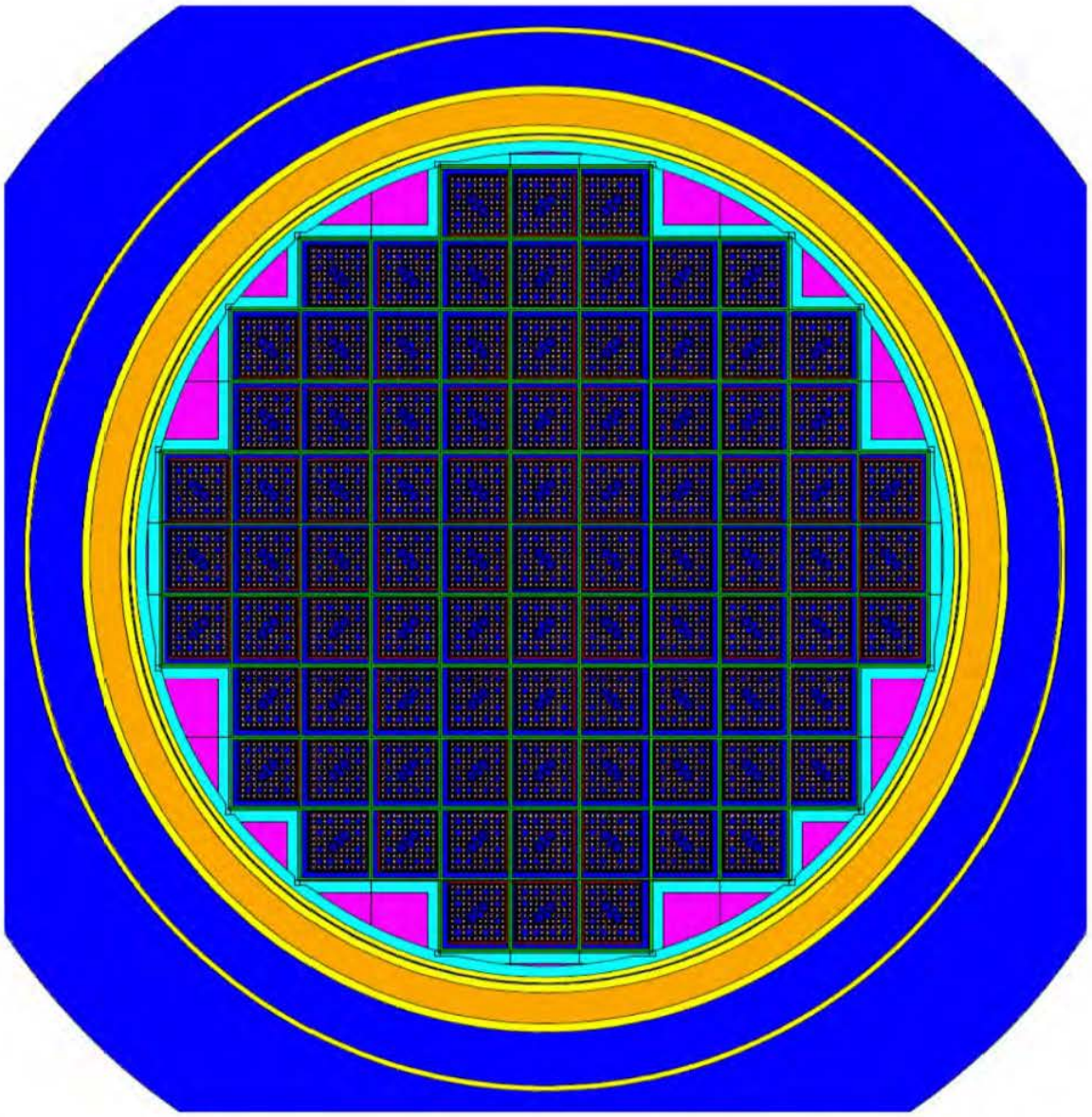

Figure generated directly from MCNP input file using the MCNP plot function. For radial dimensions of the HI-TRAC VW used in the analyses see Table 6.3.7. For true dimensions see the drawings in Chapter 1.

Figure 6.3.4: Calculational Model (planar cross-section) of the MPC-89

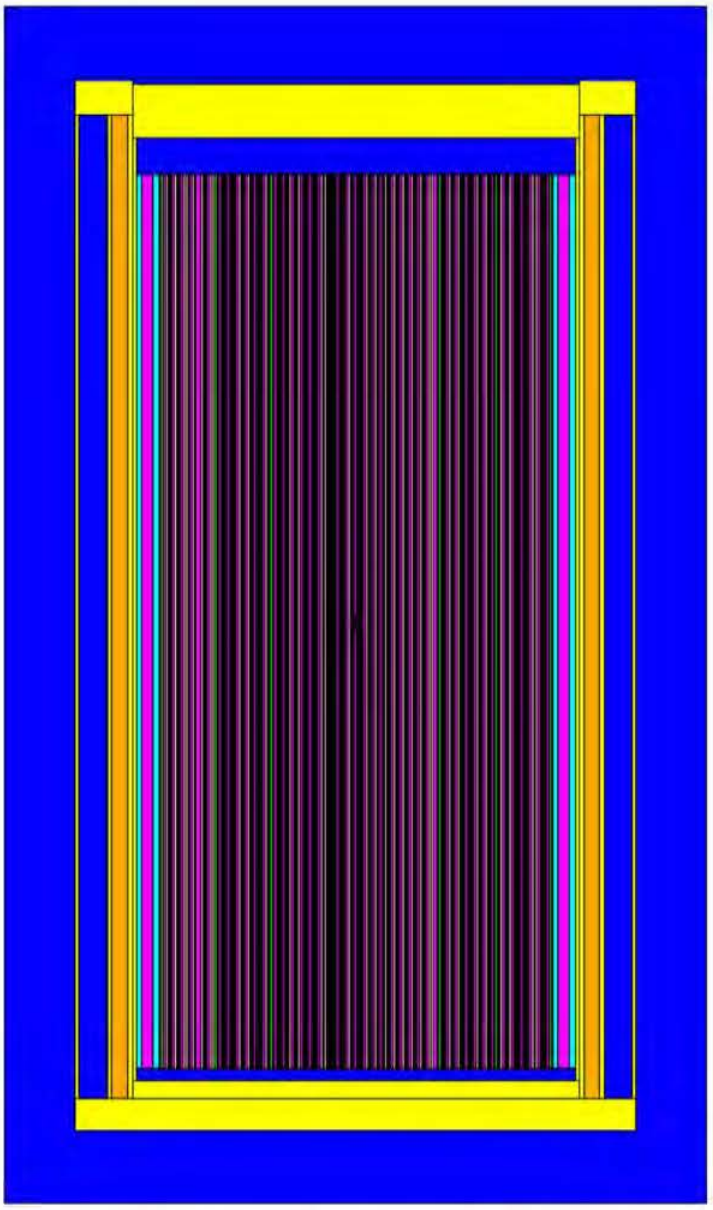

Figure generated directly from MCNP input file using the MCNP plot function. For axial dimensions of the HI-TRAC VW used in the analyses see Table 6.3.7. For true dimensions see the drawings in Chapter 1.

Figure 6.3.5: Calculational Model in Axial Direction

6.4 CRITICALITY CALCULATIONS

6.4.1 Calculational Methodology

The principal method for the criticality analysis is the general three-dimensional continuous energy Monte Carlo N-Particle code MCNP5 [6.1.4] developed at the Los Alamos National Laboratory. MCNP5 was selected because it has been extensively used and verified and has all of the necessary features for this analysis. MCNP5 calculations used continuous energy cross-section data distributed with the code [6.1.4].

The convergence of a Monte Carlo criticality problem is sensitive to the following parameters: (1) number of histories per cycle, (2) the number of cycles skipped before averaging, (3) the total number of cycles and (4) the initial source distribution. The MCNP5 criticality output contains a great deal of useful information that may be used to determine the acceptability of the problem convergence. Based on this information, a minimum of 20,000 histories were simulated per cycle, a minimum of 20 cycles were skipped before averaging, a minimum of 100 cycles were accumulated, and the initial source was specified as uniform over the fueled regions (assemblies). To verify that these parameters are sufficient, studies were performed where the number of particles per cycle and/or the number of skipped cycles were increased. The calculations are presented in Table 6.4.9, and show only small differences between the cases, with the statistical tolerance of those calculations. All calculations are therefore performed with the parameters stated above, except for some studies that are performed with 50000 neutrons per cycle for improved accuracy, and except for the calculations for the HI-STORM, which need less particles for convergence. Appendix 6.D provides sample input files for the MPC-37 and MPC-89 basket in the HI-STORM FW system.

6.4.2 Fuel Loading or Other Contents Loading Optimization

The basket designs are intended to safely accommodate fuel with enrichments indicated in Section 2.1. The calculations were based on the assumption that the HI-STORM FW system (HI-TRAC VW transfer cask) was fully flooded with clean unborated water or water containing specific minimum soluble boron concentrations. In all cases, the calculations include bias and calculational uncertainties, as well as the reactivity effects of manufacturing tolerances, determined by assuming the worst case geometry.

The discussion provided in Section 6.2.1 regarding the principal characteristics of fuel assemblies and basket poison is also important for the various studies presented in this section, and supports the fact that those studies only need to be performed for a single BWR and PWR assembly types, and that the results of those studies are then generally applicable to all assembly types. The studies and the relationship to the discussion in Section 6.2.1 are listed below. Note that this approach is consistent with that used for the HI-STORM 100.

Internal and External Moderation (Section 6.4.2.1): The studies presented in Table 6.2.3 show that all assemblies essentially behave identical in respect to water moderation, specifically, that all assemblies are undermoderated. The principal effect of changes to the internal and external moderation would therefore be independent of the fuel type.

Partial Flooding (Section 6.4.2.2): The partial flooding of the basket, either in horizontal or vertical direction, reduces the amount of fuel that partakes effectively in the thermal fission process, while essentially maintaining the fuel-to-water ratio in the volume that is still flooded. This will therefore result in a reduction of the reactivity of the system (similar to that of the reduction of the active length), and due to the similarity of the fuel assemblies is not dependent on the specific fuel type.

Pellet-to-clad Gap (Section 6.4.2.3): As demonstrated by the studies shown in Section 6.2.1, all assemblies are undermoderated. Flooding the pellet-to-clad gap will therefore improve the moderation and therefore increase reactivity for all assembly types.

Preferential Flooding (Section 6.4.2.4): The only preferential flooding situation that may be credible is the flooding of the bottom section of the DFCs while the rest of the MPC internal cavity is already drained. In this condition, the undamaged assemblies have a negligible effect on the system reactivity since they are not flooded with water. The dominating effect is from the damaged fuel model in the DFCs. However, the damaged fuel model is conservatively based on an optimum moderated array of bare fuel rods in water, and therefore representative of all fuel types. The results are therefore applicable to all fuel types.

6.4.2.1 Internal and External Moderation

Calculations in this section demonstrate that the HI-STORM FW system remains subcritical for all credible conditions of moderation.

6.4.2.1.1 External Moderator Density

Calculations for the MPC designs with external moderators of various densities are shown in Table 6.4.1, all performed for the HI-TRAC VW and the MPC fully flooded. The results show that the maximum k_{eff} is essentially independent from the external water density. Nevertheless, all further evaluations are performed with full external water density.

6.4.2.1.2 Internal Moderator Density

In a definitive study, Cano, et al. [6.4.1] have demonstrated that the phenomenon of a peak in reactivity at low moderator densities (sometimes called "optimum" moderation) does not occur in the presence of strong neutron absorbing material or in the absence of large water spaces between fuel assemblies in storage. Nevertheless, calculations were made to confirm that the phenomenon does not occur with low density water inside the casks.

Calculations for the MPC designs with internal moderators of various densities are shown in Table 6.4.5. Results show that in all cases the reactivity reduces with reducing water density, with both filled and voided guide and instrument tubes for PWR assemblies (see Section 6.4.7). All further calculations are therefore performed with full water density inside the MPCs.

6.4.2.2 Partial Flooding

Calculations in this section address partial flooding in the HI-STORM FW system and demonstrate that the fully flooded condition is the most reactive.

The reactivity changes during the flooding process were evaluated in both the vertical and horizontal positions for all MPC designs. For these calculations, the cask is partially filled (at various levels) with full density (1.0 g/cm^3) water and the remainder of the cask is filled with steam consisting of ordinary water at a low partial density (0.002 g/cm^3 or less), as suggested in NUREG-1536. Results of these calculations are shown in Table 6.4.2. In all cases, the reactivity increases monotonically as the water level rises, confirming that the most reactive condition is fully flooded.

6.4.2.3 Clad Gap Flooding

As recommended by NUREG-1536, the reactivity effect of flooding the fuel rod pellet-to-clad gap regions, in the fully flooded condition, has been investigated. Table 6.4.3 presents maximum k_{eff} values that demonstrate the positive reactivity effect associated with flooding the pellet-to-clad gap regions. These results confirm that it is conservative to assume that the pellet-to-clad gap regions are flooded. For all cases, the pellet-to-clad gap regions are assumed to be flooded with clean, unborated water.

6.4.2.4 Preferential Flooding

Two different potential conditions of preferential flooding are considered: preferential flooding of the MPC basket itself (i.e., different water levels in different basket cells), and preferential flooding involving Damaged Fuel Containers.

Preferential flooding of the MPC basket itself for any of the MPC fuel basket designs is not possible because flow holes are present on all four walls of each basket cell at the bottom of the MPC basket. The flow holes are sized to ensure that they cannot be blocked by crud deposits (see Chapter 12). For damaged fuel assemblies and fuel debris, the assemblies or debris are loaded into stainless steel Damaged Fuel Containers fitted with mesh screens which prevent damaged fuel assemblies or fuel debris from blocking the basket flow holes. Preferential flooding of the MPC basket is therefore not possible.

However, when DFCs are present in the MPC, a condition could exist during the draining of the MPC, where the DFCs are still partly filled with water while the remainder of the MPC is dry. As a simplifying and conservative approach to model this condition it is assumed that the DFCs are completely flooded while the remainder of the MPC is only filled with steam consisting of ordinary water at partial density (0.002 g/cm^3 or less). Assuming this condition, the case resulting in the highest maximum k_{eff} for the fully flooded condition (see Subsection 6.4.4) is re-analyzed assuming the preferential flooding condition. Table 6.4.4 lists the maximum k_{eff} in comparison with the maximum k_{eff} for the fully flooded condition. For all configurations, the preferential flooding condition results in a lower maximum k_{eff} than the fully flooded condition. Thus, the preferential flooding condition is bounded by the fully flooded condition.

Once established, the integrity of the MPC Confinement Boundary is maintained during all credible off-normal and accident conditions, and thus, the MPC cannot be flooded. In summary, it is concluded that the MPC fuel baskets cannot be preferentially flooded, and that the potential preferential flooding conditions involving DFCs are bounded by the result for the fully flooded condition listed in Subsection 6.4.4.

6.4.2.5 Design Basis Accidents

The analyses presented in Chapters 3 and 12 demonstrate that the damage resulting from the design basis accidents is limited to a loss of the water jacket for the HI-TRAC VW transfer cask and minor damage to the concrete radiation shield for the HI-STORM FW storage cask, which have no adverse effect on the design parameters important to criticality safety, and to minor deformation of the basket geometry, which is already considered in the analyses for the normal conditions.

In summary, the design basis accidents have no adverse effect on the design parameters important to criticality safety, and therefore, there is no increase in reactivity as a result of any of the credible off-normal or accident conditions involving handling, packaging, transfer or storage. Consequently, the HI-STORM FW system is in full compliance with the requirement of 10CRF72.124, which states that "before a nuclear criticality accident is possible, at least two unlikely, independent, and concurrent or sequential changes have occurred in the conditions essential to nuclear criticality safety."

6.4.3 Criticality Results

Results of the design basis criticality safety calculations for the condition of full flooding with water (limiting cases) and summarized in Section 6.1. To demonstrate the applicability of the HI-TRAC VW analyses, results of the design basis criticality safety calculations for the HI-TRAC VW cask (limiting cases) are also summarized in Section 6.1 for comparison. These data confirm that for each of the candidate fuel types and basket configurations the effective multiplication factor (k_{eff}), including all biases and uncertainties at a 95-percent confidence level, do not exceed 0.95 under all credible normal, off-normal, and accident conditions.

Additional calculations (CASMO-4) at elevated temperatures confirm that the temperature coefficients of reactivity are negative as shown in Table 6.3.1. This confirms that the calculations for the storage baskets are conservative.

In calculating the maximum reactivity, the analysis used the following equation:

$$k_{eff}^{max} = k_c + K_c \sigma_c + Bias + \sigma_B$$

where:

- ⇒ k_c is the calculated k_{eff} under the worst combination of tolerances;
- ⇒ K_c is the K multiplier for a one-sided statistical tolerance limit with 95% probability at the 95% confidence level [6.1.5]. Each final k_{eff} value is the result of averaging 100 (or more) cycle k_{eff} values, and thus, is based on a sample size of 100. The K multiplier corresponding to a sample size of 100 is 1.93. However, for this analysis a value of 2.00 was assumed for the K multiplier, which is larger (more conservative) than the value corresponding to a sample size of 100;
- ⇒ σ_c is the standard deviation of the calculated k_{eff}, as determined by the computer code;
- ⇒ ***Bias*** is the systematic error in the calculations (code dependent) determined by comparison with critical experiments in Appendix 6.A; and
- ⇒ σ_B is the standard error of the bias (which includes the K multiplier for 95% probability at the 95% confidence level; see Appendix 6.A).

The critical experiment benchmarking and the derivation of the bias and standard error of the bias (95% probability at the 95% confidence level) are presented in Appendix 6.A.

6.4.4 Damaged Fuel and Fuel Debris

6.4.4.1 Generic Approach

All MPCs are designed to contain PWR and BWR damaged fuel and fuel debris, loaded into DFCs. The number and permissible location of DFCs is provided in Table 2.1.1 and the licensing drawing in Section 1.5, respectively. Because the entire height of the fuel basket contains the neutron absorber (Metamic-HT), axial movement of DFC's does not have any reactivity consequence to MPC.

Damaged fuel assemblies, for the most part, are considered to be assemblies with known or suspected cladding defects greater than pinholes or hairline cracks, or with missing rods, but excluding fuel assemblies with gross defects (for the exact definition see the Glossary). Fuel debris can include a large variety of configurations ranging from whole fuel assemblies with severe damage down to individual fuel pellets.

To identify the configuration or configurations leading to the highest reactivity, a bounding approach is taken which is based on the analysis of regular arrays of bare fuel rods without cladding. Details and results of the analyses are discussed in the following subsections.

Note that since a modeling approach is used that bounds both damaged fuel and fuel debris without distinguishing between these two conditions, the term 'damaged fuel' as used throughout this chapter designates both damaged fuel and fuel debris.

Note that the modeling approach for damaged fuel and fuel debris is identical to that used in the HI-STORM 100 and HI-STAR 100.

Bounding Undamaged Assemblies

The undamaged assemblies assumed in the basket in those cells not filled with DFCs are those that show the highest reactivity for each group of assemblies, namely

- 9x9E for BWR 9x9E/F, 8x8F and 10x10G assemblies
- 10x10F for BWR 10x10F assemblies
- 10x10A for all other BWR assemblies;
- 16x16A for all PWR assemblies with 14x14 and 16x16 arrays; and
- 15x15F for all PWR assemblies with 15x15 and 17x17 arrays.

Since the damaged fuel modeling approach results in higher reactivities, requirements of soluble boron for PWR fuel and maximum enrichment for BWR fuel are different from those for undamaged fuel only. Those limits are listed in Table 6.1.4 (PWR) and Table 6.1.5 (BWR) in Section 6.1. Note that for the calculational cases for damaged and undamaged fuel in the MPC-89, the same enrichment is used for the damage and undamaged assemblies.

Note that for the first group of BWR assemblies listed above (9x9E/F, 8x8F and 10x10G), calculations were performed for both 9x9E and 10x10G as undamaged assemblies, and assembly class 9x9E showed the higher reactivity, and is therefore used in the design basis analyses. This may seem contradictory to the results for undamaged assemblies listed in Table 6.1.2, where the 10x10G shows a higher reactivity. However, the cases in Table 6.1.2 are not at the same enrichment between those assemblies.

All calculations with damaged and undamaged fuel are performed for an active length of 150 inches. There are two assembly classes (17x17D and 17x17E) that have a larger active length for the undamaged fuel. However, the calculations for undamaged fuel presented in Table 6.1.1 show that the reactivity of those undamaged assemblies is at least 0.0050 delta-k lower than that of the assembly class 15x15F selected as the bounding assembly for the cases with undamaged and damaged fuel. The effect of the active fuel length is less than that, with a value of 0.0026 reported in Table 6.2.1 for a much larger difference in active length of 50 Inches. The difference in active length between the 17x17D/E and 15x15F is therefore more than bounded, and the

15x15F assembly class is therefore appropriate to bound all undamaged assemblies with 15x15 and 17x17 arrays.

Bare Fuel Rod Arrays

A conservative approach is used to model both damaged fuel and fuel debris in the DFCs, using arrays of bare fuel rods:

- Fuel in the DFCs is arranged in regular, rectangular arrays of bare fuel rods, i.e., all cladding and other structural material in the DFC is replaced by water.

- For cases with soluble boron, additional calculations are performed with reduced water density in the DFC. This is to demonstrate that replacing all cladding and other structural material with borated water is conservative.

- The active length of these rods is assumed to be the same as for the intact fuel rods in the basket, even for more densely packed bare fuel rod arrays where it results in a total amount of fuel in the DFC that exceeds that for the intact assembly.

- To ensure the configuration with optimum moderation and highest reactivity is analyzed, the amount of fuel per unit length of the DFC is varied over a large range. This is achieved by changing the number of rods in the array and the rod pitch. The number of rods are varied between 16 (4x4) and 324 (18x18) for BWR fuel, and between 64 (8x8) and 576 (24x24) for PWR fuel.

This is a very conservative approach to model damaged fuel, and to model fuel debris configurations such as severely damaged assemblies and bundles of individual fuel rods, as the absorption in the cladding and structural material is neglected.

Further, this is a conservative approach to model fuel debris configurations such as bare fuel pellets due to the assumption of an active length of 150 inch (BWR and PWR). The actual height of bare fuel pellets in a DFC would be significantly below these values due to the limitation of the fuel mass for each basket position.

All calculations are performed for full cask models, containing the maximum permissible number of DFCs together with undamaged assemblies.

As an example of the damaged fuel model used in the analyses, Figure 6.4.1 shows the basket cell of an MPC-37 with a DFC containing a 14x14 array of bare fuel rods.

Principal results are listed in Table 6.4.6 and 6.4.7 for the MPC-37 and MPC-89, respectively. In all cases, the maximum k_{eff} is below the regulatory limit of 0.95.

For the HI-STORM 100, additional studies for damaged fuel assemblies were performed to further show that the above approach using arrays of bare fuel rods are bounding. The studies considered conditions including

- Fuel assemblies that are undamaged except for various numbers of missing rods
- Variations in the diameter of the bare fuel rods in the arrays
- Consolidated fuel assemblies with cladded rods
- Enrichment variations in BWR assemblies

Results of those studies were shown in the HI-STORM 100 FSAR, Table 6.4.8 and 6.4.9 and Figure 6.4.13 and 6.4.14 (undamaged and consolidated assemblies); HI-STORM 100 FSAR Table 6.4.12 and 6.4.13 (bare fuel rod diameter); and HI-STORM 100 FSAR Section 6.4.4.2.3 and Table 6.4.13 (enrichment variations). In all cases the results of those evaluations are equivalent to, or bounded by those for the bare fuel rods arrays. Since the generic approach of modeling damaged fuel and fuel debris is unchanged from the HI-STORM 100, these evaluations are still applicable and need not be re-performed for the HI-STORM FW.

6.4.5 Fuel Assemblies with Missing Rods

For fuel assemblies that are qualified for damaged fuel storage, missing and/or damaged fuel rods are acceptable. However, for fuel assemblies to meet the limitations of undamaged fuel assembly storage, missing fuel rods must be replaced with dummy rods that displace a volume of water that is equal to, or larger than, that displaced by the original rods.

6.4.6 Sealed Rods replacing BWR Water Rods

Some BWR fuel assemblies contain sealed rods filled with a non-fissile material instead of water rods. Compared to the configuration with water rods, the configuration with sealed rods has a reduced amount of moderator, while the amount of fissile material is maintained. Thus, the reactivity of the configuration with sealed rods will be lower compared to the configuration with water rods. Any configuration containing sealed rods instead of water rods is therefore bounded by the analysis for the configuration with water rods and no further analysis is required to demonstrate the acceptability. Therefore, for all BWR fuel assemblies analyzed, it is permissible that water rods are replaced by sealed rods filled with a non-fissile material.

6.4.7 Non-fuel Hardware in PWR Fuel Assemblies

Non-fuel hardware as defined in Table 2.1.1 are permitted for storage with all PWR fuel types. Non-fuel hardware is inserted in the guide tubes of the assemblies, except for ITTRs, which are placed into the instrument tube.

With the presence of soluble boron in the water, non-fuel hardware not only displaces water, but also the neutron absorber in the water. It is therefore possible that the insertion results in an increase of reactivity, specifically for higher soluble boron concentrations. As a bounding approach for the presence of non-fuel hardware, analyses were performed with empty (voided) guide and instrument tubes, i.e., any absorption of the hardware is neglected. Table 6.4.10 shows results for all PWR assembly classes at 5% enrichment with filled and voided guide and instrument tubes. These results show that for all classes, the condition with filled guide and instrument tubes bound those, or are statistically equivalent to those, with voided guide and instrument tubes. For the higher soluble boron concentration required in the presence of damaged fuel, the same is shown in Table 6.4.5 (two columns on the right). In this case, only the bounding case (Assembly class 15x15F as undamaged fuel) was analyzed.

In summary, from a criticality safety perspective, non-fuel hardware inserted into PWR assemblies are acceptable for all allowable PWR types, and, depending on the assembly class, can increase the safety margin.

6.4.8 Neutron Sources in Fuel Assemblies

Fuel assemblies containing start-up neutron sources are permitted for storage in the HI-STORM FW system. The reactivity of a fuel assembly is not affected by the presence of a neutron source (other than by the presence of the material of the source, which is discussed later). This is true because in a system with a k_{eff} less than 1.0, any given neutron population at any time, regardless of its origin or size, will decrease over time. Therefore, a neutron source of any strength will not increase reactivity, but only the neutron flux in a system, and no additional criticality analyses are required. Sources are inserted as rods into fuel assemblies, i.e., they replace either a fuel rod or water rod (moderator). Therefore, the insertion of the material of the source into a fuel assembly will not lead to an increase of reactivity either.

6.4.9 Low Enriched, Channeled BWR fuel

The calculations in this subsection show that low enriched, channeled BWR fuel with indeterminable cladding condition is acceptable for loading in all storage locations of the MPC-89 without placing those fuel assemblies into DFCs, hence classifying those assemblies as undamaged. The main characteristics that must be assured are:

- The channel is present and attached to the fuel assembly in the standard fashion; and
- The channel is essentially undamaged; and
- The maximum planar average enrichment of the assembly is less than or equal to 3.3 wt% ^{235}U

This analysis covers older assemblies, where the cladding integrity is uncertain, and where a verification of the cladding condition is prohibitive. An example of this type of fuel is the so-called CILC fuel, which has potential corrosion-induced damaged to the cladding but does not have grossly breached spent fuel rods.

The presence of the essentially undamaged and attached channel confines the fuel rods to a limited volume and the low enrichment, required for all assemblies in the MPC, limits the reactivity of the fuel even under optimum moderation conditions. Due to the uncertain cladding condition, the analysis of this fuel follows essentially the same approach as that for the Damaged Fuel and Fuel Debris, i.e. bare fuel rod arrays of varying sizes are analyzed within the confines of the channel. This is an extremely conservative modeling approach for this condition, since reconfiguration is not expected and cladding would still be present. The results of this conservative analysis are listed in Table 6.4.8 and show that the system remains below the regulatory limit with these assemblies in all cells of the MPC-89, without DFCs.

These results confirm that even with unknown cladding condition the maximum k_{eff} values are below the regulatory limit when fully flooded and loaded with any of the BWR candidate fuel assemblies, therefore if the cladding is not grossly breached and the fuel assembly structurally sound it can be considered undamaged when loading in an MPC-89.